Environmental Laboratory

US Army Corps
of Engineers®
Engineer Research and
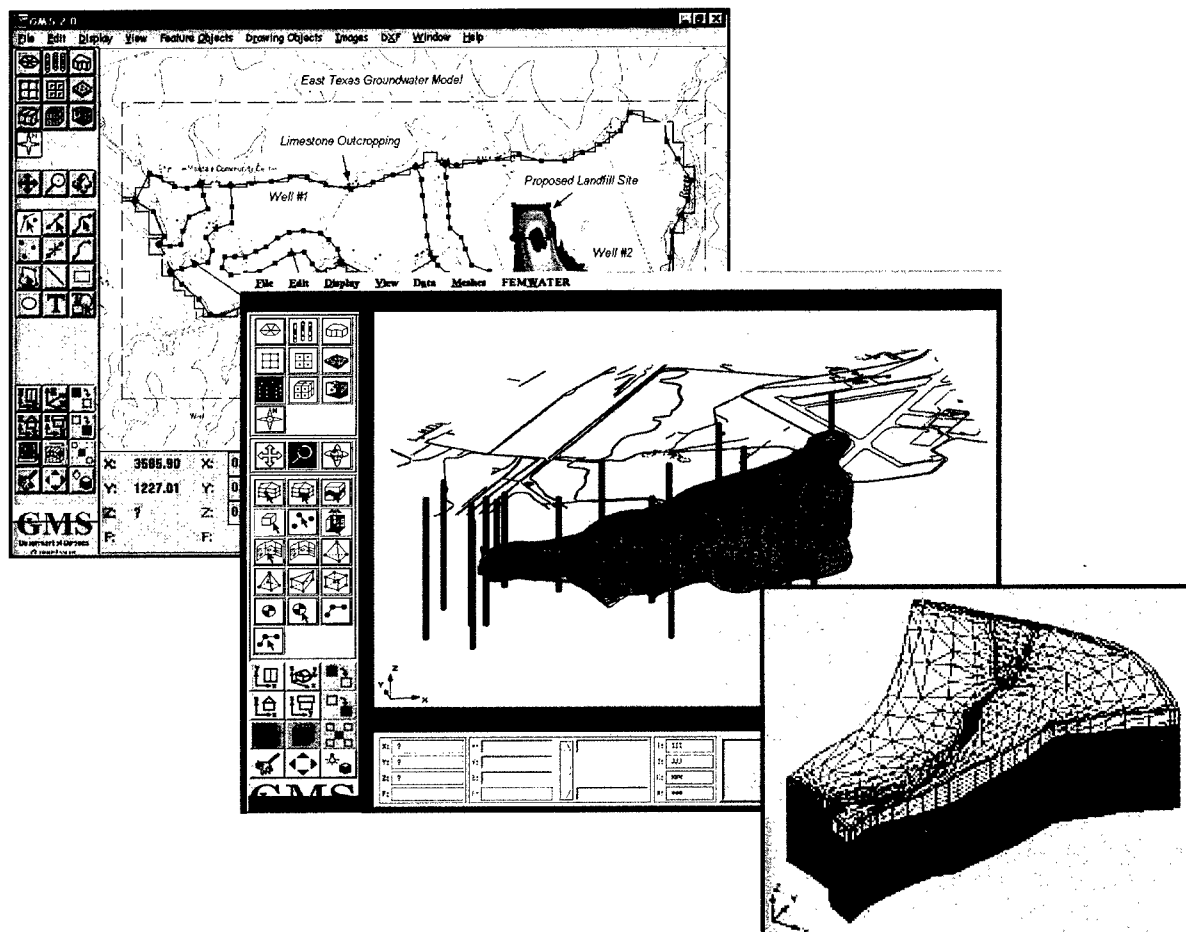Development Center

20020312 034

Strategic Environmental Research and Development Program

Development of Simulators for In Situ Remediation Evaluation, Design, and Operation: Final Report

Mark S. Dortch, Christian J. McGrath, John J. Nitao, Mark A. Widdowson, and Steve Yabusaki

September 2001

The contents of this report are not to be used for advertising, publication, or promotional purposes. Citation of trade names does not constitute an official endorsement or approval of the use of such commercial products.

The findings of this report are not to be construed as an official Department of the Army position, unless so designated by other authorized documents.

Development of Simulators for In Situ Remediation Evaluation, Design, and Operation: Final Report

by   Mark S. Dortch and Christian J. McGrath

Environmental Laboratory
U.S. Army Engineer Research and Development Center
3909 Halls Ferry Road
Vicksburg, MS 39180-6199

John J. Nitao

Lawrence Livermore National Laboratory
U.S. Department of Energy
7000 East Avenue
Livermore, CA 94550-9234

Mark A. Widdowson

The Charles E. Via, Jr., Department of Civil and Environmental Engineering
Virginia Polytechnic Institute and State University
Blacksburg, VA 24061-0105

Steve Yabusaki

Pacific Northwest National Laboratory
U.S. Department of Energy
P.O. Box 999
Richland, WA 99352

Final report

Contents

List of Figures

List of Tables

Preface

This report is the final, summary report for Work Unit CU-1062, "Development of Simulators for In Situ Remediation Evaluation, Design, and Operation," which was under the Cleanup Pillar of the Strategic Environmental Research and Development Program (SERDP), sponsored by the U.S. Department of Defense, U.S. Environmental Protection Agency, and U.S. Department of Energy. Work Unit CU-1062 was conducted by U.S. Army Engineer Research and Development Center (ERDC), under the purview of the Environmental Laboratory (EL), Vicksburg. MS. ERDC involvement in SERDP was coordinated by Dr. John Cullinane, Program Manager for the EL Installation Restoration Research Program (IRRP). Mr. Charles Miller, EL, was Assistant Manager for the IRRP. Ms. Catherine Vogel was the Cleanup Program Manager for SERDP.

The technical leader and point of contact for Work Unit CU-1062 was Dr. Mark S. Dortch, Chief, Water Quality and Contaminant Modeling Branch (WQCMB), Environmental Processes and Engineering Division (EPED), EL. Other principal investigators participating in the project included Mr. Christian J. McGrath, WQCMB; Dr. Carlos E. Ruiz, WQCMB; Dr. Stacy E. Howington, Groundwater Systems Group, Modeling Systems Branch, Coastal and Hydraulics Laboratory, ERDC; Mr. Steve Yabusaki, U.S. Department of Energy (DOE), Pacific Northwest National Laboratory (PNNL), Richland, WA; Dr. John J. Nitao, DOE, Lawrence Livermore National Laboratory (LLNL), Livermore, CA; and Dr. Thomas B. Stauffer, U.S. Air Force, Armstrong Laboratory/EQ, Wright-Patterson Air Force Base, Ohio. Additionally, work within this project was conducted through contracts with Brigham Young University, Provo, UT; University of Texas, Austin; Virginia Polytechnic Institute (VPI) and State University, Blacksburg; University of Alabama, Tuscaloosa; and Tennessee Valley Authority, Norris, TN. This report was prepared by Drs. Dortch, Nitao, and Mark A. Widdowson of VPI and Messrs. McGrath and Yabusaki.

This study was conducted under the general supervision of Dr. Richard E. Price, Chief of EPED, and Drs. John Keeley and Edwin A. Theriot, Acting Directors of EL.

At the time of publication of this report, Dr. James R. Houston was Director of ERDC, and COL John W. Morris III, EN, was Commander and Executive Director.

This report should be cited as follows:

1 Introduction

Background

The Departments of Defense (DoD) and Energy (DOE) are involved in the cleanup of thousands of sites at an estimated cost of over hundreds of billions of dollars. Significant resources will be consumed in the evaluation of alternative or combined remediation technologies, particularly where in situ or innovative technologies are considered. Yet there is no expedient means to quantitatively evaluate alternatives. Such methods could provide more accurate and technically defensible evaluations. Expensive remediation decisions based on inadequate information will become even more expensive if they result in inefficient design or failure. These failures may result in increased human and environmental risk, thereby reducing public confidence and negatively impacting DoD and DOE readiness. Methods to streamline the evaluation process would also save time and money. The ultimate goal in remediation modeling is to minimize remediation costs and environmental and human health risks while maximizing cleanup. Toward this end, the general goals of this project were to (a) develop reliable simulators for promising technologies of interest to DoD, DOE, and the regulatory community including the U.S. Environmental Protection Agency (EPA); and (b) provide efficient access to multiple remediation simulators through a common user environment amenable to multidisciplinary cleanup teams. A common graphical user environment has been developed for these simulators: the DoD Groundwater Modeling System (GMS).

The GMS provides conceptualization, characterization, model parameterization and setup, visualization, and animation capabilities. GMS extensions, either ongoing or planned, will provide capabilities for conducting parameter estimation, uncertainty analysis, optimization, and cost analyses. The U.S. Army Engineer Research and Development Center (ERDC) leads the GMS development, which has been a Tri-Service, multiagency activity involving multiple DoD, DOE, and EPA researchers and 20 university partners. The GMS is employed by hundreds of users within the Tri-Services, DOE, and EPA. Commercial versions of the GMS are used by many groups within the cleanup industry.

Objectives

The overall objective of this project was to provide DoD, DOE, EPA, and other GMS users with the ability to simulate in situ remediation and natural attenuation of subsurface contamination. This capability allows the evaluation of the effectiveness of various cleanup strategies and improvement of system design prior to implementation. Simulators also provide a means to evaluate cleanup system operational strategies and improvements. Additionally, products from this project provide the computational capability to assess future exposure concentrations, enabling efficient analysis of tradeoffs between environmental risk (cleanup level) and costs for a variety of cleanup alternatives prior to their implementation.

The specific technical objectives of this project were as follows:

a. Develop and/or enhance state-of-the-art remediation simulators for the following technologies:

   (1) Engineered or enhanced in situ bioremediation.

   (2) Natural attenuation of petroleum and chlorinated hydrocarbons and explosives (NAX).

   (3) In situ chemical treatment (ISCT), such as permeable reactive walls.

   (4) Surfactant/cosolvent flushing to recover nonaqueous phase liquids (NAPLs).

   (5) Venting technologies, such as soil vapor extraction (SVE), air sparging, and bioventing/sparging.

b. Validate simulators for most of these technologies against available laboratory and field data.

c. Document the simulators and incorporate them into the GMS.

The purpose of this report is to summarize the results achieved during the course of this 4-year project.

Technical Approach

Remediation simulator development could have proceeded along three paths, in order of priority: (a) use existing, proven remediation simulators where available and consistent with project goals; (b) modify promising groundwater model codes to simulate additional technologies as appropriate; or (c) develop new codes as required for efficient simulation of innovative technologies. All simulator codes selected or developed within this project were required to be in the public domain. Prior to this project, the major thrust in remediation simulation within the GMS had been toward using existing codes for the simpler remediation technologies, such as pump-and-treat and physical barriers. Codes within the GMS prior to this project included FEMWATER (Lin et al. 1997), MODFLOW (McDonald and Harbaugh 1988) and MT3D (Zheng 1990). The approach used during this project

followed (a) and (b), i.e., to use existing codes and to modify, adapt, and enhance existing codes to simulate additional technologies as necessary.

A plan for GMS integration of additional simulators existed prior to this project (Hadala et al. 1993) that placed priority on certain technologies based on remediation technology maturity and effectiveness, user demand for a given remedial technology, and the degree to which the additional simulator would complement existing GMS capabilities. Based on these guidelines, a suite of three-dimensional, groundwater/subsurface simulation codes was selected as shown in Table 1. All of these codes existed prior to this project, but were modified during this project to better represent the targeted in situ remediation technologies.

Table 1
CU-1062 Simulators, Technologies, and Validation Sites

Simulator	Technology Simulation Validated	Validation Site
Sequential Electron Acceptor Model in 3D (SEAM3D)	Engineered in situ bioremediation	Defense Fuel Supply Point (DFSP), SC
	Natural attenuation of petroleum hydrocarbons (BTEX)	Natural Attenuation Test Site (NATS), Columbus AFB
	Natural attenuation of chlorinated hydrocarbons (solvents)	Pensacola Naval Air Station
University of Texas Chemical Flood Simulator (UTCHEM)	NAX	Louisiana Army Ammunition Plant (LAAP) in collaboration with CU-715
	Surfactant flushing	Hill AFB
	Cosolvent flushing	Lab studies and Dover AFB
Operator Splitting in 3D (OS3D)	ISCT, permeable reactive walls	Dover AFB, in collaboration with CU-107 and Moffett Field
Nonisothermal, Unsaturated/ Saturated Flow and Transport in 3D (NUFT3D)	SVE Biosparging	Lawrence Livermore National Laboratory Building 518, DOE Hill AFB
Note: SEAM3D is a reaction module that must be coupled with a transport module. SEAM3D is coupled to the MT3DMS transport code, which resides within the GMS and has the option of using either SEAM3D or RT3D for reactions.		

The four targeted simulators can simulate multiple technologies. For example, UTCHEM (University of Texas Chemical Flood Simulator) is applicable to cosolvent flushing and surfactant flushing. Through a separate EPA effort, UTCHEM has been modified to include bioremediation (aerobic and anaerobic respiration and cometabolism). UTCHEM is a multiphase flow/transport code, so it potentially offers other simulation capabilities. NUFT (Nonisothermal Unsaturated/ Saturated Flow and Transport) can simulate SVE, steam- or thermally-enhanced SVE, air sparging, as well as other multiphase flow/transport problems. NUFT has also been modified for bioremediation. There is some overlap of simulator capabilities, such as multiphase flow/transport with UTCHEM and NUFT and bioremediation simulation with SEAM3D (Sequential Electron Acceptor Model, 3-Dimensional), NUFT, and UTCHEM. However, these overlaps are a strength

rather than a weakness since each of these codes has its unique capabilities. Additionally, model selection for a particular application should be based on satisfying study needs while using the code that is easiest to use.

All simulators were validated against available laboratory and field data, with preference given to Strategic Environmental Research and Development Program (SERDP) National Environmental Technology Test Sites (NETTS). Table 1 lists the technology simulations that were validated and the validation sites. Results of all validation applications either have been or are in the process of being documented as technical reports or papers, with references cited herein. Each simulator has been documented and implemented in the GMS. Also, a tutorial for each model is available with the GMS for assistance in application.

Before any model is used for decision making, it should be validated by application to at least one field study. Validation provides the assurance that the algorithms embodied in the computer code correctly represent the physical processes or system to which the model is applied (Beljin 1988). A model is said to be validated when sufficient testing shows an acceptable degree of matching the actual systems through model versus data comparisons. However, a model should be revalidated every time it is modified or is applied to a new system. In practice, validation is a never-ending process since models of any value tend to stay in use for a long time, and are eventually applied to a wide variation of field systems. Additionally, model developers/users are always striving for perfection in terms of adding new features to make models more closely resemble the real system. Therefore, numerical models are assessed (validated) by repeated application to laboratory experiments and monitored field data. Repeated successful applications enhance confidence in the model, while unsatisfactory results stimulate either improvements to the model or its abandonment by the user community. While the validation applications undertaken during this project may not be the first for a particular model, they most likely will not and should not be the last.

This report provides a summary of the work conducted under this project. The next four chapters focus on each of the four simulators that were under development. Each chapter describes the simulator, its enhancements or improvements, its validation, its incorporation within the GMS, and recommendations for future work. For more detail, readers should refer to other reports and papers cited in each chapter.

SEAM3D

Basic Transport Package

Advection Package

MT3DMS

Dispersion Package

Source/Sink Mixing Package

Reaction Package

Biodegradation Package

NAPL Dissolution Package

Reductive Dechlorination Package

Cometabolism Package
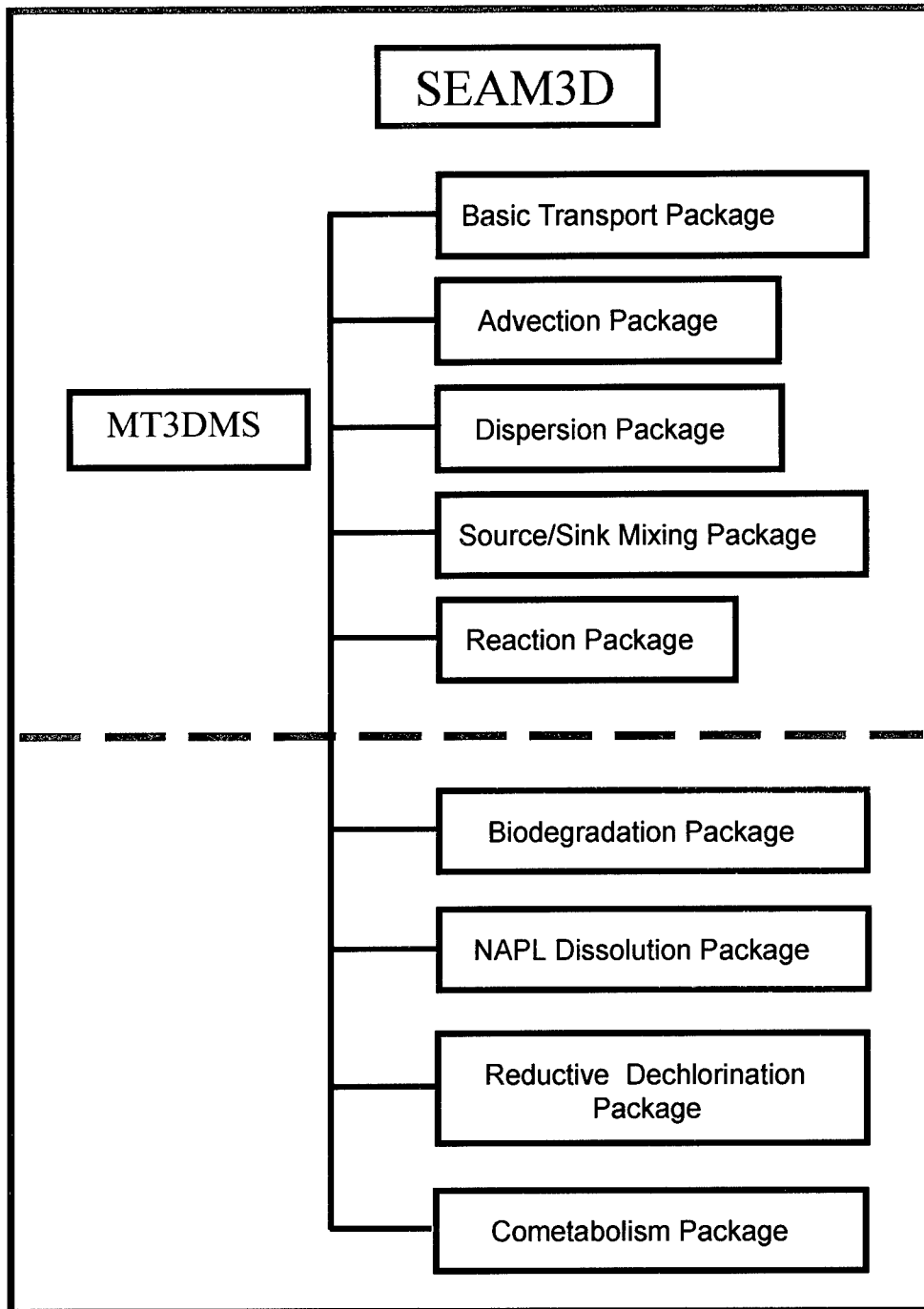
Figure 1. SEAM3D incorporates MT3DMS packages (blue) for advective-dispersive transport, sorption, and fluid source/sinks and additional packages unique to SEAM3D (red), including the Biodegradation, NAPL Dissolution, Cometabolism, and Reductive Dechlorination Packages.

2 SEAM3D and MT3DMS

Model Description

SEAM3D is a computer code for the numerical simulation of solute transport with aerobic and sequential anaerobic biodegradation. The model can depict multiple constituents in a three-dimensional, anisotropic, heterogeneous domain. SEAM3D is designed for application to engineered (accelerated) bioremediation systems and intrinsic bioremediation (natural attenuation).

The parent code is MT3DMS (Zheng and Wang 1999), which is designed to simulate physical transport, sorption, and mass injection/extraction due to fluid sources and sinks. As shown in Figure 1, SEAM3D consists of four additional packages: Biodegradation, NAPL Dissolution, Cometabolism, and Reductive Dechlorination. The Biodegradation and NAPL Dissolution Packages were developed and verified in the original version of SEAM3D (Waddill and Widdowson 2000). The latter two packages were recently developed, and that work is outlined in this report.

The Biodegradation Package is the main subroutine of SEAM3D. Hydrocarbon contaminants are simulated as electron donors (i.e., substrates) for microbial growth, with available electron acceptors (EAs) used in the following sequence based on energy yield: oxygen (O_2), nitrate (NO_3^-), oxidized manganese (Mn(IV)), ferric iron (Fe(III)), sulfate (SO_4^{2-}), and carbon dioxide (CO_2). Mineral nutrients and biodegradation end products and daughter products are also simulated. Biodegradation of each substrate follows Monod kinetics, modified to include the effects of EA and nutrient availability. Inhibition functions allow any EA to inhibit utilization of all other EAs that provide less energy to the microbes. Microbial biomass is simulated as scattered microcolonies attached to the porous medium. Equations used in the Biodegradation Package are described in Waddill and Widdowson (1998).

The NAPL Dissolution Package simulates the transfer of mass from a NAPL to the aqueous phase. When using the Biodegradation Package with the NAPL Dissolution Package, the user specifies the number of tracers and hydrocarbon substrates and the characteristics of each constituent, and the characteristics, distribution, and concentration of a light nonaqueous phase liquid (LNAPL) such as gasoline. Equations used in the NAPL Dissolution Package are described in Waddill and Widdowson (1998).

Model Enhancements

Model enhancements to SEAM3D are summarized here. Enhancements to MT3DMS can be found in Zheng and Wang (1999).

Reductive dechlorination package

The SEAM3D Reductive Dechlorination Package (SEAM3D-RDP) is a numerical model designed to simulate intrinsic bioremediation of chlorinated ethenes in groundwater. SEAM3D-RDP is designed to simulate transport and biodegradation of chlorinated compounds perchloroethene (PCE), trichloroethene (TCE), 1,2-dichloroethene (cis-DCE), and vinyl chloride (VC). End products simulated in SEAM3D-RDP include ethene and chloride. The model is solved numerically using the core packages of MT3DMS and the Biodegradation Package. SEAM3D-RDP may be executed with or without the NAPL Dissolution and Cometabolism Packages. The NAPL Dissolution Package was updated to simulate PCE or TCE dissolution from a dense nonaqueous phase liquid (DNAPL), such as a solvent. When the Cometabolism Package and SEAM3D-RDP are used, only TCE, cis-DCE, and VC (or any combination) may be specified as subject to cometabolism.

SEAM3D-RDP is designed to simulate two or three significant biological degradation mechanisms: reductive dehalogenation (or dechlorination) and direct oxidation. A third mechanism, cometabolism, is simulated in the Cometabolism Package, if this option is specified by the user. The mechanisms for degradation are summarized in Table 2 for the four chlorinated ethenes. The conceptual and mathematical models for SEAM3D-RDP and relevant equations are discussed in depth in a progress report to ERDC and in a peer-reviewed journal paper under preparation. In addition, this work as been presented in part at two international conferences and at the SERDP 2000 Symposium.

Recent experimental studies have demonstrated aerobic and anaerobic oxidation of VC and cis-DCE, but direct oxidation appears limited to higher energy-yielding terminal electron accepting processes (TEAPs). All four simulated

Table 2			
Biodegradation Mechanisms Considered in the Model for Perchloroethene (PCE), Trichloroethene (TCE), Dichloroethene (DCE), and Vinyl Chloride (VC)			
	Mechanism		
Compound	Direct Oxidation	Reductive Dechlorination	Cometabolism
PCE	No	Yes	No
TCE	No	Yes	Yes[1]
DCE	Yes	Yes	Yes[1]
VC	Yes	Yes	Yes[1]
[1] If specified by user in the Cometabolism Package.			

chlorinated ethenes may undergo reductive dechlorination with the rate of trans-
formation dependent on the prevailing TEAP simulated in any given model cell.
SEAM3D simulates the prevailing TEAP in each model cell and at every time-
step using the Biodegradation Package, and this information is linked to the
Reductive Dechlorination Package. VC and cis-DCE may serve as electron donors
in the SEAM3D-RDP when conditions in a model cell favor direct oxidation.

Cometabolism package

The SEAM3D Cometabolism Package (SEAM3D-CP) is a numerical model
designed to simulate engineered or intrinsic bioremediation of recalcitrant com-
pounds in groundwater. SEAM3D-CP is designed to simulate transport and
biodegradation of chlorinated ethenes (TCE, cis-DCE, trans-DCE, VC) or other
compounds known to cometabolize in the presence of a single growth substrate,
oxygen, and an aerobic microbial population. The model is solved numerically
using the core packages of MT3DMS and the Biodegradation Package.
SEAM3D-CP may be used in conjunction with the NAPL Dissolution Package,
SEAM3D-RDP, or both.

When SEAM3D-CP is run, one hydrocarbon compound is designated in the
Biodegradation Package as the growth substrate linked to cometabolism. A frac-
tion of the aerobic population (designated in the Biodegradation Package) is
assumed responsible for cometabolism. Methane, an end product of aerobic bio-
degradation, may also serve as the growth substrate. In this case, a methanotrophic
population, separate from the main aerobic population, is designated in the
Biodegradation Package. Up to three recalcitrant compounds may be designated in
the SEAM3D-CP. Equations used in the SEAM3D-CP were modified from
Semprini and McCarty (1991 and 1992).

Microbial populations

The SEAM3D Biodegradation Package originally included as many as six
bacterial populations: aerobes, facultative nitrate reducers, anaerobic manganese
reducers, anaerobic iron reducers, anaerobic sulfate reducers, and methanogens
(Table 3). Three new microbial groups have been added. Two biomass concen-
tration variables are simulated in SEAM3D-RDP, both responsible for the reduc-
tion of chlorinated ethenes. One population utilizes only PCE and TCE as EAs,
preferentially using PCE, but inhibited by higher energy-yielding EAs. The
second population utilizes only cis-DCE and VC as EAs, preferentially using cis-
DCE, but potentially inhibited in the presence of PCE and TCE. As noted in the
preceding paragraph, a seventh microbial population, the methanotrophs, was
added directly to the Biodegradation Package. This group is relevant only to the
SEAM3D-CP, when cometabolism is simulated. The methanotrophic population
may be simulated either with or without the methanogenic population.

Table 3
Electron Acceptors Used by the Microbial Populations for Biodegradation of Hydro-carbon Substrates

Microbial Population x = SEAM3D Bio Y = SEAM3D-RDP	Index of Electron Donor Is	Index of Electron Acceptor Ie[1]	Utilization Inhibited by[2]	End Products
x=1 strict aerobes	User-specified hydrocarbon (UHC)	Ie=1 O_2	--	
x=2 facultative NO_3 reducers	UHC	Ie=1 O_2	--	
	UHC	Ie=2 NO_3	O_2	NO_x
x=3 anaerobic Mn(IV) reducers	UHC	Ie=3 $Mn_{(x)}$	O_2, NO_3, Mn(IV), Fe(III), SO_4	Mn(II)
x=4 anaerobic Fe(III) reducers	UHC	Ie=4 $Fe_{(x)}$	O_2, NO_3, Mn(IV), Fe(III), SO_4	Fe(II)
x=5 anaerobic SO_4 reducers	UHC	Ie=5 SO_4	O_2, NO_3, Mn(IV), Fe(III), SO_4	HS^-
x=6 methanogens	UHC		O_2, NO_3, Mn(IV), Fe(III), SO_4	CH_4
x=7 methanotrophs	Methane	Ie=1 O_2	--	--
y=1 PCE/TCE reducers	Not simulated		O_2, NO_3, Mn(IV), Fe(III), SO_4	CI
y=2 cis-DCE/VC reducers	Not simulated		O_2, NO_3, Mn(IV), Fe(III), SO_4	CI, ethene

[1] Electron acceptors are listed in order of highest to lowest Gibbs free energy per half reaction.
[2] Utilization of each electron acceptor is inhibited by the presence of an electron acceptor that provides higher energy.

Model Validation

Waddill and Widdowson (2000) demonstrated the use of SEAM3D at a gasoline-contaminated site where the uncontrolled release resulted in a benzene, toluene, ethylbenzene, xylene (BTEX) plume that included methyl tertiary butyl ether (MTBE). The model was validated using monitoring well data collected over 5 years. The SEAM3D Biodegradation and NAPL Dissolution Packages were more recently validated at the Natural Attenuation Study (NATS) located at Columbus Air Force Base (AFB), Mississippi. Progress was also made toward validation of the SEAM3D-RDP at the Pensacola Naval Air Station (NAS).

NATS

NATS consisted of the release and subsequent monitoring of a NAPL mixture of BTEX, naphthalene, decane, and bromide into the shallow, unconfined aquifer underlying Columbus AFB in eastern Mississippi. During the present study, both conceptual and mathematical models were developed for NAPL source release, sequential aerobic/anaerobic biodegradation, and sorption during NATS. SEAM3D was used to simulate fully three-dimensional transport and aerobic, anoxic, ferrogenic, and methanogenic hydrocarbon biodegradation. Simulation results matched individual BTEX concentration distributions collected 5 and 9 months following NAPL release.

NATS was initiated by placing a known mass of NAPL into the Columbus aquifer. The mass fraction of BTEX and naphthalene in the NAPL was propor-tional to a typical JP-4 jet fuel, with decane serving as an octane surrogate for the

remaining inert fraction of the fuel. The NAPL was mixed with 30 m^3 of clean sand and placed in an excavated trench (hereafter referred to as the source trench), which was backfilled to land surface with uncontaminated sand. Sheetpiling, which had been installed along the walls of the trench to establish hydraulic control, was removed, and the natural groundwater gradient in the source area was restored to allow petroleum hydrocarbon (PHC) dissolution into the groundwater. Solute concentrations were measured from selected ports in a multilevel sampling network. The most comprehensive collection and analysis were conducted during the sampling events 5 months and 9 months after source removal. Analysis of solute concentrations indicated that multiple microbial processes were active during the NATS experiment.

Figure 2 presents contour plots of field data (left column) at time $t = 5$ months and calibrated single porosity model results (right column) for a vertical cross section located 4 m west of the source center line for benzene, toluene, ethyl-benzene, p-xylene, and naphthalene. Comparison between columns in Figure 2 shows that the calibrated model recreated the fingering observed for the 1-mg/L BTEX contour, and generally reproduced the vertical and longitudinal extent of BTEX concentration plumes. The vertical and longitudinal dimensions of the naphthalene plume were also reproduced, but field-measured naphthalene concentrations in and around the source area were approximately five times higher than model-predicted values at $t = 5$ months (possibly due to increased solubility effects). A comparison of model results at $t = 9$ months (results not shown) showed a stable plume and the persistent fingering on the hydrocarbon plume.

Horizontal slices of the field-measured and model-simulated PHC concentrations, taken at an elevation z that passed through the source trench (i.e., 60 m), showed that the reactive transport model also captured horizontal variations in PHC transport. As an example, Figure 3 depicts horizontal contour plots of toluene concentration developed from field data (left column) and the calibrated single porosity model (right column) for $t = 5$ months and 9 months. Figure 3 shows agreement between field observations and model simulations in that toluene migration in the western portion (negative transverse distance) of the plume was greater than in the eastern portion.

SEAM3D mass balance calculations indicated that biodegradation consumed 49 percent of the aqueous phase hydrocarbon compounds, while 13 percent of this mass was sorbed and 38 percent remained in the aqueous phase. Mass calculations further indicated that aerobic biodegradation accounted for the majority of hydro-carbon attenuation (37 percent of the attenuated mass), followed by ferrogenesis (23 percent), sorption (21 percent), nitrate reduction (16 percent), and methan-ogenesis (< 4 percent). Model results were particularly sensitive to the NAPL release rate, the initial Fe(III) concentration, hydrocarbon utilization rates, initial condition for the anaerobic microbial populations, and dispersivity. Results of this study have helped to confirm the validation of SEAM3D for simulating the transport and attenuation of petroleum hydrocarbon compounds in groundwater. The results of the SEAM3D validation for the NATS are documented in Brauner and Widdowson (accepted for publication). Validation of MT3DMS for the NATS is
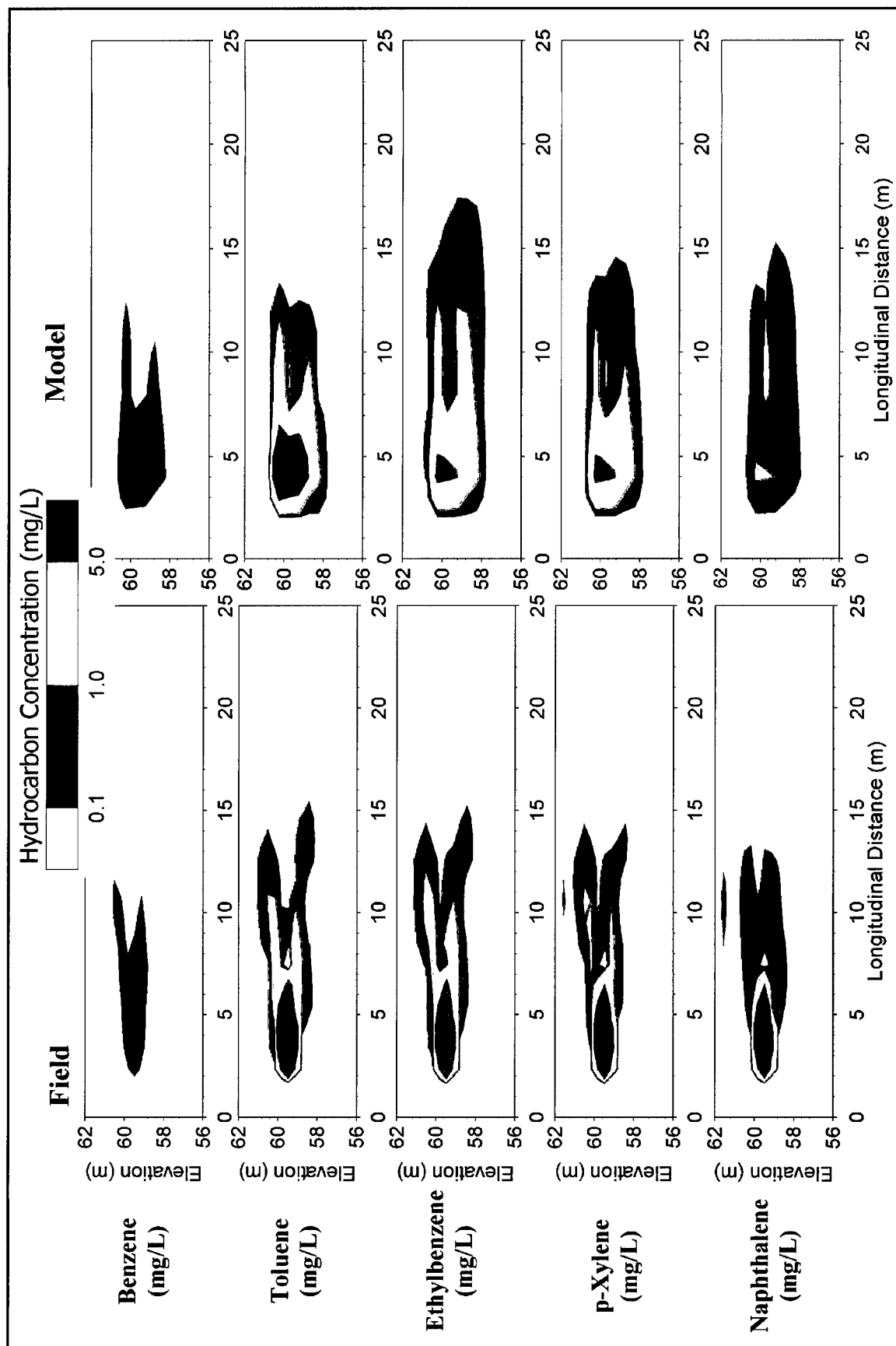
Figure 2. Comparison of field-measured BTEX and naphthalene concentrations with model simulations for the single porosity model along a vertical cross section 4 m west of the source center line for t = 5 months
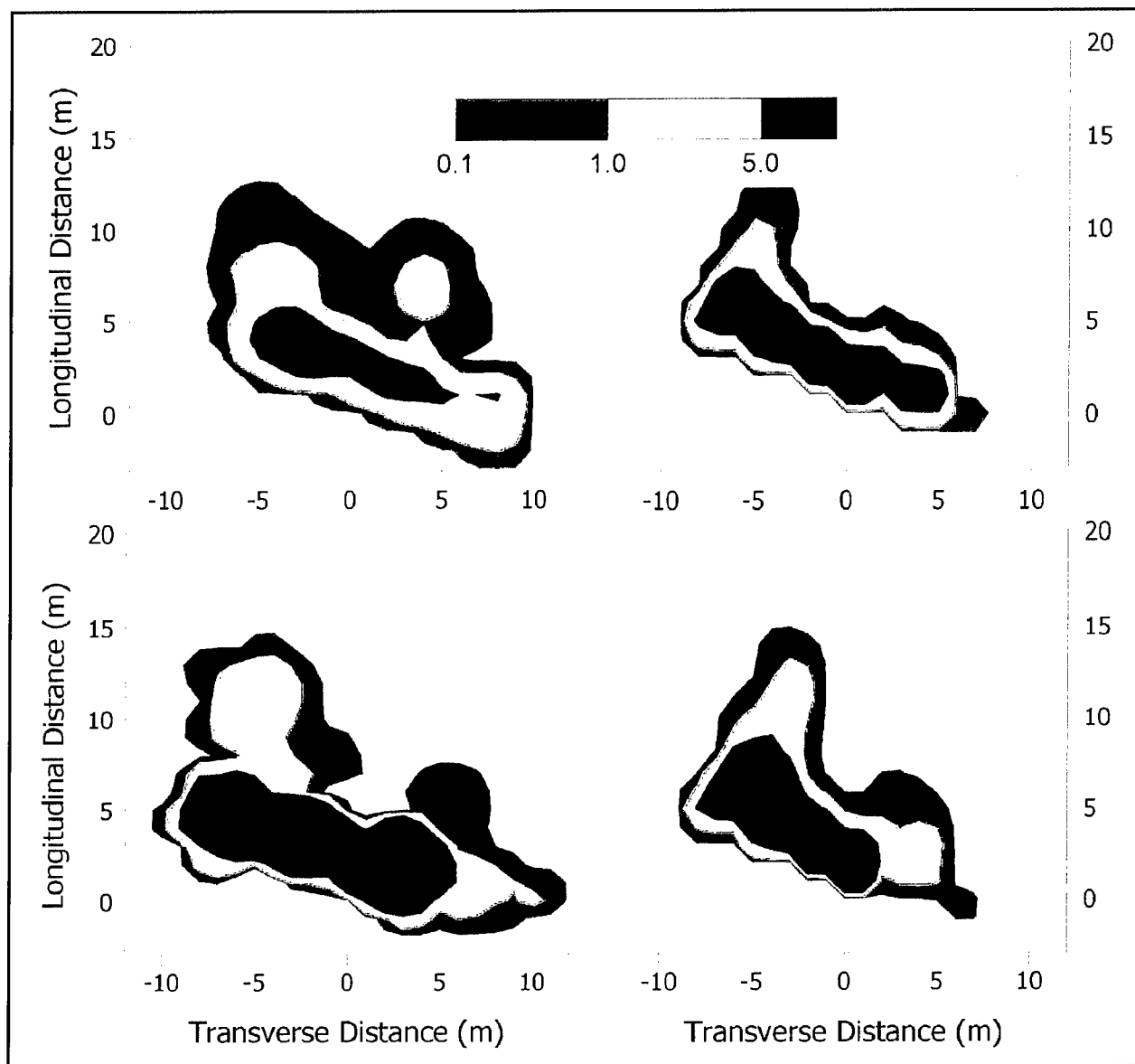
Figure 3. Comparison of field-measured toluene concentrations (left) with model-simulated toluene concentrations (right) for a horizontal cross section at z = 60 m at t = 5 months (top) and 9 months (bottom)

documented in Julian et al. (in review). Additionally, the transport scheme in MT3DMS is documented and verified in Zheng, Wang, and Dortch (in review).

NAS Pensacola

Model validation was confirmed at NAS Pensacola Wastewater Treatment Plant (WWTP), where natural attenuation of chlorinated ethene compounds has been monitored and documented. Past disposal of industrial wastewater into an unlined holding pond led to contamination of the surficial aquifer underlying the WWTP. Trichloroethene is present with a concentration range of 2.5 mg/L to

nondetect along the 91-m (300-ft) flow path. Chlorinated daughter products are also present, including cis-DCE and VC. Groundwater monitoring data demonstrate the removal of all three chlorinated ethenes in wells immediately up-gradient of Pensacola Bay.

Marine and fluvial terrace sediments underlie the WWTP, consisting primarily of fine to medium sands to a depth of 12 m (40 ft) below land surface. The unconfined aquifer is underlain by a 6-m- (20-ft-) thick confining layer. An upward hydraulic gradient prevents downward transport. Local groundwater flow is to the west, which results in discharge to the adjacent Pensacola Bay, 91 m (300 ft) to the west of the source area. Geochemical data indicate that iron-reducing and sulfate-reducing conditions are the primary redox processes in the aquifer but that methanogenesis is also active.

The modeling objective was to calibrate the model to contaminant concentration data (TCE, cis-DCE, and VC) and geochemical parameters along the main transect of the plume. A flow and transport model of the NAS Pensacola WWTP site was developed to simulate the transport and attenuation of TCE, cis-DCE, and VC using MODFLOW and SEAM3D, respectively. Reduction in the source concentration of TCE due to chemical oxidation treatment is being simulated using the calibrated site model as a verification step.

Figures 4 and 5 show TCE and cis-DCE with VC concentration, respectively, versus distance along the plume center line for both the measured and simulated cases. Results of the calibrated model show a stable TCE plume with an accurate representation of the down-gradient peaks of cis-DCE and VC. The site model using SEAM3D will be used to simulate the residual TCE plume following source remediation using chemical oxidation. SEAM3D will be used to determine the time required for the TCE plume to restabilize following chemical oxidation of the source and the time to reach remediation goals under a monitored natural attenuation program. The final results of the NAS Pensacola validation will be documented in a paper.

Interface with GMS

A revised SEAM3D interface to GMS has been developed that will incorporate the Reductive Dechlorination and Cometabolism Packages. In addition, the "define species" menu has been revised to incorporate chlorinated ethenes and methanotrophs. The NAPL Dissolution Package input was also revised to account for solvents derived from a DNAPL.

Recommendations

Recommendations for further validation work and improvements to the SEAM3D code include the following:
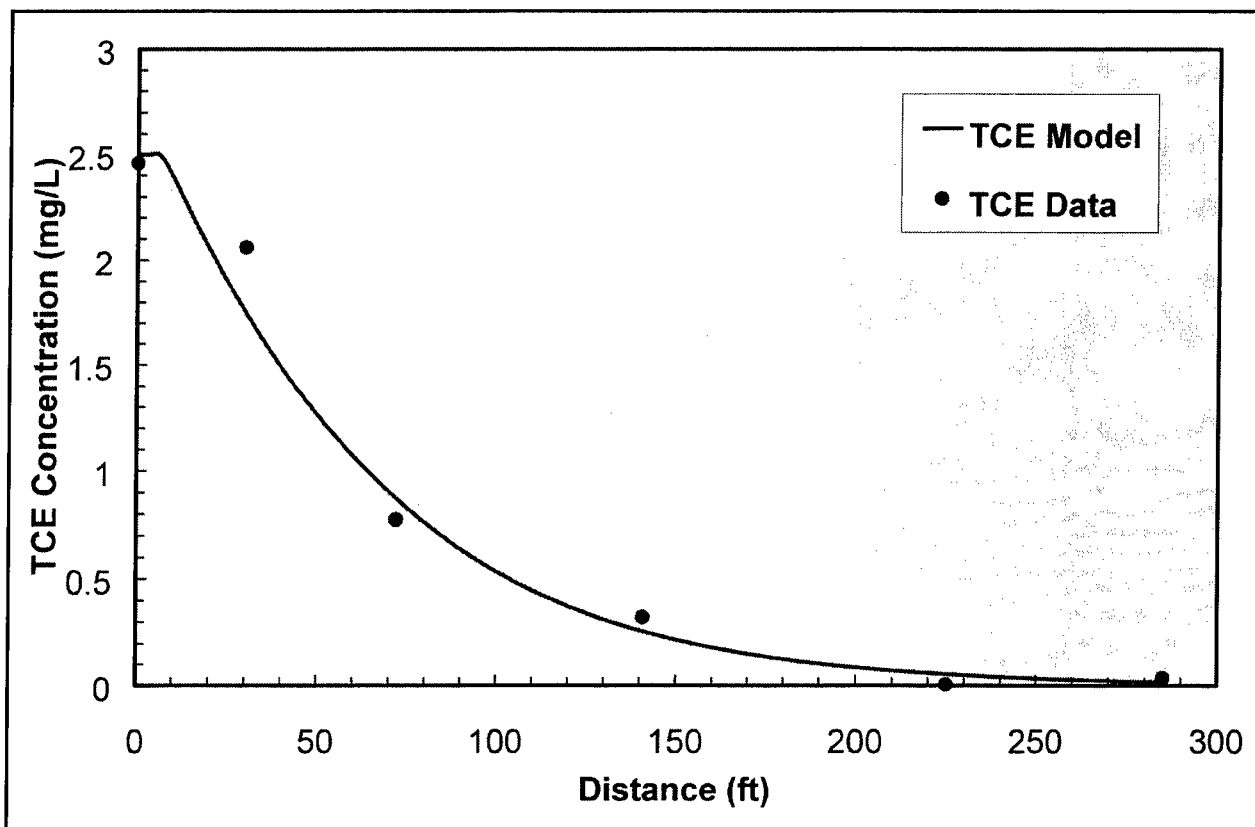
Figure 4. Measured and simulated (SEAM3D-RDP) concentration of TCE along the main plume transect showing a steady-state distribution for each solute prior to chemical oxidation treatment of source area (to convert distance into meters, multiply by 0.3048)

    a. Validate the SEAM3D Cometabolism Package using field data from a pilot test or full-scale bioremediation project.

    b. Validate the SEAM3D Reductive Dechlorination Package at a field site where a biostimulant (e.g., vegetable oil or formate) has been injected in the source area to enhance reductive dechlorination of PCE/TCE in the source area.

    c. Develop and test a SEAM3D Bioaugmentation Package and validate at a controlled pilot test or full-scale field demonstration.

    d. Develop and test a SEAM3D Package for modeling with inhibition kinetics, which could be validated at the Laurel Bay, SC, U.S. Geological Survey study site.
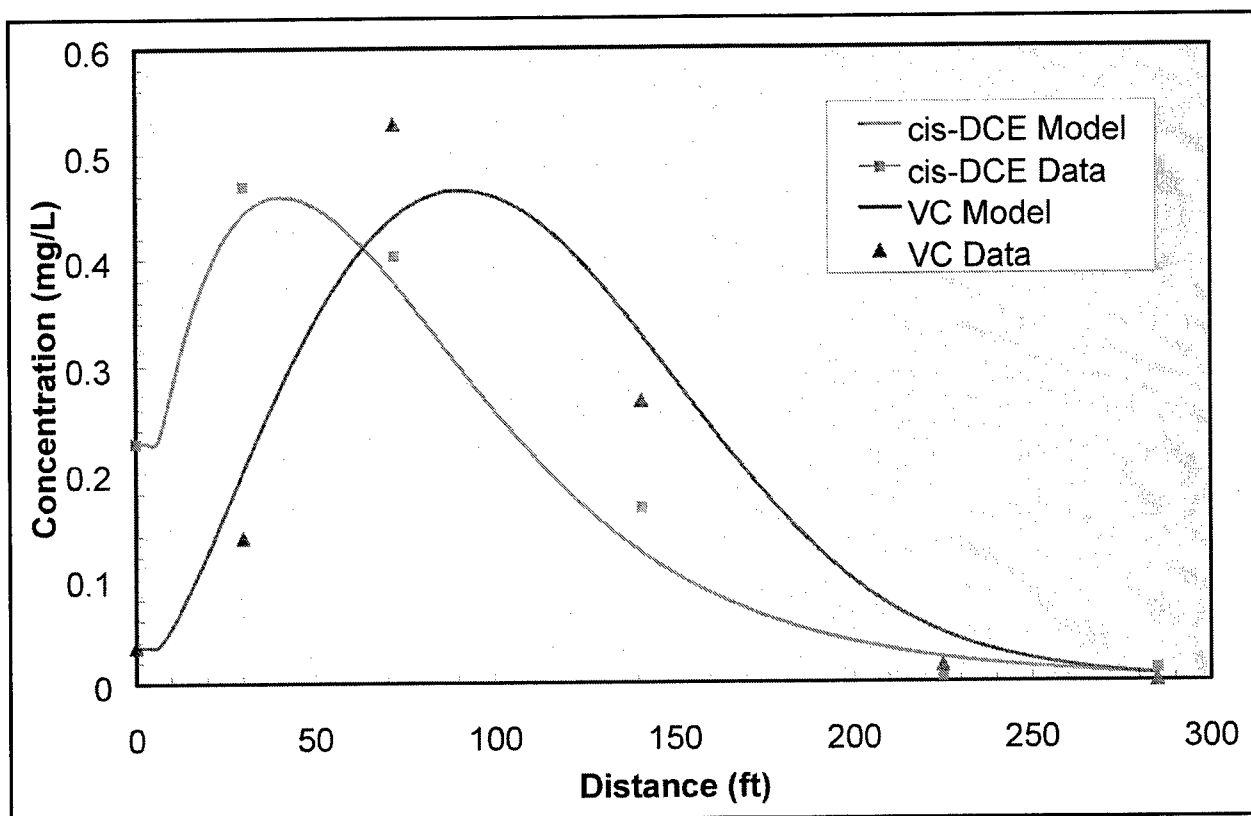
Figure 5.   Measured and simulated (SEAM3D-RDP) concentration of cis-DCE and VC along the main plume transect showing a steady-state distribution for each solute prior to chemical oxidation treatment of source area (to convert distance into meters, multiply by 0.3048)

3 UTCHEM

Model Description

UTCHEM is a three-dimensional, finite difference, multiphase flow, multi-component, reactive transport model. This is a mature, multipurpose model with too many facets to detail here. Major features are summarized, followed by discussions of the enhancements made during the current project, benchmarking and validation of the model, development of the GMS interface, and the preparation of documentation and training materials.

The key UTCHEM features include the following:

a. Multidimensional: fully three-, two-, or one-dimensional or nondimensional (batch) in Cartesian, radial, or stretched vertical coordinate systems.

b. Multiphase flow: water, oil, air, microemulsion; the aqueous phase is either water or microemulsion depending on local surfactant concentration.

c. Multicomponent reactive transport: any number of user-defined, organic and/or inorganic contaminants, microbes, or additives (e.g., reactants, nutrients, etc.).

d. Constitutive models for relative permeability–saturation–capillary pressure (k_r-S-P_C) relations: Brooks-Corey Imbibition and First-drainage models.

e. Hysteretic models (Parker-Lenhard) for capillary pressure and relative permeability in water-wet media and for two-phase flow (oil-water) in mixed-wet media.

f. Liquid phase densities functions of composition.

g. Liquid phase viscocities functions of composition, including viscosity-enhancing polymers with non-Newtonian rheology.

h. Full tensor coefficients for dispersivity and molecular diffusion in each phase.

i. Microemulsion phase behavior: empirical models dependent on complex function of surfactant/cosolvent, oil composition, water chemistry.

j. Surfactant/cosolvent effects on constitutive models, i.e., enhanced oil mobilization (versus dissolution) as a function of viscous and buoyancy forces (trapping number).

k. Partitioning interwell tracer tests (PITTs): characterization of oil saturations in the vadose or phreatic zones by assessing the relative transport of alcohols, varying in their hydrophobicity (preferential partitioning into any oil phase).

l. Wells: flexible module for any number of injection, withdrawal, or monitor wells, completed (or screened) in user-specified cells, in any orthogonal orientation.

m. Equilibrium or rate-limited mass transfer (dissolution) of NAPL components.

n. Equilibrium adsorption to aquifer solids (linear, Langmuir, or Freundlich isotherms); cation exchange.

o. Boundary conditions: impermeable by default; user may specify head and compositional conditions at two opposing boundaries; flow may be confined or unconfined.

p. Initial conditions: user may specify initial phase saturations, solute concentrations.

q. Zero-order, first-order (a common, empirical approach), and higher-order biogeochemical models accommodated.

r. Bioremediation package: highly flexible in terms of reaction pathways and kinetics (first-order and higher), microbial biomass (microcolony concept).

s. Geochemistry package: limited accommodation of user-defined, equilibrium reactions, e.g., speciation, precipitation–dissolution.

t. Heterogeneous media: parameters for flow and transport models can be assigned as homogeneous, stratified, or fully heterogeneous fields.

u. Dual porosity approximation of fractured media.

v. Heat transport (polythermal conditions) coupled to other properties (e.g., viscosity).

w. Implicit pressure explicit saturation (IMPES) type formulation; third-order-accurate finite-difference methods with total-variation-diminishing (TVD) flux limiter.

Detailed documentation and user information regarding all of these features are available (Reservoir Engineering Research Program 2000a, 2000b). The new GMS interface will expedite the preparation of input for most UTCHEM 9.0 features, particularly those relevant to environmental applications. The remaining features, for which a GMS interface is not developed, still can be used, but will require editing of the input file independent of the GMS.

UTCHEM employs a three-dimensional, block-centered, finite-difference scheme. The solution method is implicit in pressure and explicit in concentration

(an IMPES type method). Options for one- and two-point upstream and third-order spatial tessellation are available. A TVD flux limiter has been added to increase the stability and robustness (reducing overshoot and undershoot) of the second- and third-order methods. Of course, the third-order method gives the most accurate solution.

UTCHEM was developed originally in the late 1970's (Pope and Nelson 1978) as a design simulator for surfactant-polymer flooding in enhanced oil recovery. The model continued to evolve and improve in terms of both the processes described and numerical methods used. One of the essential requirements of a surfactant enhanced aquifer remediation (SEAR) design simulator is accurate and flexible treatment of microemulsion phase behavior, which is central to the treatment of other phenomena such as partitioning, interfacial tension, capillary pressure, capillary number, and microemulsion viscosity. Adaptation of the mature and successful modeling approach to enhanced oil recovery evident in UTCHEM was deemed a rational and cost-effective approach to the development of a SEAR simulator. Some modifications were required in the adaptation to environmental concerns, arising primarily from the focus on much lower oil saturations (subresidual) and very low concentrations of organic contaminants in the aqueous phase (parts per billion (ppb) level). These adaptations have been affected under efforts supported recently by the EPA and the current SERDP Project CU-1062. Two goals of the current project were to develop a graphical user interface within the GMS and to continue the evolution of UTCHEM as an advanced remediation simulator.

UTCHEM is a flexible, multifaceted model that would be useful in the design and evaluation of a variety of remediation technologies. However, the current effort is focused on surfactant and cosolvent flushing for NAPL cleanup. The validation process was accomplished by assessment of the revised model in application to several surfactant/cosolvent flushing experiments at the laboratory and field scales. Equally important was the thorough beta testing of the GMS interface as it developed. Several of these applications will serve as tutorials in the self-directed training of new UTCHEM-GMS users.

Model Enhancements

The enhancements to UTCHEM under SERDP CU-1062 have been achieved in three basic areas: (a) expanding model capabilities for environmental applications, particularly for SEAR-related processes, (b) developing a graphical user interface to improve ease of use, and (c) improving numerical methods. Each of these enhancement areas is discussed more thoroughly in this section. Applications demonstrating these enhancements are presented in the "Model Validation" section.

Several enhancements to UTCHEM are either "invisible" to the user or involve processes that could be useful in the design/evaluation of multiple remediation technologies. The former would include the shift to dynamic memory allocation and other changes in numerical methods to take advantage of FORTRAN 90 features. The dynamic memory allocation allows array sizes to adjust

automatically to match the input, thereby avoiding the need to redimension the arrays explicitly and recompile the entire model for each application. Enhancements that could benefit the design and evaluation of multiple remediation technologies include the following:

    a.   The addition of Freundlich and Langmuir adsorption isotherms.

    b.   Adaptation of input and output file formats for GMS compatibility.

    c.   Expansion of boundary condition options.

Independent efforts, concurrent with CU-1062, also have contributed to UTCHEM enhancement, which are incorporated in UTCHEM-GMS (version 9.0). These enhancements supported by DOE, the petroleum industry, or others corroborate the broad appeal and utility of this simulator.

The numerous enhancements to UTCHEM necessitated an update to the documentation (Reservoir Engineering Research Program 2000a, 2000b). The revised user's guide includes descriptions of new input parameters and formats. The technical documentation, which is a thorough suite of brief reviews of underlying theory and mathematical descriptions of key UTCHEM features, is revised to reflect the more fundamental changes. Guidance is offered as to parameter determination and typical values and ranges for select parameters, with an emphasis on those unique to SEAR. The revised user's guide and technical documentation accompany any release of the GMS interface and currently are available in PDF format from the UTCHEM page at the GMS Web site, http://chl.wes.army.mil/software/gms/docs.htp.

Validation of the model and testing of the GMS interface will be documented in separate reports and/or integrated into the GMS documentation as tutorials. The reports will include discussion of the rationale for parameter selection, particularly for parameters unique to surfactant/cosolvent flush simulation. Finally, the GMS documentation for UTCHEM, to accompany each public release, will incorporate portions of each of these documents, with an emphasis on the graphical interface features.

Enhancements to surfactant/cosolvent flushing simulation

UTCHEM is already well established as one of the most comprehensive models available for SEAR design and evaluation. In addition to the GMS interface, there are several SEAR-related enhancements including the following:

    a.   Nonequilibrium mass transfer to the micellar phase.

    b.   Hysteretic constitutive models (relative permeability-capillary pressure).

    c.   Constitutive models for mixed-wet media (for oil-water systems).

All of these enhancements were completed and tested in Fiscal Year (FY) 1999. The GMS interface will serve only to accelerate the acceptance of both UTCHEM and surfactant/cosolvent-flushing technologies by raising the level of understanding in the user community and providing the requisite tools to design and implement SEAR. UTCHEM also provides a tool for the forward modeling

assessment of PITTs for estimating NAPL saturations prior to SEAR and in the subsequent assessment of its effectiveness.

Most experienced SEAR practitioners would concur that simulation is critical in the design and preinstallation evaluation phase and is not a peripheral or academic exercise. At the very least, design/evaluation simulation is the best approach for the quantitative integration of multiple, coupled, physical and chemical processes that can affect SEAR performance. There is no alternative for the integration of complex calculations of compositional effects on such factors as phase equilibria or constitutive models for flow in a heterogeneous medium.

Enhancements to the bioremediation features of UTCHEM

Natural or engineered microbial processes can be described or designed using the highly flexible, input-controlled definition of reaction pathways and mechanisms available in UTCHEM. These features may be useful in the evaluation of the post-SEAR cleanup of any residual NAPL or contaminated groundwater, as well as any unrecovered surfactant/cosolvent.

The monitored natural attenuation of organic contaminants can be an attractive, cost-effective cleanup alternative where tenable. The attenuation of certain recalcitrant contaminants, such as solvents and explosives, can involve slow, subtle processes under the predominantly aerobic, oligotrophic conditions present in most aquifers. Thus, long-term fate and transport predictions become indispensable in the evaluation of monitored natural attenuation efficacy. Groundwater modeling provides the only rigorous approach to consider and evaluate monitored natural attenuation alternatives and assess exposure risk.

UTCHEM has been made more readily applicable to the simulation of natural attenuation and the design of engineered bioremediation. The major enhancements to UTCHEM bioreaction features under CU-1062 included adding the following:

a. A first-order kinetic model alternative that accommodates product generation.

b. A microcolony-type, bioreaction kinetics model.

c. A built-in transport time-step control, based on dimensionless parameters conditioned upon the relative influence of reaction kinetics versus diffusive mass transfer on bioreaction rates.

d. Option to consider the coupled effect of microbial biofouling (growth) on flow.

e. Option to specify initial conditions for aqueous phase transport.

These features build on the bioreaction module developed for EPA (UTCHEM version 6.0).

Bioreaction kinetics can be influenced by solute mass transfer between pore water and biomass. The error associated with neglecting mass transfer limitations

to biomass is a function of both the rate of biodegradation and the rate of mass transfer. The rate of biodegradation also influences the operator splitting error (a small error inherent in the solution scheme), so that it is difficult to distinguish between errors introduced from neglecting mass transfer and errors introduced by operator splitting. To resolve this difficulty, the following tasks were completed: (a) the dependence of the operator splitting error on the flow rate and biodegradation rate has been established in terms of dimensionless numbers, and confirmed with a large number of one-dimensional simulations; and (b) UTCHEM will automatically select the appropriate biodegradation kinetics time-step, independent of the advection-dispersion time-step. The Damköhler and Peclet dimensionless numbers are used to determine when diffusive mass transfer to/from biomass is significant. Generally, a Damköhler number below 0.1 indicates that mass transfer is not limiting the bioreactions. The automatic time-step feature greatly reduces simulation times by solving the biodegradation equations only as often as necessary to keep the operator splitting error beneath a given threshold. This approach also allows better comparisons between runs with and without mass transfer.

Biofouling of porous media by overstimulating microbial growth is a phenomenon to be avoided in bioremediation design. The biofouling algorithm incorporated into UTCHEM is based on porosity loss due to a constrained biomass growth. The altered permeability is expressed using a Kozeny-Carmen equation. Biomass growth is limited to occupying up to 90 percent of the available pore space. Biomass transport and adsorption also have been added to UTCHEM with the adsorption modeled as linear partitioning.

UTCHEM has been applied to a variety of bioreaction problems, including evaluation of explosives reactions at the Louisiana Army Ammunition Plant[1] and bioremediation of post-SEAR, residual solvent and surfactant at the Hill AFB pilot demonstration site (de Blanc 1998). One or more of these will serve as tutorials for the GMS documentation.

Model Validation

A variety of conditions have been simulated with UTCHEM 9.0 to validate the model and to evaluate/test its GMS interface. The immediate goal was to ferret out as early as possible the coding errors that are inevitable in models as complex as UTCHEM and GMS. Validation of the more unique and advanced process models within UTCHEM, most of which are not amenable to exact (analytical) solution, requires model application to a variety of well-controlled and/or well-monitored experiments at laboratory and field scales. Repeated success enhances confidence in the model, while unsatisfactory results stimulate either improvements to the model or its abandonment by the user community. This natural selection phenomenon in model evolution is driven by the same market pressures at work in the remediation business in which the better, faster, cheaper technologies survive.

---

[1]   C. J. McGrath and M. Zakikhani. (1998). "Numerical modeling of the natural attenuation of explosives," presentation at 3rd Tri-Service Environmental Technology Workshop, San Diego, CA, 18-20 August 1998.

UTCHEM has been demonstrated, benchmarked, and validated in application to a variety of scenarios, including (a) surfactant flushing for the removal of residual DNAPL at Hill AFB, Utah; (b) PITTs at Hill AFB; (c) ethanol flushing to recover residual benzene from packed columns, (d) an alcohol flushing demonstration for DNAPL removal at Dover AFB, and (e) post-SEAR bioremediation at Hill AFB. Each of these UTCHEM applications was supported, at least in part, under SERDP CU-1062, while the experimental/field data were collected for other projects.

Surfactant flushing, Hill AFB

UTCHEM simulations were indispensable in the design of the highly successful surfactant flush demonstration at Hill AFB, Utah (Brown et al. 1996). These simulations have been revised to reflect the flow conditions actually employed (versus designed) and with an updated format for UTCHEM and GMS (Martino, in preparation). The purpose was to provide a well-documented, three-dimensional example of UTCHEM application to SEAR to be included with the code documentation. This history matching exercise generally improved the agreement between predicted and observed data. Most model parameters, such as those related to phase properties, constitutive models, hydrogeology, and the numerical grid were unchanged.

The PITT represents an innovative method to estimate in situ NAPL saturations and possibly the distribution (Figure 6). Saturations are estimated based on the relative retardation of tracers of contrasting partitioning coefficient K_p, with more hydrophilic tracers being effectively conservative (e.g., isopropyl alcohol (IPA), $K_p = 0$), while relatively hydrophobic tracers (e.g., 1-heptanol, $K_p = 140.5$; pentanol, $K_p = 3.9$) are more severely retarded in the presence of NAPL. PITTs were used to assess the initial DNAPL saturations at the Hill site (Jin 1995; Jin et al. 1997; Duke Engineering and Services 1998). A second ("intermediate") PITT was conducted after a brief initial surfactant flush (Phase I). A third ("final") PITT was performed after a second, more substantial surfactant flush (Phase II). The similarity in arrival times for IPA, pentanol, and heptanol in the final PITT suggests the absence of significant NAPL saturation.

UTCHEM can simulate the effects of adding water-soluble polymers or forming foam to further enhance the effectiveness of SEAR. The addition of a water-soluble, food-grade polymer to enhance viscosity or air injection to induce foaming increases the sweep efficiency of the flushing solution. Greater sweep efficiency enhances the recovery of NAPL that otherwise might be bypassed and left behind in lenses of lower permeability. This capability of UTCHEM has been demonstrated for creosote removal (Wu et al. 2000).

Ethanol flushing

Alcohol flushing for the recovery of residual NAPL from porous media has been documented in the laboratory and under controlled field demonstrations.
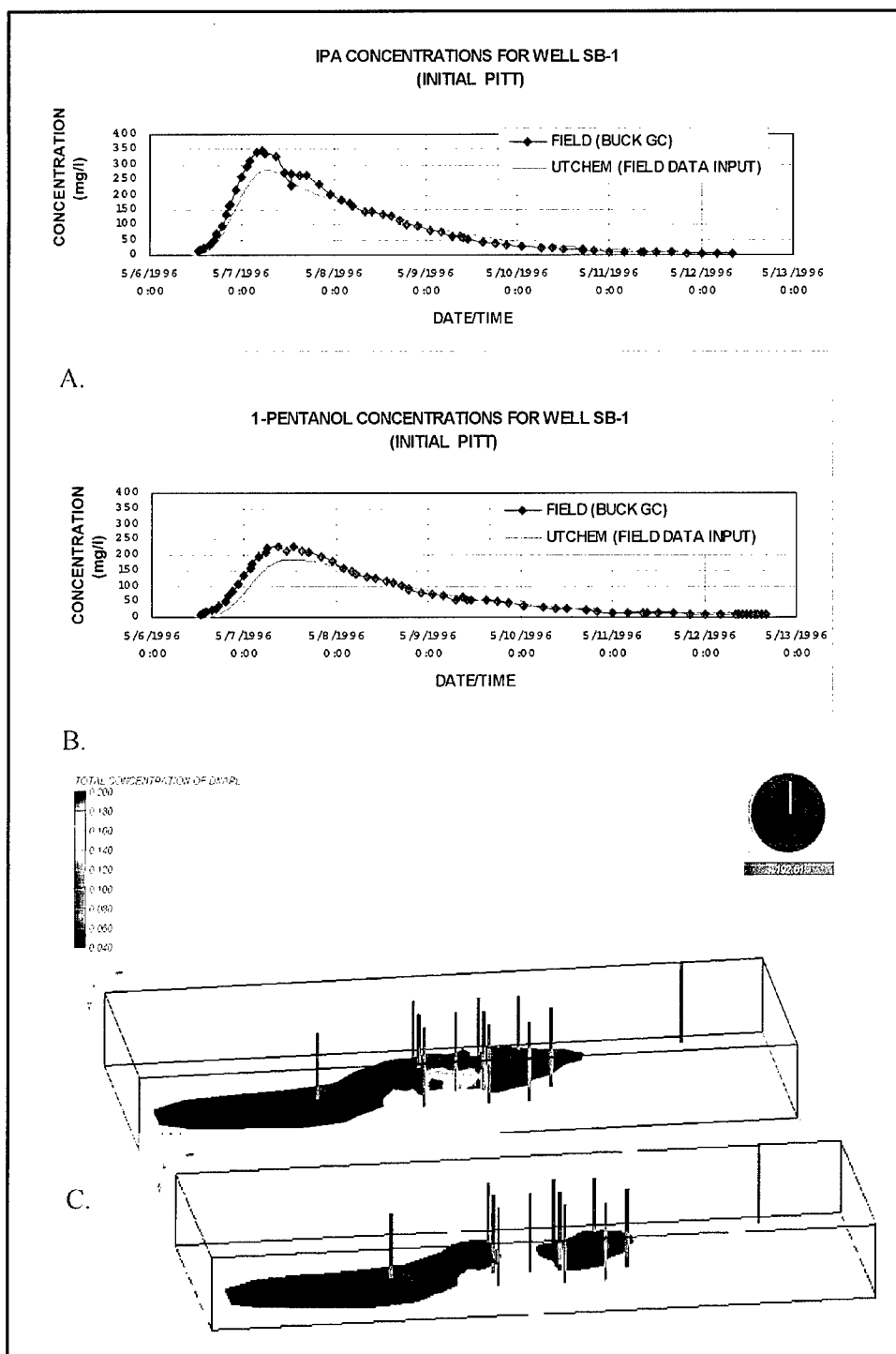
Figure 6. UTCHEM simulations of PITT and SEAR at Hill AFB OU-2:
(A) Predicted versus observed PITT for 2-propanol breakthrough at
well SB-1; (B) Predicted versus observed PITT for 1-pentanol; note
that breakthrough of the more lipophilic pentanol (K_p = 3.9) is retarded
slightly relative to IPA (K_p = 0); and (C) Simulated oil saturations
before and after SEAR

Though the procedure is technically feasible, issues of efficiency and cost remain to be addressed. Lower molecular weight alcohols such as methanol and ethanol serve to enhance the solubility of NAPL contaminants in aqueous solution, thus the term cosolvent.

UTCHEM has been applied to a series of column experiments designed to elucidate critical flow and transport phenomena involved in ethanol flushing for residual NAPL (benzene) recovery (McGrath, in preparation). Several concentrations of ethanol in aqueous solution were flushed through a 40-cm column of very fine sand (~0.10 ± 0.05 mm) containing residual benzene saturation (residual saturation S_{ro} = 0.20). At low ethanol concentration (0.50 volume fraction (VF)), benzene dissolution was enhanced, but no mobilization was evident. At 0.67 VF ethanol, benzene solubility into the aqueous phase was enhanced as expected and a small amount of benzene was mobilized as an unstable macroemulsion (Figure 7). At 0.75 VF ethanol, benzene mobilization was sufficiently effective to form a distinct oil bank in advance of the ethanol front. Magnetic resonance imaging (MRI), used to monitor the advance of the fluids through the columns, revealed some interesting displacement phenomena (Figure 7b). The effluent was analyzed by pulse nuclear magnetic resonance (NMR).

Simulation of the alcohol flush experiments with UTCHEM (Figure 7a, c) reproduced most of the flow phenomena that this model could be reasonably expected to capture, such as enhanced dissolution, NAPL mobilization, the buoyant override of the alcohol. Effluent flow rates and bulk concentrations are reproduced quite well. However, observed phenomena such as viscous fingering and the formation of macroemulsions are random or nonthermodynamic phenomena that are too poorly understood to predict/model accurately. The use of UTCHEM for alcohol flushing requires a few ad hoc redefinitions of model parameters that are intended for surfactant flushing. For example, the requisite definition of the critical micelle concentration (CMC) has no meaning in alcohol flushing. If the alcohol is modeled essentially as a poor surfactant, as has been done here, a "pseudo-CMC" may be redefined by the user as the alcohol concentration above which the aqueous solubility of NAPL constituents is substantially enhanced. Such compromises are not unusual when pushing the limits of a still evolving code such as UTCHEM. These compromises are not problematic as long as the limitations are understood. However, a more general cosolvent model that captures the full range of concentration-dependent partitioning could be developed for UTCHEM or any alcohol flush simulator. Additionally, UTCHEM assumes negligible cosolvent (surfactant) solubility in the oil phase (i.e., plait point is set at the oil apex), which is generally not the case with low molecular weight alcohols and definitely not the case for larger, more hydrophobic alcohols. Again, this appears to be a minor limitation, but a more general liquid-liquid equilibria model would be preferable.

The UTCHEM simulator continues to be evaluated further in application to the cosolvent flush demonstration recently completed at Dover AFB. The Dover demonstration involves the controlled release of a known amount of DNAPL (Figure 8) within a laterally contained section of natural, mildly heterogeneous, sandy aquifer. An extensive, high-resolution (spatially and temporally),
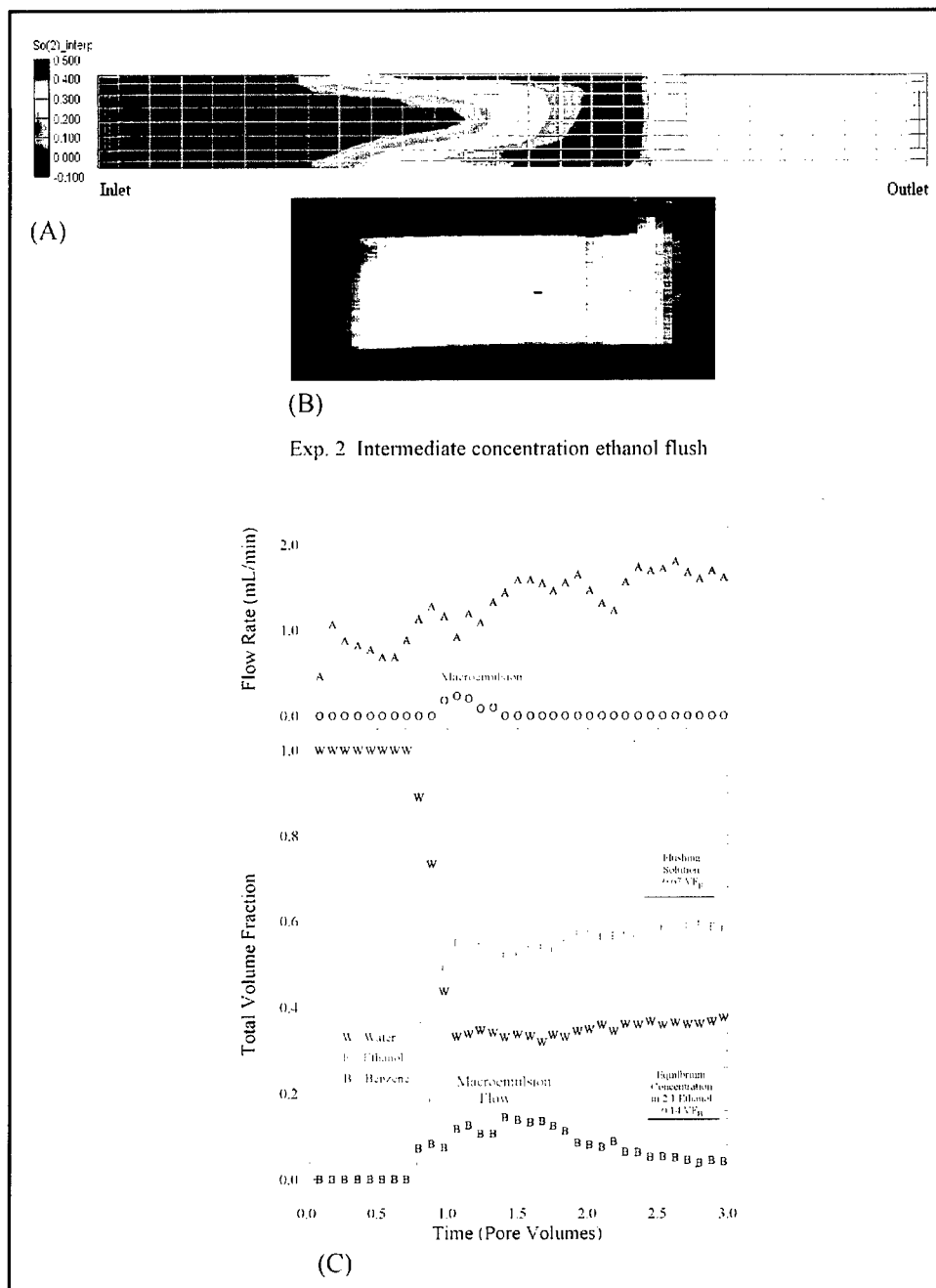
Figure 7. Cosolvent flush (0.67 VF ethanol) of NAPL (benzene) removal from a
horizontal packed column: (A) UTCHEM-predicted oil saturation
distribution at 0.5 pore volume (PV) flush. (B) MRI of column section at
approximately 0.5 PV flush; note the near-vertical advanced front,
followed by an axial, convex-forward front, similar to the predicted
phenomena. (C) UTCHEM-predicted (dashed lines) versus observed
(points) effluent flow rate (upper plot) and total composition deter-
mined by pulse NMR
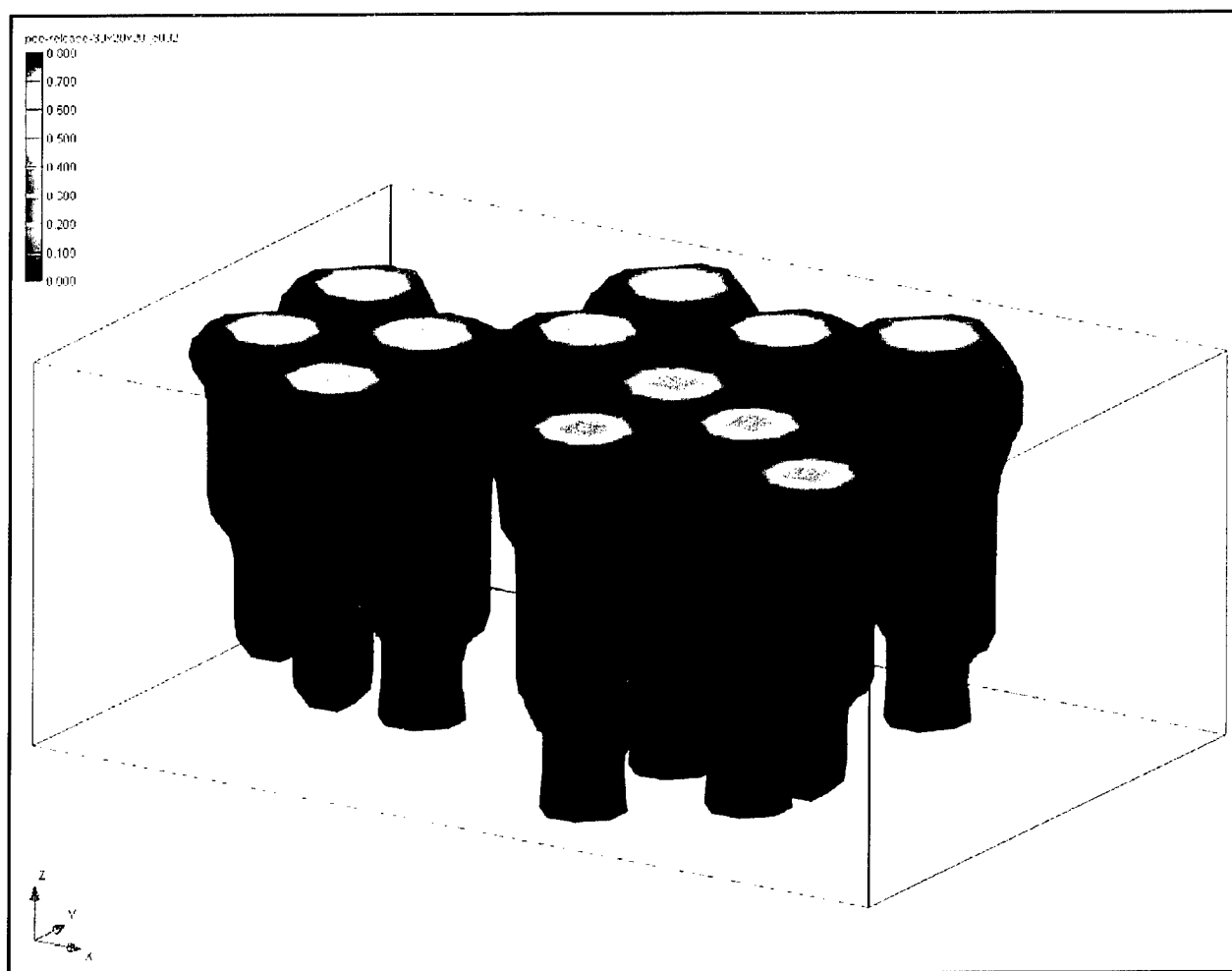
Figure 8.   UTCHEM simulation of PCE release prior to the cosolvent flush demonstration at the Dover AFB test cell. A total of 92 L of PCE was introduced via 12 wells (eight 9-L and four 5-L injections) within the 4.6- by 3.0-m test cell

three-dimensional data set for both preflush and postflush PITTs as well as the alcohol flush are providing the benchmark against which to evaluate UTCHEM as an alcohol flush simulator.

Post-SEAR bioremediation at Hill AFB

The bioremediation features of UTCHEM have been demonstrated in the design simulation of cometabolic bioremediation of postsurfactant flush residuals after the SEAR demonstration at Site O-2, Hill AFB, Utah (de Blanc 1998). The intent was to demonstrate these new model features and verify that they are fully functional and predict reasonable results. Injection of dissolved methane and oxygen (peroxide) was simulated to assess the cometabolic biodegradation of the TCE by indigenous methanotrophic microorganisms. Initial quantities of TCE included approximately 5 L of residual TCE (of the ~1,890 L present initially) and dissolved TCE leaching into the SEAR-treated zone from adjacent untreated areas. Dissolved oxygen in the aquifer was depleted initially due to heterotrophic

degradation of residual surfactant. The TCE is presumed to have suppressed the indigenous methanotroph population. Three injection wells and three recovery wells were used to establish a plug flow. Pump-and-treat was considered as a baseline scenario for which oxygen-saturated water was injected for 200 days. Much of the surfactant was removed, but TCE remained high due to continued dissolution of remaining NAPL traces and/or diffusion from low-permeability zones. Injection of methane-saturated (~20 mg/L), highly oxygenated (300 mg/L as hydrogen peroxide) water rejuvenated the methanotrophs, particularly near the injection well, where TCE concentrations were reduced due to the cometabolic biodegradation. Unfortunately, the methane was consumed quickly, precluding significant penetration into the aquifer, compared to a nonreactive tracer. The surfactant concentrations were also lower than those for the pump-and-treat scenario due to the higher oxygen influx. Although cost savings over pump-and-treat could be realized by this methane-peroxide approach, performance might be enhanced still further by considering alternative scenarios such as groundwater reinjection and cycled injection of methane and peroxide. This simple example demonstrates one of the advantages of modeling during the design phase to screen viable alternatives for the most promising.

GMS Implementation

A three-phase approach was adopted for the development of the GMS interface to UTCHEM, compatible with the comprehensive but modular structure of the model. Phase 1, completed early in FY 99, yielded an interface to the grid module only. The Phase 2 release (FY 00) included an interface to the essential input/output variables for surfactant and/or cosolvent flushing. The third and final phase (to be released in 2001) includes development of the interface to the partitioning interwell tracer features and the comprehensive and flexible bioremediation package.

The first UTCHEM-GMS Workshop was held on 16-18 November 1998 at the University of Texas at Austin. This workshop provided an opportunity for the interface developers, UTCHEM users (new and old), and SEAR practitioners to exchange ideas regarding the model and interface. Over 25 groundwater professionals from DoD, DOE, EPA, academia, and private consulting firms were invited to participate. Both the numerical aspects of UTCHEM and the biogeochemical processes involved in SEAR and other cleanup-related features of UTCHEM were discussed. Several model applications were presented, including SEAR, alcohol flushing, and natural attenuation of explosives, followed by a half-day GMS training session.

All releases of UTCHEM-GMS will be accompanied by the tutorials described in this section and additional tutorials as they become available. Tutorials expedite the learning of a new code by example and are particularly useful when learning comprehensive simulators such as UTCHEM. These tutorials are designed to lead the UTCHEM and/or GMS novice through applications, introducing additional features with each tutorial.

Tutorial-1 (T-01)

The first tutorial simulates a PCE spill in a simple, structured heterogeneous media (Figure 9). This tutorial reproduces the familiar DNAPL experiments of Kueper (1989) familiar to most investigators of DNAPL flow phenomena. This tutorial demonstrates the following:

a. Setting up a uniform numerical grid.

b. Assigning heterogeneous media properties for multiphase flow.

c. Definition of a simple GMS map overlay (the media interfaces).

The tutorial also demonstrates the numerical stability of UTCHEM. Figure 9 shows the PCE saturation predicted by UTCHEM at 310 sec after the initiation of PCE release.

Tutorial-2 (T-02)

The second tutorial simulates a PCE spill and redistribution followed by a long cleanup by pump-and-treat (Figure 10). A steady release of 28.32 m^3 (1,000 ft^3) of PCE near the surface of a horizontally stratified, sandy medium is
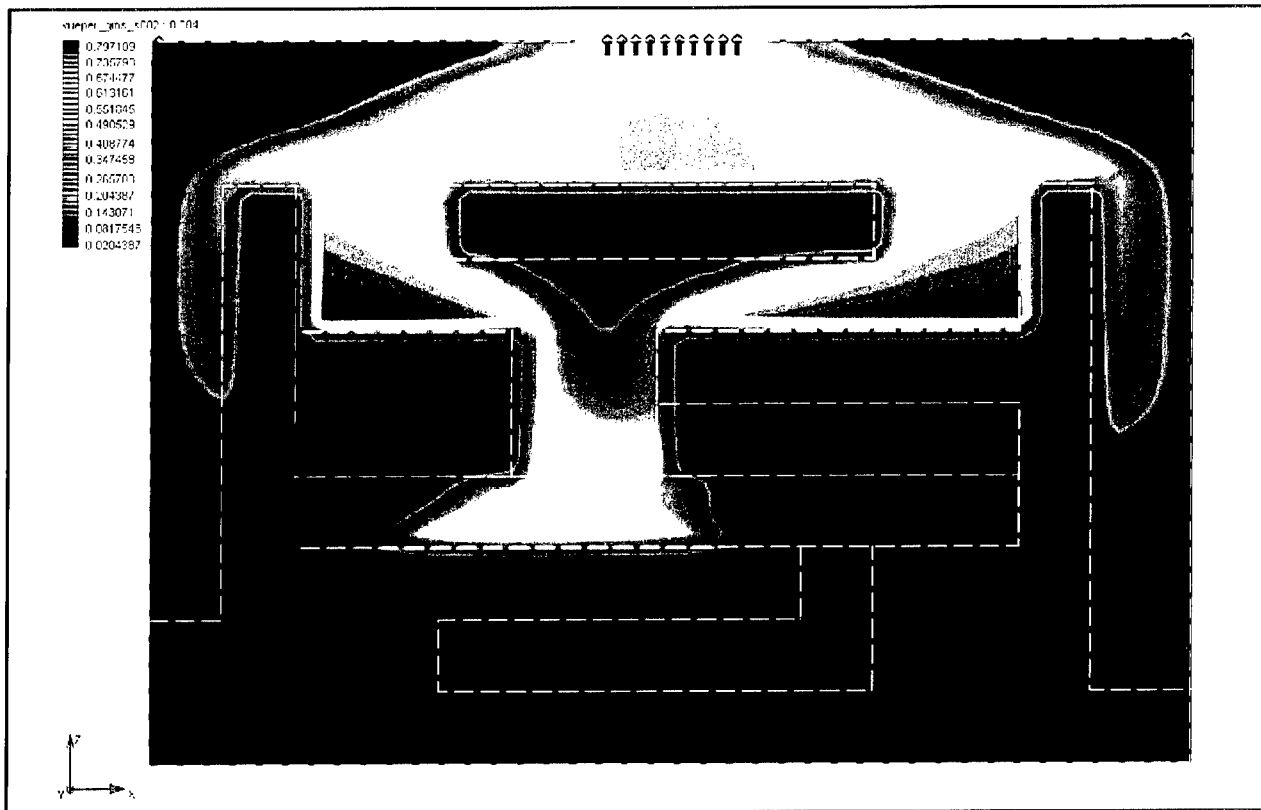
Figure 9. UTCHEM simulation of DNAPL (PCE) flow through heterogeneous media for Tutorial-1. Media boundaries are outlined by dashed lines. PCE was injected at the center top and allowed to flow for 310 sec (5.17 min). This GMS tutorial based on experiments by Kueper (1989) demonstrates the stability of UTCHEM in heterogeneous media
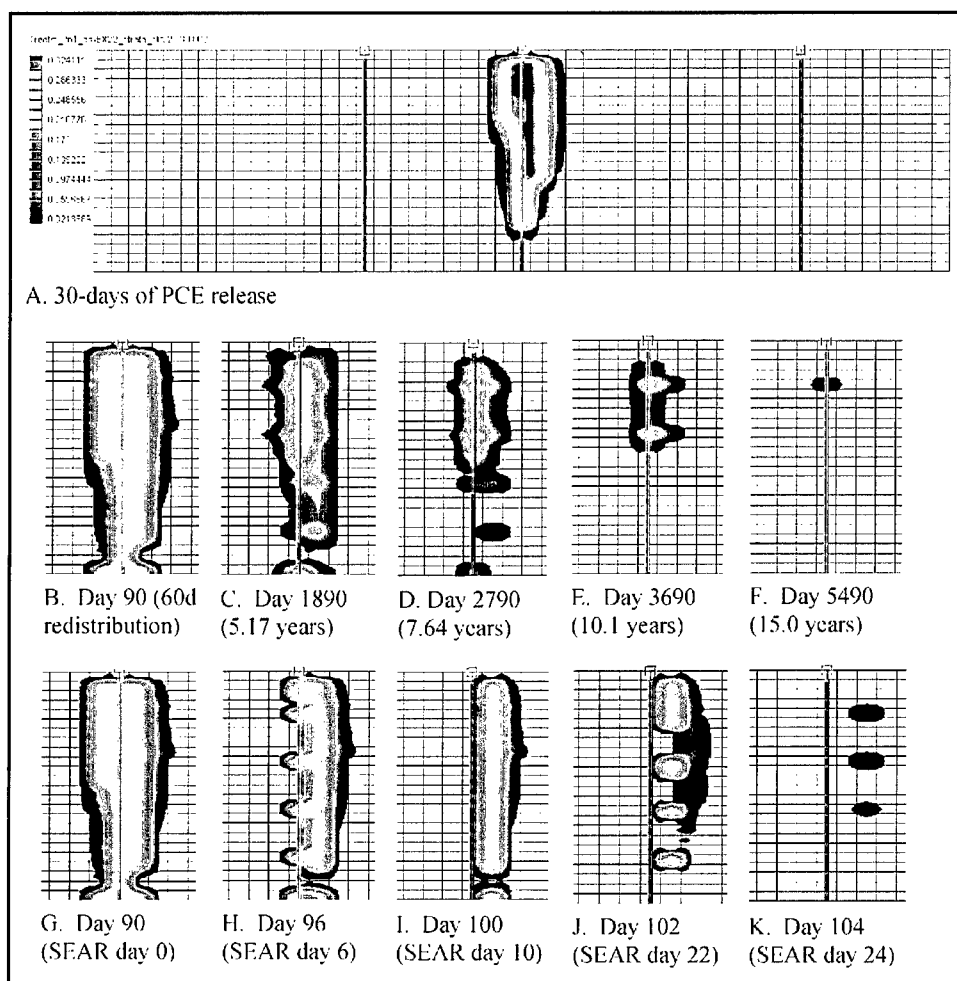
Figure 10. UTCHEM simulations for UTCHEM-GMS Tutorial-2 (water flush) and Tutorial-3 (surfactant flush), based upon the Borden SEAR demonstration. Images are DNAPL saturations (PCE) using a uniform scale. (A) Distribution after 30 days of PCE release (0.943 m³/day (33.3 ft³/day)); the central withdrawal well is flanked by two injection wells; regional flow gradient is left to right. (B and G) Distribution after 60 days of redistribution. (B-F) Time series of water flush, analogous to a pump-and-treat scenario; PCE is dissolved after ~15 years. (G-K) Time series of surfactant flush; removal is completed in approximately 25 days. Note that surfactant from the left well reaches the recovery well on day 94, while surfactant from the right well (further away and down gradient) does not break through until day 102, thus the asymmetry and delay beyond 10 days of surfactant flush

simulated. The PCE is allowed to redistribute for 60 days within a moderate regional gradient, reaching the aquifer base to form a small pool. DNAPL saturations are up to about 0.27 at day 90. A pump-and-treat scheme is imposed using one fully penetrating recovery well beneath the spill location, flanked by two injection wells (at about 9 and 16 m (30 and 52 ft) away). The trapped DNAPL dissolves slowly, being most persistent in the four lower-permeability horizons and a basal pool. The PCE saturations reach zero by day 5600, i.e., 15 years of pump-and-treat.

Tutorial-3 (T-03)

The third tutorial builds upon T-02 by replacing the lengthy pump-and-treat period with a 16-day surfactant flush to achieve complete DNAPL removal (Figure 10). This UTCHEM simulation introduces the user to the additional input parameters required for SEAR simulation. Tutorials T-02 and T-03 are based on the SEAR demonstration at the Borden site and UTCHEM simulations by Brown (1993) and Jin (1995). In practice this scenario would probably use a surfactant flush much less than the 16 days simulated, and may involve a pre-surfactant slug of high-salinity water to condition the aquifer for optimal SEAR effectiveness.

The research site at Canadian Forces Base, Borden, Ontario, subsequently referred to as the Borden site, is well characterized in terms of aquifer hydro-geology, solute transport properties, and multiphase flow properties. Several tracer dispersion and remediation technology demonstration studies have been con-ducted at the Borden site, including the first demonstration of zero-valent iron for in situ treatment of dissolved chlorinated organic solvents. The thin surficial/unconfined aquifer consists of relatively homogeneous, medium- to fine-grained, siliciclastic sands underlain by a thick clay unit at a depth of ~9 m (~30 ft). The water table is 2 to 3 m (6.5 to 10 ft) below the ground surface. The hydraulic conductivity is ~0.00723 cm/sec (~20.5 ft/day), typical for clean sands.

Additional tutorials in preparation will highlight many of the other useful features of UTCHEM and the GMS interface. Specifically, these tutorials include demonstration of the following: (a) partitioning interwell tracers with which to characterize NAPL saturations in either saturated or unsaturated media; (b) the bioremediation features and how they may be coupled to the fate of NAPL con-taminants; and (c) cosolvent flushing for NAPL removal. Still more tutorials will be prepared in the future as the capabilities of UTCHEM continue to expand.

Recommendations

UTCHEM-GMS brings a powerful and practical remediation simulator to the GMS suite. UTCHEM-GMS is an advanced, multifaceted model well suited to the following common, environmentally significant groundwater problems:

a. NAPL (dense or light) spills into saturated or unsaturated media.

b. NAPL cleanup by flushing with surfactant/cosolvent/polymer or surfactant/foam.

c. PITTs in saturated or unsaturated media.

d. Bioremediation by natural or engineered microbial processes.

e. Geochemical reactions (e.g., heavy metals, radionuclides).

There are very few multiphase-flow, multicomponent transport models in the public domain, and still fewer are as well documented and maintained as UTCHEM. The capabilities for simulating NAPL flow, multicomponent transport, PITTs, SEAR, and bioremediation within a single model make UTCHEM-GMS unique among remediation simulators. The goal of the GMS graphical interface is

to reduce any impedance to users taking advantage of this advanced remediation simulator.

UTCHEM, like all models, has its limitations and idiosyncrasies, rooted in its developmental history. UTCHEM was developed initially to describe microemulsion phase behavior in petroleum reservoirs. The terminology and units used in UTCHEM reflect this heritage. Though groundwater modelers without a chemical or petroleum engineering background may find this distracting, the inconvenience is minor.

UTCHEM was not originally developed for cosolvent-only flushing, general vapor phase transport, geochemical reactions, or vadose zone problems; but due to a series of modifications over the past several years, the code can be applied to a wide variety of conditions. However, for some types of applications, users may find it necessary to use some approximations. For example, cosolvent behavior can be approximated as a poor surfactant. Limitations in application to cosolvent-only flushing will be addressed in a separate report. Vapor phase transport can be simulated for the special case of air-oil partitioning tracers; thus, UTCHEM (version 9) should not be applied to the simulation of vapor extraction, as the NUFT code can. A geochemical package has been added to UTCHEM; however, this package is not presently part of the GMS interface. UTCHEM should be applicable to vadose zone problems, although this feature was not validated during this project.

Models evolve as the user community develops a more complete, quantitative understanding of the processes being modeled and/or the need arises to extend model capabilities to describe new processes. Continuous development to address new model needs is the mark of a vibrant or "living" code; failure to evolve leads inevitably to abandonment of an outdated model. UTCHEM likely will continue to be improved to take advantage of new ideas.

The GMS interface developed under the current project does not provide graphical access to all UTCHEM capabilities. The neglected features are those either designed for petroleum reservoir applications or those deemed to be of lesser utility in environmental applications. These features remain in the model (version 9.0), but utilization would require editing of the input files outside the GMS. Specialized UTCHEM features such as horizontal wells, radial grids, and stretch grid options are also not included in the current GMS interface.

The geochemical reaction package is the only UTCHEM package entirely missing from the current GMS interface (version 3.1). The geochemical package is somewhat limited and geared toward chromium cross-linking reactions important in surfactant-polymer floods for enhanced oil recovery. Another GMS model (OS3D) is designed specifically for environmental geochemical reactive transport modeling, e.g., in situ chemical treatment.

The current versions of UTCHEM and GMS visualize the distribution of fluid phase saturations and total concentration for each component. It may also be useful in the design phase to be able to visualize the distribution of other parameters and conditions such as phase flow velocities or relative permeabilities, total

component concentrations in each phase separately, interfacial tension, and trapping number. UTCHEM calculates and outputs all of the variables mentioned, but the output is not presently formatted for GMS visualization. Future improvements to the GMS interface for UTCHEM should consider adding these additional output options.

The enhancements to UTCHEM under CU-1062 advance the practice of both multiphase flow modeling and evaluation and design of SEAR as a remediation technology. UTCHEM continues to be an excellent vehicle for the quantitative description and evaluation of remediation processes that may be coupled to synergistic or competing processes. GMS interface development should continue to complete graphical input-output to the ever-expanding model options in UTCHEM.

4 NUFT Model

Model Description

NUFT is a general-purpose computer code for modeling multiphase fluid flow and multispecies reactive transport in porous media under nonisothermal or isothermal conditions (Nitao 1998a). It has been used for various field applications in environmental remediation: soil vapor extraction (Nitao, Martins, and Ridley 2000), soil vapor extraction combined with groundwater dewatering (Rueth et al. 1998), bioventing (Sun et al. 2000), dynamic steam stripping and contaminant hydropyrolysis (Newmark et al. 1999), and electrical heating (Carrigan and Nitao 2000). NUFT has also been used in field studies for research in vadose zone flow and transport processes (Lee and Nitao 2000; Carrigan 1999), as well as for evaluation of vadose zone contaminated sites (Demir et al. 1999). Other field applications include nuclear waste disposal (Nitao and Buscheck 1995), nuclear treaty verification (Carrigan et al. 1996), containment of gases during subcritical test explosions, and enhanced petroleum recovery (Sahni, Kumar, and Knapp 2000).

NUFT is a robust code that can solve highly computationally demanding problems. It runs on IBM PC-compatibles and various Unix operating systems such as Sun Solaris, IBM AIX, HP-UX, DEC OSF, and 386 Linux. The input file format is highly flexible. The code is written in the C++ language. Because it uses dynamically allocated memory, the code does not have to be recompiled for different problem dimensions.

NUFT consists of several modules contained in a single source code. Each module has its own set of simplifying assumptions so that the user can select the most physically appropriate mathematical module and computationally efficient numerical solution method. The following are current modules:

a. UCSAT = unconfined aquifer flow model.

b. US1P = Richard's equation flow model.

c. US1C = single-component, single-phase transport model.

d. USNT = general multiphase, multicomponent flow and transport under either isothermal or nonisothermal conditions.

e. JOULE = electrical heating.

The distinct modules in the code use a common set of utility routines and input file format. Because the various modules are essentially isolated from each other, future modules can be added without affecting existing ones. Input data are in the form of that used by the LISP language. An internal LISP interpreter for the Scheme dialect of LISP is part of the simulator to parse and store input data information, to perform input error checking, and to set default input parameter values.

USNT is the NUFT module (Nitao 1998b) that is the focus of this report. The USNT module solves the multiphase flow and multispecies flow and transport equations under nonisothermal or isothermal conditions. Local thermodynamic equilibrium for partitioning of species between fluid phases is assumed. Vapor pressure lowering of components is available as an option. A multiporosity model is also available as an option for modeling fractured porous rock systems. Kinetic reaction rate laws can be turned on, such as first-order, power law, sequentially first-order, Monod, and dual-substrate Monod reactions.

Unlike some other multiphase codes, the NUFT-USNT module can handle full disappearance of the NAPL, or any fluid phase, due to, for example, dissolution or evaporation. This is in contrast to some codes that require at least a small amount of NAPL to be present everywhere in the domain, which means that, for those models, the predicted groundwater concentrations can never go below the contaminant solubility.

The NUFT-USNT module solves the partial differential equations for the conservation of mass and energy using the integrated finite-difference method. The resulting nonlinear system of equations is solved at each time-step by the Newton-Raphson method. Each iteration of the Newton-Raphson method requires the solution of a system of linear equations arising from the linearization of the nonlinear system. Options for solution of the linear equation system are the variably banded Gaussian elimination method and the iterative conjugate gradient method with various options for preconditioners. See the NUFT Reference Manual (Nitao 1998a) and the NUFT USNT User's Manual (Nitao 1998b) for the actual balance equations and references to numerical methods.

Model Enhancements

Monod-type reactions were implemented as part of the kinetic reaction capability in the NUFT-USNT module to model bioremediation of contaminants, such as by bioventing, and to model natural degradation. The general form of the implemented reaction law is a product of factors of the form $b_i/(b_i+C_i)$, $C_i/(s_i+C_i)$, and $C_i^{p_i}$ where C_i is the concentration of the ith reactant species, b_i is the inhibition constant, s_i is the saturation constant, and p_i is some power. The index i can run over any set of contaminants or other mass components such as oxygen or methane. An additional temperature-dependent factor proportional to the Arrhenius-type rate law $\exp(-E/RT)$ is also optionally present. Here, R is the gas constant, T is absolute temperature, and E is activation energy, J/mol. Documentation of the Monod rate laws using NUFT is given by Sun et al. (2000).

Another enhancement in NUFT was the capability to generate a hetero-geneous field of saturated and unsaturated hydrological properties. This feature allows for more realistic modeling of remediation sites where natural heter-ogeneity plays an important role. In the approach described in this report, the physical domain is subdivided into any number of lithological material types. Up to three statistically independent random fields are generated for each material type. Hydrologic properties in a particular material are specified as functions of these multiple random fields so that the generated air entry pressure field, for example, can be statistically correlated with the saturated permeability field. The random fields are generated by the spectral method (Lee and Nitao 2000) using the fast Fourier transform algorithm. Figure 11 shows an example of random fields generated for a model of a steam flooding test performed at a creosote-contaminated site at Visalia, CA (Newmark et al. 1999). Here three random fields were generated, one for each zone. The air entry pressure parameter for the capil-lary pressure curves were also varied spatially by assuming that they scale as the square root of the permeability.
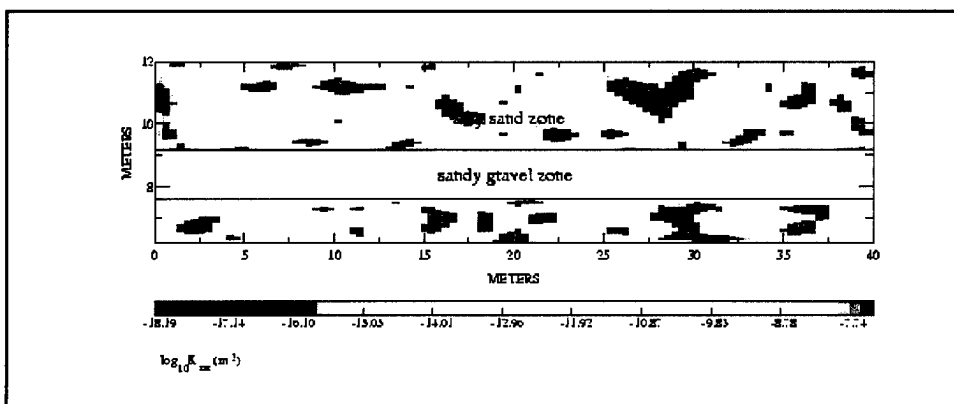
Figure 11. Heterogeneous random fields generated for saturated intrinsic permeability for a model of a steam flooding test performed at a creosote-contaminated site at Visalia, CA

A multicontinua option was implemented into NUFT that enables the code, for example, to model sites with fractured porous rock by treating the fracture network and the porous rock matrix as separate porous medium continua. Theo-retically, any number of continua can be specified to model separate fracture sets. Exchange of fluids between continua is governed by various flow options. The random field generation also works with this capability. In particular, each con-tinuum can have material types with each material type having up to three statisti-cally independent random fields. The file **addendum.doc** distributed with the NUFT code documents the multicontinua and random property field options. Figure 12 shows the isosurface of 50 percent liquid water saturation (saturation is the fractional occupied void space) in the fractures due to infiltrating water within a heterogeneous domain.
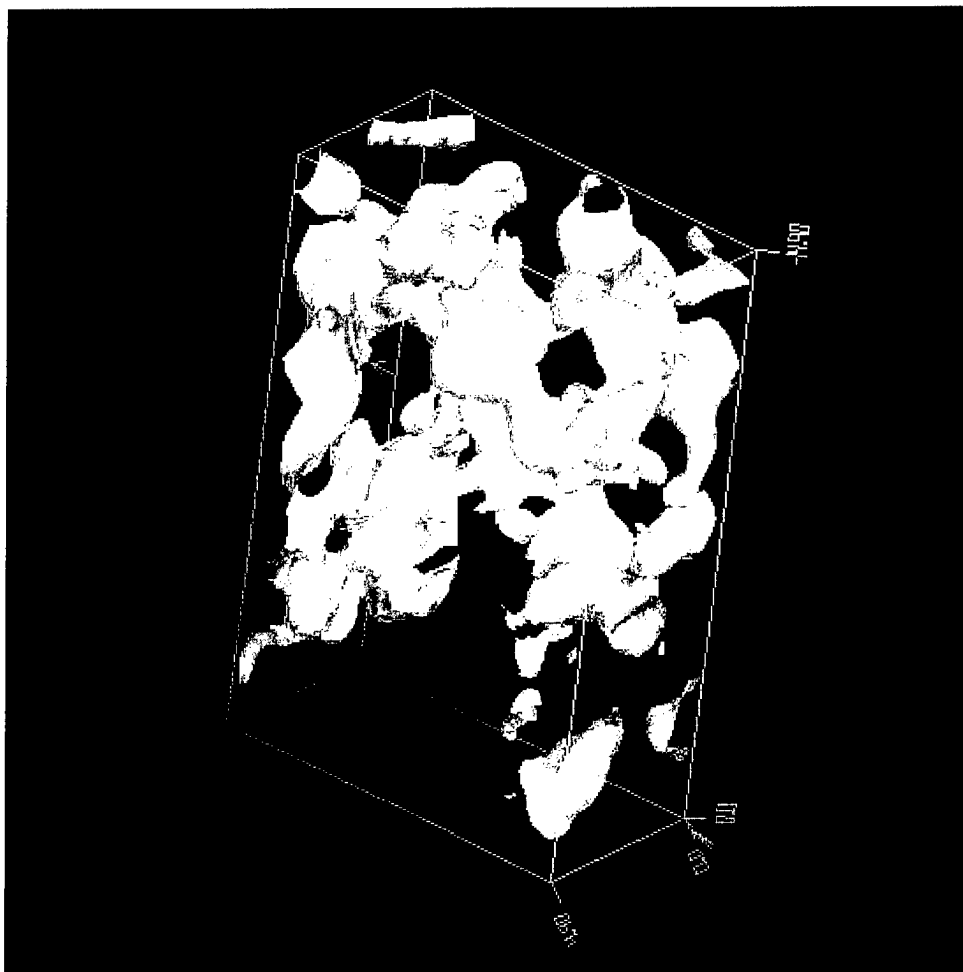
Figure 12. Water infiltrating within a heterogeneous fracture continuum where the 50 percent liquid water saturation isosurface is shown

Model Validation

A primary objective of this project was to validate NUFT for SVE. Code enhancements and general support provided by this project contributed to the preparation and documentation of other validation efforts. A broad suite of validation tests is preferable to a single test because each one is able to focus on a subset of processes modeled in NUFT. Therefore, the results of these other field validation exercises are described as well.

Validation of SVE at the LLNL B-518 Site

A detailed description of the SVE validation at the Lawrence Livermore National Laboratory (LLNL) Building 518 (B-518) site is given in Nitao, Martins, and Ridley (2000). SVE is a commonly used remediation method for removing volatile organic contaminants (VOCs) from the vadose zone. Soil gas is extracted

from the subsurface by applying a vacuum to one or more boreholes. In many cases, clean air is also injected at other locations to enhance air flow rates.

Building 518 was constructed in 1958 and used as a gas cylinder, solvent drum, and oil drum facility. Several sites around the former facility were identified to have potentially high concentrations of VOC, primarily TCE. In 1993 a 2-day field test was performed at a borehole located in the area of the highest soil concentrations to demonstrate the treatability of the site. The mean permeability of the model was calibrated based on the wellhead pressure and the total extracted vapor flux. The initial total contaminant mass was calibrated using the vapor concentrations from the borehole. The shape of the vapor concentration history curve agreed well with calibrated model predictions (Figure 13). It was found that the initial mass had to be increased up to five times the initial estimates using simple spatial interpolation, indicating that initial estimates were probably too low.
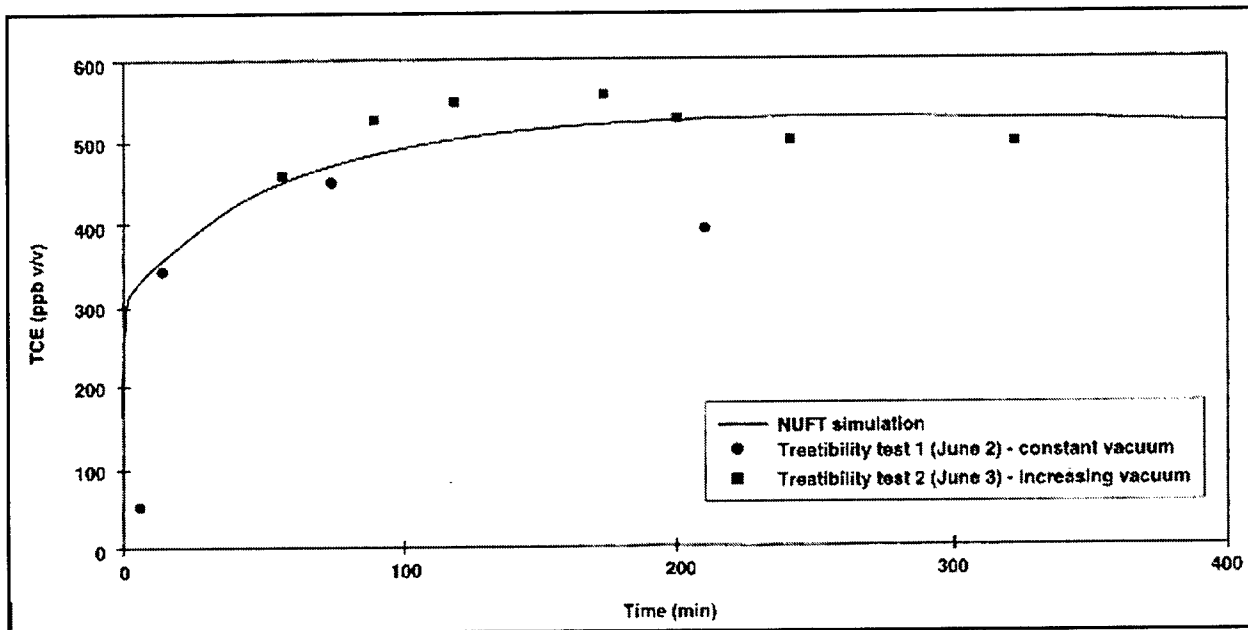
Figure 13. Comparison of SVE vapor concentrations from calibrated model with field data during the pre-remediation test

In September 1995, actual remediation of the site was begun using vapor extraction from the same borehole. The remediation was modeled using the model calibrated in 1993 with the focus on the first 19 months of extraction because after that period other extraction boreholes began operation, which would extend the range of remediation beyond that of the 1993 calibration. The total vapor flux history measured in the field was input to the calibrated NUFT model in the form of a specified flux well condition. The resulting comparison with the field data and model prediction is shown in Figure 14. Increasing the initial mass in the model by 10 percent shows the sensitivity to the mass estimate. Most of the VOC stream is TCE, but other relatively minor volatile contaminants that are present, but not included in the model, will cause total VOC to be underpredicted.
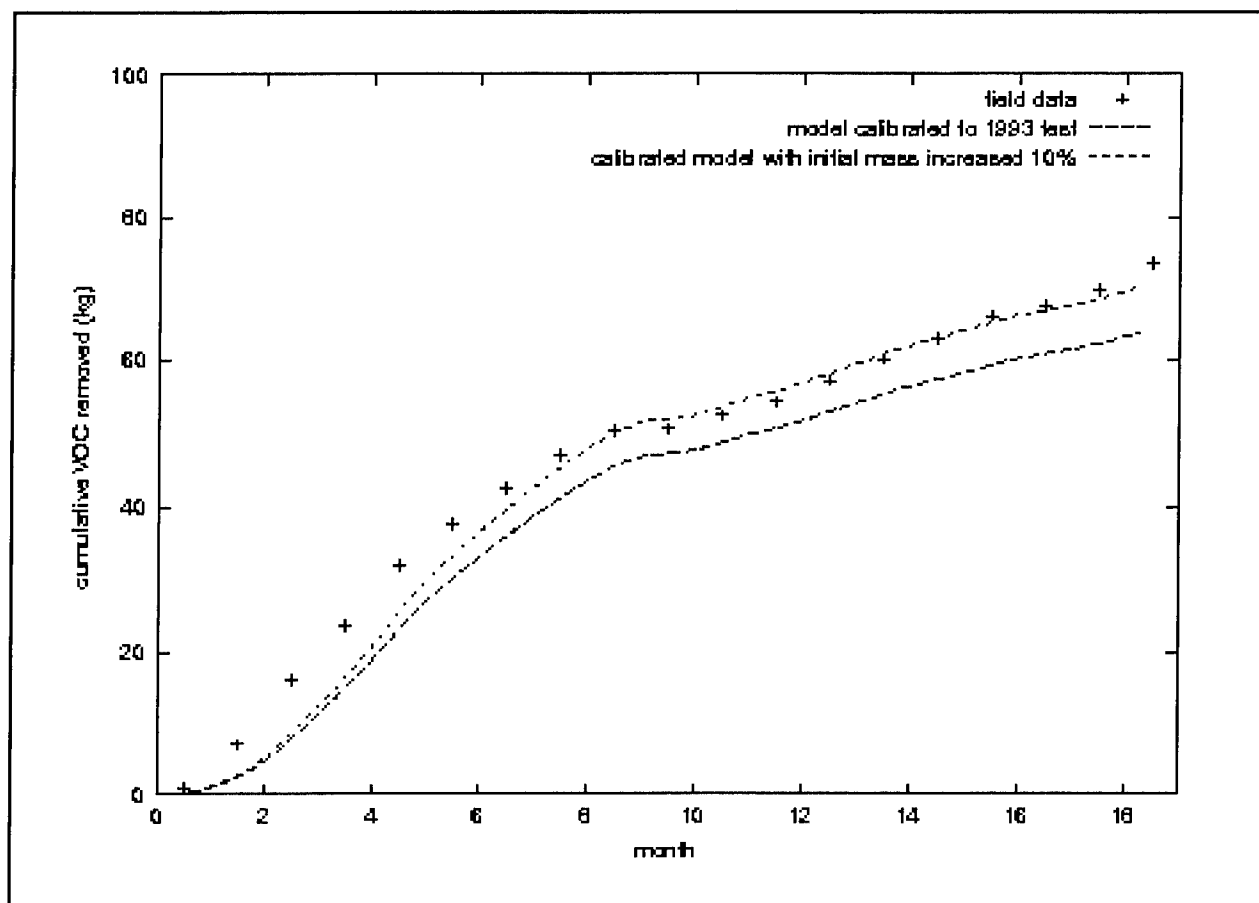
Figure 14. Comparison of cumulative total VOC mass from field measurements of TCE beginning
September 1995 versus those predicted by the model during first 19 months of SVE, 1993

Using the same homogeneous model that was calibrated against the 2-day treatability test in 1993, very good agreement with the produced stream was obtained during the first 19 months of remediation using SVE from the same well. Although the main goal of the study was model validation against SVE, the study also showed how a numerical model can be used to improve initial contaminant mass estimates.

Modeling of bioventing at Site 280, Hill AFB

An initial modeling effort was performed for bioventing at Site 280, Hill AFB, near Ogden, UT. Bioventing is the remediation of hydrocarbons from the vadose zone by injecting air into the vadose zone to enhance aerobic biodegradation of hydrocarbons from naturally occurring microbes. Compared to SVE, the required flow rates are low. The vadose zone at Site 280 was contaminated with jet fuel.

The components modeled were water, N_2, O_2, CO_2, and benzene (C_6H_6). All components can partition into both gaseous and aqueous phases, which, for example, allows for evaporation of water and dissolution of benzene in the aqueous

phase. Both diffusive and advective transport of all components in both fluid phases were considered. Since no NAPL has been observed at the site, no free phase was considered.

Stoichiometry of the biodegradation process was described by the following reaction

$$C_6H_6 + 7.5\ O_2 \Longrightarrow 6\ CO_2 + 3\ H_2O \tag{1}$$
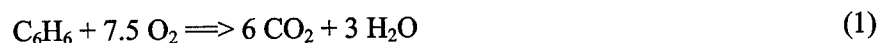
An irreversible, dual-substrate Monod kinetic reaction was used to model this reaction. The coefficient for the rate equation was calibrated based on plume size and total mass removal.

Modeling without bioventing showed, as expected, that biodegradation is limited by the lack of oxygen. Natural biodegradation was predicted to destroy 15.4 percent of the contaminant mass while bioventing was predicted to destroy 99.6 percent. Further work ended because of re-prioritization from the SERDP Office. Sun et al. (2000) documents this study.

Modeling dynamic steam stripping—the Visalia Test

In the summer of 1997 a test was performed at Visalia, CA, that injected steam into a creosote-contaminated formation (Newmark and Aines 1998; Newmark et al. 1999). Water sampling and temperature monitoring were performed at an extraction well 23 m (75 ft) from the extraction well. A NUFT model was developed that incorporated heterogeneous distribution of hydrological properties as given in Figure 11. The predicted breakthrough of the steam front at the extraction well was approximately 48 hours, which was very close to the observed breakthrough time.

Several noble gas tracers added to injected water and steam to track their movement were subsequently monitored at the extraction well. Figure 15 shows the breakthrough curves at the extraction well from xenon that was injected along with the steam. The different curves represent different initial conditions. The decrease in measured concentrations, as shown in the figure, that begins at 15 hours was caused by partial failure of the extraction well due to emulsification of NAPL. The NUFT model did not include the pump failure because its exact degree of impact is uncertain. Also, it should be noted that most of the simulations were done before the field test was actually performed. The agreement between field data and model prediction is considered to be good considering the complexities involved in the steam stripping process and the high degree of uncertainties involved in modeling a site that had relatively little quantitative characterization of hydrologic properties.

Benchmarking of NAPL movement and steam stripping

NUFT has the capability to model heating of porous media through AC electrical heating (Carrigan and Nitao 2000). LLNL has been performing scoping
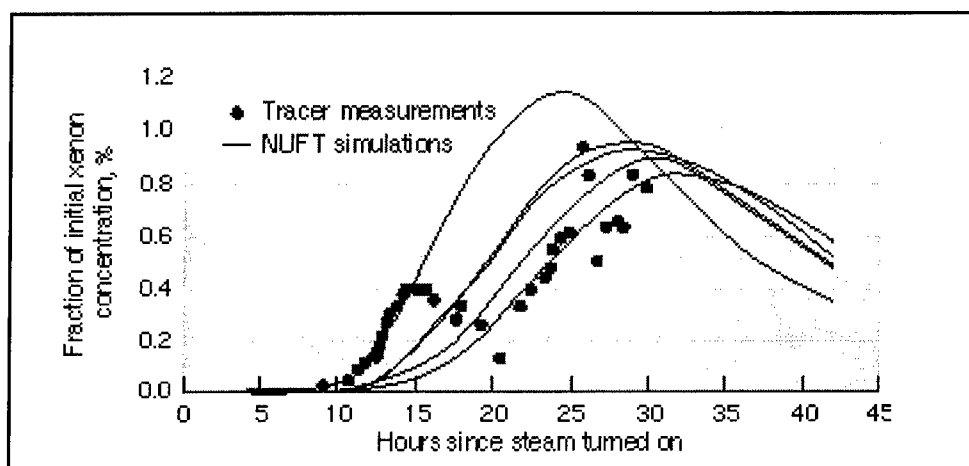
Figure 15. Breakthrough curves for xenon tracer that was injected with the steam (from Newmark and Aines 1998)

studies to model the enhancement of production from heavy oil reservoirs by this process (Sahni, Kumar, and Knapp 2000). The sponsor requested that NUFT be verified against an established petroleum industry reservoir simulator, in particular, the CHEARS code developed by Chevron Oil Company (Chien and Northrup 1993). The selected test problem was the steam flooding of a hypo-thetical reservoir. Of course, simulation of this condition has implications for modeling recovery of NAPL source contamination.

CHEARS was run in this exercise as a black oil simulator; that is, the petro-leum is treated as a single nonvolatile component. Because the NUFT-USNT module cannot model a nonvolatile component, the oil phase had small amounts of dissolved noncondensable gas. The benchmark problem consisted of a three-dimensional rectangular domain (109 m (358 ft) wide by 109 m (358 ft) deep and 18.3 m (60.04 ft) tall) with a steam injection well at the center and a fully pene-trating production well at each corner of the domain. The formation was a perme-able sandstone with two low-permeability shale zones of thickness 1.524 m (5 ft), starting at 3.05 m (10 ft) from the bottom of the model and 3.05 m (10 ft) from the top of the model. Steam was injected only in the sandstone between the two shale zones. The bottom and top of the model formed impervious boundaries. The formation was tilted by 10 degrees from the vertical along one of the sides of the model.

Figure 16 shows the oil phase (NAPL) saturation at time 0.58 year from the start of the simulation for a cross section that runs through the injection well. The formation is tilted upwards going from the left to right. An oil bank, as indicated by the red, developed around the steam injection well. The right portion of the bank that is shown progressed farther because of the imposed tilt. The bluish zones are the shale zones, which have very little oil saturation. Figure 17 shows the plan view of the oil saturation at the same time period, at a horizontal plane underneath the upper shale zone, clearly showing the resulting oil bank.
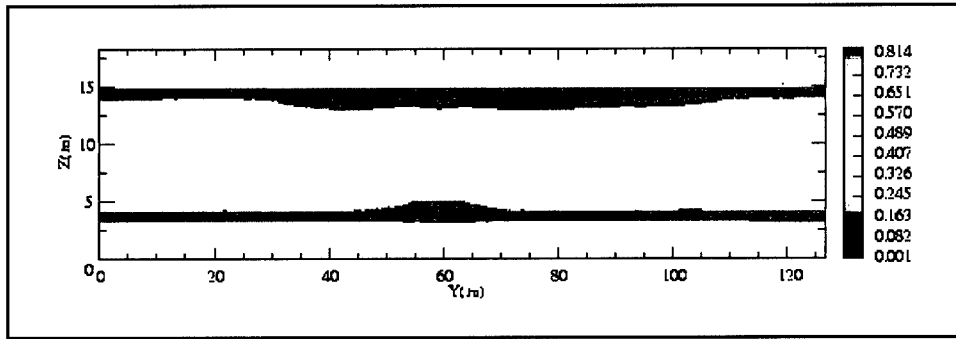
Figure 16. Oil phase saturation along a vertical cross section through the injection well parallel to the sides of the model (the model tilts upward by 10 degrees from left to right)
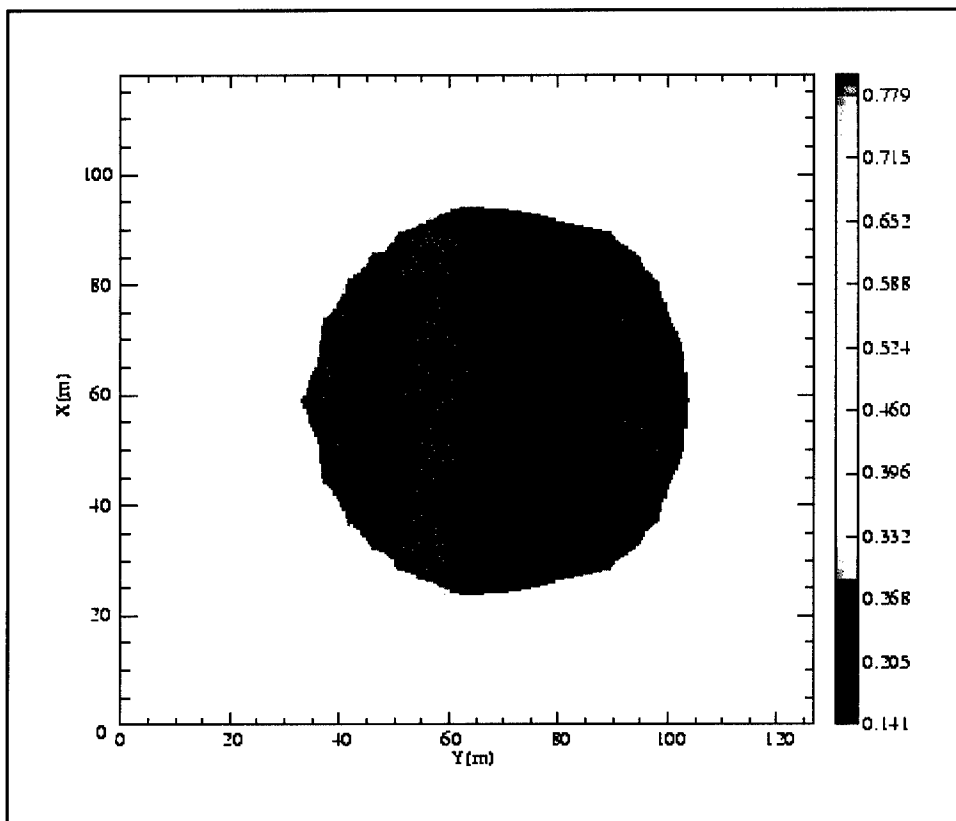
Figure 17. Plan view of oil phase saturation in the sand layer just below the upper shale layer (the model tilts upwards from left to right)

Figure 18 shows the total oil flux and water flux produced from the field as predicted by the CHEARS and NUFT models. The underprediction of oil by NUFT compared with the CHEARS model is probably due to the reduction in oil flow from evolution of noncondensable gas around production wells in the NUFT calculation. Comparison between the models is considered good, especially when compared to other industry code benchmarking exercises (Aziz, Ramesh, and Woo 1987). Note that differences can also arise from the manner in which the
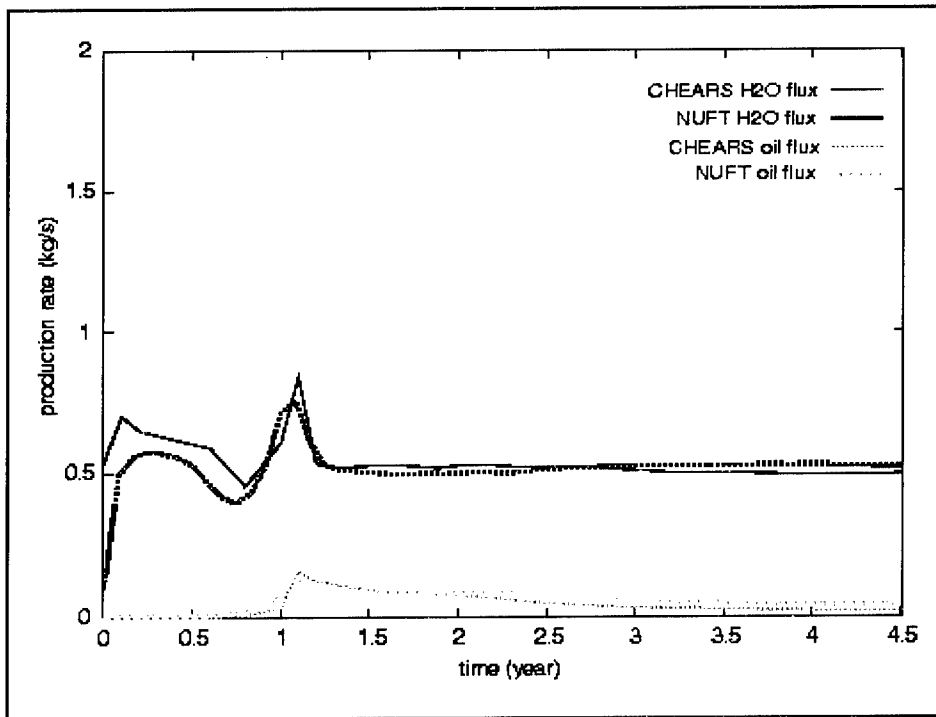
Figure 18. Comparison of oil and water fluxes from the NUFT and CHEARS
models (courtesy of R. Knapp, Geosciences and Environment
Technologies Division, Lawrence Livermore National Laboratory,
Livermore, CA, 6 October 2000)

models control their time-steps and other aspects of their numerical solution
algorithms.

Implementation into the GMS Interface

A sophisticated NUFT interface for GMS was developed using information
about NUFT input from the author of NUFT.[1] Because most environmental
remediation methods modeled by NUFT use the USNT module, it was decided to
implement only this module. Because of the many options available in NUFT and
because of its generality, considerable programming effort was required to
program the GMS-NUFT interface.

Some modifications to the NUFT code were also required because NUFT was
originally written to be run at the MS-DOS or Unix command line, instead of
interactively under a graphical user interface, such as GMS. First, a new output
option in NUFT was implemented and tested that allows NUFT to create output
files in the standard GMS binary output format so that GMS can read NUFT
output directly for graphical output. The output times for the data can be specified
by the user through the GMS interface. Next, NUFT and its program build system
were ported from the GNU C++ compiler to the Microsoft Visual C++ compiler

---

[1] Personal Communication, 1999, J. J. Nitao, Lawrence Livermore National Laboratory,
Livermore, CA.

to support long file names under Windows NT. NUFT assumes that all user output files should be created in the directory in which it is being run whereas GMS passes the full directory path of the input file and expects all output files to go in the directory of the input file. A function supplied by Brigham Young University (BYU) to extract the executable and input file directory paths was integrated into NUFT to be consistent with the GMS convention. A similar change was made with regard to the directory location of the NUFT start-up files, which is now based on parsing the full directory path of the NUFT executable. All of these changes had to be made while maintaining compatibility with non-PC platforms.

The following steps for building a NUFT simulation using GMS are from the GMS help utility:

a. A cell-centered three-dimensional grid is constructed.

b. The basic NUFT options are selected including general options, equations, time-steps, and solver.

c. Regions of the grid are selected and marked as ranges.

d. All boundary conditions and sources/sinks are assigned to ranges. The ranges also define material zones.

e. The material, phase, and component properties are defined.

f. Boundary conditions and phase and component sources are assigned to predefined ranges.

g. Wells are created and assigned the appropriate phase and component fluxes.

h. Initial conditions are defined.

i. Output control options are selected.

j. The model is saved and NUFT is launched from the GMS menu.

k. The NUFT solution is read into GMS for postprocessing.

An existing NUFT simulation can be read into GMS using the "Read Simulation" command in the NUFT menu. Once a NUFT simulation is saved to disk, NUFT can be launched by selecting the "Run NUFT" command from the NUFT menu. The command brings up a dialog listing the path to the NUFT executable and the most recently saved NUFT simulations. In most cases, these paths do not need to be edited. When the "OK" button is selected, NUFT is launched and the input file is passed to NUFT as a command line argument. NUFT is launched in a separate window and the console output from NUFT is displayed.

Figure 19 shows an example dialog menu for specifying the phase- dependent material properties of a NUFT material type.

Figure 19. GMS dialog menu in the NUFT interface for specifying the phase-dependent material properties of a single material type

Recommendations

Because multiple flow and transport mechanisms occur during most remediation processes, preferably more than one field test should be used to verify computer models. Each test in a broad suite of tests can be used to focus the validation on a particular subset of dominant processes.

Table 4 is a matrix diagram listing various physical processes modeled by NUFT with x's indicating appropriate tests validating each process. If a process plays only a minor role in a test, it is not checked. For example, aqueous phase transport due to infiltration occurs in the LLNL B-518 SVE remediation test, but at that site it is unimportant relative to gaseous phase transport, so it is not marked. However, in less arid regions, aqueous phase transport can play a significant role in contaminant transport during SVE, at least during periods of high rainfall. Aqueous phase transport is an important part of SVE in such circumstances. Thus, it is important to have other tests for validating aqueous phase advection such as a trench infiltration test, which has been performed.

The Visalia field test and the steam-flood simulator test are important for modeling thermal remediation processes and for problems where there is NAPL

Table 4
NUFT Process Validation Matrix

Main Processes Validated	Field Tests					
	A	B	C	D	E	F
Gaseous flow	X	X	X		X	
Gaseous transport	X	X			X	
Aqueous flow			X	X	X	X
Aqueous transport			X	X	X	X
NAPL flow						X
Steam flow					X	X
Steam transport					X	
Thermal advective transport				X	X	X
Thermal conductive transport				X	X	X
Fluid phase changes					X	X
Heterogeneous systems				X	X	
Barometric pumping effects		X				
Transport in fractures		X				
Infiltration flow			X			
Infiltration transport			X			
Injecting and producing wells	X				X	X

Notes:
Field Tests
A. LLNL B-518 SVE remediation
B. Nuclear treaty test (Carrigan et al. 1996)
C. CAMBRIC trench study, personal communication with F. B. Thompson, Geosciences and Environmental Technologies Division, Lawrence Livermore National Laboratory, 15 November 2000.
D. Cheshire nuclear test (Maxwell et al. 2000; Tompson et al. 2000)
E. Visalia field test
F. Steam-flood simulator benchmark
X = Appropriate test for validating the process.

movement. NAPL movement is important at SVE sites where there is free product.

The results of the validation tests modeled by NUFT were very encouraging. Although it is impossible to rigorously prove the validity of NUFT, or any computer code for that matter, the tests that were performed give confidence that the code can be used for modeling SVE, thermal remediation methods such as dynamic steam stripping, and general prediction of vadose zone flow and transport processes. However, it should be recognized that NUFT is a fairly complex simulator offering much flexibility. Thus, it will take time for this simulator to arrive at a state where it is widely applied.

5   OS3D

Model Description

OS3D is a simulator for multidimensional, multicomponent reactive transport in porous media. It predicts the behavior of multiple interacting chemical components by modeling subsurface reaction and transport processes in a quantitatively mechanistic framework that accounts for spatially variable geochemical conditions and properties. These reactive components include minerals, aqueous chemical species, and species sorbed to mineral surfaces. The modeling technology spans multiple disciplines (e.g., hydrology, geology, chemistry, biology, numerical analysis, and computational methods) to address multiple end user applications (e.g., diagenesis, mineral extraction, remediation, and waste management).

OS3D, originally developed by Steefel and Yabusaki (1996) in 1995, has been updated over the intervening years. This latest version of OS3D is written entirely in the FORTRAN 90 language and is now part of a reactive transport package called CRUNCH (Steefel, in preparation). The GMS implementation of OS3D and the development of a parallel processing version is a collaborative effort among ERDC, LLNL, and Pacific Northwest National Laboratory.

Transient and steady-state phenomena can be addressed in batch, reaction path, one-, two-, and three-dimensional systems that include advective, dispersive, and diffusive transport. The OS3D reactive transport simulator can be used in conjunction with nonuniform, single-phase-fluid velocity fields provided by the MODFLOW (McDonald and Harbaugh 1988) groundwater flow simulator. OS3D solves a set of nonlinear partial differential equations describing coupled reactions and transport in a multicomponent system using a finite volume discretization of the problem domain. A mixed system of equilibrium and kinetic reactions representing aqueous and surface complexation, ion exchange, precipitation, and dissolution can be solved (Steefel 2000). An extended Debye-Huckel model is used to calculate activity corrections. OS3D uses an extensible version of the EQ3/EQ6 (Wolery 1992) temperature-dependent thermodynamic database for reaction stoichiometry, stability constants, mineral molar volume, and activity model parameters. Constant temperature and temperature gradient conditions can be simulated.

Total component concentrations are transported in both the dispersion and advection routines, and form the basis for mass balance equations in the reactive chemistry step. The actual unknowns, however, are the individual "primary" or

"component" species concentrations. This approach effectively folds a speciation calculation into the nonlinear ordinary differential equations describing the conservation of solute mass in the system. The approach also allows for mixed equilibrium and kinetic reactions within the overall reaction network. The following are major reactive chemistry components included in OS3D:

a. Equilibrium aqueous complexation.

b. Kinetically controlled aqueous phase reactions (e.g., redox and biological).

c. Mineral dissolution/precipitation kinetics.

d. Multicomponent ion exchange.

e. Surface complexation with a double-layer model used for an electrostatic correction.

f. Redox catalysis on mineral surfaces.

g. Radioactive decay.

h. Linear adsorption isotherms K_d.

In theory, there are no restrictions on the number of different processes included in a simulation since physical memory for each of these is allocated at run time. The code is also accompanied by an initialization routine that allows the use of a variety of different constraints (e.g., total concentration, equilibrium with a mineral phase, equilibrium with a gas phase, charge balance) to speciate initial or boundary conditions. Given a choice of primary component species, the code searches a version of the EQ3/EQ6 database, which has been augmented with surface complexation and ion exchange thermodynamic data along with kinetic rate laws for aqueous and mineral reactions.

At startup, the code allows the specification of a number of different zones within the domain of interest, which have distinct initial solute concentrations, mineral abundances, and/or grid spacing. The code also includes a distribution of species calculation to specify the initial and boundary solute concentrations. The code reads a thermodynamic database based on the EQ3/EQ6 database, which covers temperatures between 0 and 300 °C along the water saturation curve for a large number of mineral and aqueous species. The code also allows for a range of mineral-water reaction rate laws, including parallel reactions (e.g., pH-dependent and pH-independent rates) and proton-promoted and/or ligand-promoted dissolution.

The operator splitting solution methodology comprises an explicit, third-order accurate TVD advection scheme; an implicit, second-order accurate dispersion and diffusion scheme; and an implicit backward Euler scheme for the system of algebraic equations representing the differential equations for reactions. Concentration fronts are accurately preserved with the high-resolution, shock-capturing TVD method.

An adaptive time-stepping algorithm is used to control the convergence of the nonlinear iteration scheme within the limits of the maximum allowable time-step

that maintains the stability of the explicit numerical scheme for advective transport. Fully coupled or "global implicit" approaches can also provide solutions to reactive transport problems; however, OS3D has some real advantages in terms of memory usage, CPU time required per time-step, the ability to handle up to three-dimensional transport, and the coupling to higher order advective transport schemes. This made it an attractive choice for incorporation into the GMS software suite.

Inquiries about the code should be directed to:

Carl I. Steefel
Lawrence Livermore National Laboratory
Geosciences and Environmental Technologies
Phone: 925-424-9807
FAX: 925-423-1997
E-mail: steefel@llnl.gov

Postal Address:	Street Address:
LLNL, L-204	LLNL, L-204
PO Box 808	7000 East Avenue
Livermore, CA 94551-9900	Livermore, CA 94550-9900

Model Enhancements

OS3D contains a number of enhancements over previous versions of the code that have been released (Steefel and Yabusaki 1996). The present version has been entirely rewritten in FORTRAN 90, incorporating data structure modules, run time dimensioning of arrays, and dynamic memory allocation. These improvements allow (a) problem initialization routines to be executed without loading memory for the global spatial arrays; (b) problem restart that skips the initialization routines altogether; and (c) more information that can be used in the parallel implementation. A keyword-based input has been implemented that allows the entry of data categories in any order and the ability to comment entries so they will be ignored by the code.

OS3D now allows for the importation of a transient or steady-state flow field from MODFLOW. With this added capability comes the ability to simulate a variety of source terms, including injection and pumping wells, drains, rivers, and other fixed-head boundary conditions. New routines were developed to accommodate data transfer from MODFLOW and the GMS interface to OS3D. MODFLOW input data are now transferred through the GMS interface into the OS3D input file. In the GMS, MODFLOW initial and boundary conditions and flow fields are written to output files for use by transport routines in the MT3DMS (Zheng and Wang 1999) simulator. These same files are now read by OS3D. This condition required the modification of the OS3D transport routines to be consistent with the MODFLOW for (a) three-dimensional cell thickness variability; (b) flows (rather than Dacy velocities) that are specified at cell faces; (c) source/sinks (recharge, evapotranspiration, wells, drains, rivers, streams); and (d) inactive cells.

Enhancements to the chemical processes simulated with OS3D include the following:

a. Option to automatically include every relevant secondary chemical species in the database after specifying a set of primary species. This is typically done early in the development of a problem specification when a geochemically consistent set of component concentrations is being initialized to ensure that key reactions are not omitted.

b. Multicomponent (multivalent) ion exchange with multiple exchange sites. The user may choose to use either the Gaines-Thomas, Gapon, or Vanselow conventions for calculating exchange species activities (e.g., Appelo and Postma 1993).

c. Multisite surface complexation, with or without an electrostatic correction accounting for the effect of surface charge on mineral surfaces. The electrostatic or "coulombic" correction is based on the double layer model (Davis and Kent 1990; Parkhurst 1995; Bethke 1996).

d. Aqueous phase (homogeneous) kinetics including

    (1) Biodegradation using Monod-type rate laws or variable order (zeroth-, first-, second-order) rate laws.

    (2) Radioactive decay chains.

e. Solid phase reactions using either transition state theory types of rate laws with various catalytic or inhibitory functions or with Monod-type kinetics.

Unlike previous versions of the code, only total component concentrations are transported in the present version, so no basis switching (Steefel and Yabusaki 1996) is allowed.

Model Validation

The OS3D simulator was applied to a field study (Battelle 1998) of a pilot-scale funnel and gate treatment system at Moffett Field, California, that used zero-valent iron (Fe^0) to engineer TCE destruction (Yabusaki et al. 2001). To date, Fe^0 has been emplaced in a variety of subsurface barrier geometries in a variety of subsurface settings, e.g., Moffett Field, Elizabeth City, Dover AFB, and Denver Federal Center (U.S. Environmental Protection Agency 1999). While it is clear that Fe^0 can be effective in transforming chlorinated hydrocarbons to benign byproducts, there are many other components in the groundwater that will also be affected by the presence of Fe^0. Of concern are reactions that could adversely affect the long-term performance of the iron barrier or create secondary contaminants. Since the solution chemistry (e.g., pH, E_H, alkalinity, dissolved gases, major cations and anions) of groundwater will vary from site to site, the long-term performance of a "standard" implementation of an iron barrier may also be expected to vary. Understanding the impact of the local groundwater chemistry on the performance of the iron barrier provides opportunities to assess the feasibility of the technology and adapt the engineering design to site-specific conditions.

Problem description

The funnel and gate methodology emplaces impermeable walls in a saturated aquifer to "funnel" contaminated groundwater through one or more "gates" where passive treatment takes place (Starr and Cherry 1994). Shallow (< 15 m (50 ft) below ground surface) aquifers underlain by a continuous bottom-confining layer are the best candidates for the technology. Sheet piles with sealable joints are typically used to construct the impermeable walls, whereas the gates contain reactive cells filled with varying amounts and geometries of granular Fe^0. As contaminated groundwater passes through the reactive cell, transformation of the target contaminants occurs.

In the Moffett Field case, the gate is 5.5 m (18 ft) deep, 3.0 m (10 ft) long, and 3.0 m (10 ft) wide (Figure 20). The reactive iron cell is as wide and deep as the gate but is 1.8 m (6 ft) long with 0.6-m- (2-ft-) long pea gravel zones on either end. The pea gravel has a porosity of 0.33. The granular iron in the reactive cell was manufactured by Peerless Metal Powders, Inc., in the –8 to +40 mesh particle size range. The iron was characterized with a packed porosity of 0.66 and a specific surface area of 1.5 m^2/gm, which are typical for these materials (Johnson, Scherder, and Tratnyek 1996).

After installation of the funnel and gate in April 1996, a very comprehensive field data collection effort comprising five quarterly monitoring events after the installation of the permeable reactive barrier was performed through October 1997 (Battelle 1998). Chlorinated volatile organic compounds (CVOCs), hydrocarbons, major ions, dissolved gases, temperature, E_H, pH, and alkalinity were measured. Unless otherwise noted, the measured data reported are from Battelle (1998), which also includes a description of the sampling and analytical procedures.

Model specification

Selection of aqueous components. Based on the observed changes to the groundwater chemistry from the aquifer through the iron zone, the following aqueous species were modeled:

   a. Organic chemistry: TCE, *cis*-1,2-DCE, CH_4, C_2H_4, Cl^-

   b. Carbonate chemistry: H^+, OH^-, HCO_3^-, CO_2(aq), CO_3^{-2}

   c. Major metal ions: Ca^{+2}, Mg^{+2}

   d. Redox couples: Fe^{+3}/Fe^{+2}, O_2 (aq)/H_2O, H_2O/H_2(aq), SO_4^{-2}/HS^-, NO_3^-/NH_4^+

   e. Metal complexes:
$FeOH^{+2}, Fe(OH)_2^+, Fe(OH)_3 (aq), Fe(OH)_4^-, Fe(OH)^+, Fe(OH)_2 (aq),$
$Fe(OH)_3^-, FeCO_3 (aq), FeHCO_3^+, CaHCO_3^+, CaCO_3 (aq), MgHCO_3^+,$
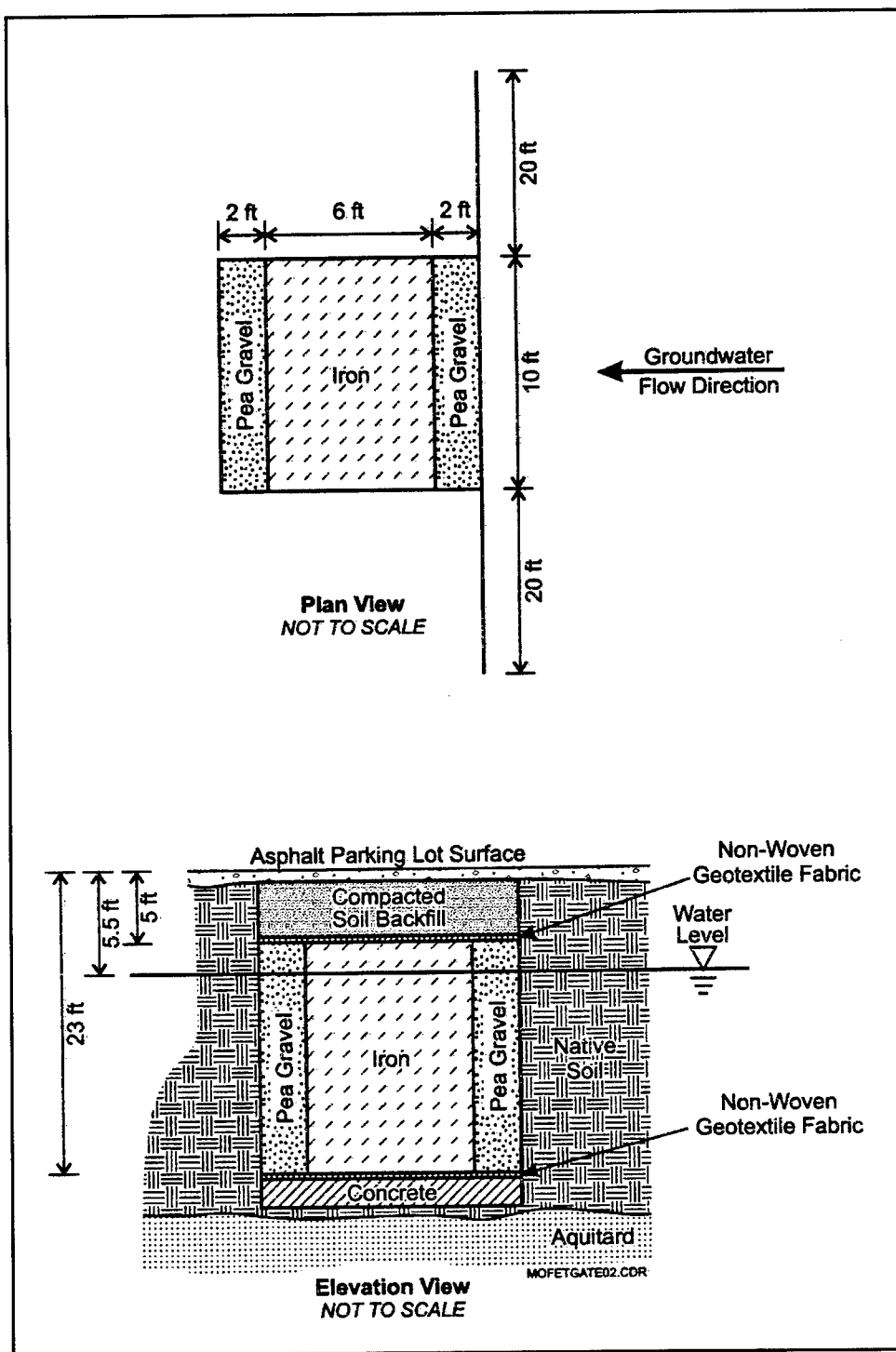$MgCO_3 (aq), CaSO_4 (aq), MgSO_4 (aq), FeSO_4 (aq)$

Figure 20. Permeable reactive barrier plan view and elevation view at Moffett Field (to convert measurements to meters, multiply by 0.3048)
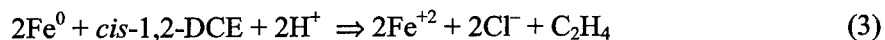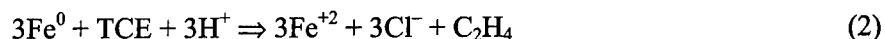
As a first approximation, the homogeneous reactions were modeled as equilibrium reactions using the stoichiometry and thermodynamics from the EQ3/EQ6 database (Wolery 1992). A temperature of 25 °C was assumed for the reaction

thermodynamics, which was appropriate given observed temperatures in the 20-22 °C range.

Selection of minerals. Other than the chemical reduction of aqueous components, the precipitation of secondary minerals was assumed to be the primary mechanism for removing calcium, magnesium, carbonate, hydroxide, and sulfate from solution in the iron cell. Based on observed concentrations in the field and the analyses of the iron cores, a set of candidate minerals was individually tested for geochemical consistency (i.e., under or at saturation in the background aquifer and over saturation in the iron cell) using the batch equilibrium mode of the OS3D simulator. For example, $CaCO_3(s)$ is indicated as a potential secondary mineral, but it is aragonite, rather than calcite, that is thermodynamically consistent with the observed concentrations.

Based on these equilibrium modeling analyses, the following secondary minerals were included in the model: ferrihydrite $(Fe(OH)_3(am))$, $Fe(OH)_2(am)$, FeS(am), brucite $[Mg(OH)_2]$, siderite $(FeCO_3)$, aragonite $(CaCO_3)$, and green rust $[Fe_4^{II}Fe_2^{III}(OH)_{12}][SO_4 3H_2O]$. Both mackinawite $(Fe_{1+x}S)$ and "amorphous FeS" have nearly the same free energy of formation (Lennie and Vaughan 1996). Although subsequent sulfidation to form marcasite and pyrite is expected, the exact sulfidation sequence and kinetics of each step have not been characterized well enough to be included in the model. The green rust reaction thermodynamics are from Hansen, Borggaard, and Sorensen (1994). The reaction thermodynamics for the remaining secondary minerals are from the 25 °C EQ3/EQ6 database.

Reaction rates. The degradation kinetics of TCE and *cis*-1,2-DCE were modeled using the beta elimination pathway (Roberts et al. 1996) as a bulk first-order kinetic reaction that includes the oxidation of iron in addition to the transformation of the chlorinated organics to undifferentiated hydrocarbons and chloride. In this case, ethene is used as the nominal hydrocarbon byproduct as follows:

$$3Fe^0 + TCE + 3H^+ \Rightarrow 3Fe^{+2} + 3Cl^- + C_2H_4 \tag{2}$$

$$2Fe^0 + cis\text{-}1,2\text{-}DCE + 2H^+ \Rightarrow 2Fe^{+2} + 2Cl^- + C_2H_4 \tag{3}$$

Bench scale column studies (PRC Environmental Management, Inc., 1995) using granular iron from Peerless Metal Powders, Inc., were performed on 50:50 mixtures of iron and sand to determine degradation rates for these two reactions. The results were scaled to the 100 percent iron and packing conditions used in the field resulting in TCE half-life of 0.4 hour and *cis*-1,2-DCE half-life of 1.35 hours.

Other than the iron dissolution that occurs in conjunction with the transformation of the chlorinated hydrocarbons, a reversible rate law for mineral precipitation and dissolution is used that is based loosely on transition state theory (e.g., Lasaga 1984):

$$r_m = A_m k_m \prod_{i=1}^{N_S} a_i^p \left[\left(\frac{Q_m}{K_m} \right) - 1 \right] \qquad (4)$$

where

r_m = rate of precipitation (>0) or dissolution (<0) of mineral m

A_m = surface area of the reacting mineral

k_m = rate constant

N_s = number of species

a_i = activity of a species

p = empirically determined exponent

Q_m = ion activity product

K_m = equilibrium constant for the mineral − water reaction

For dissolution, the intrinsic rate constant k_m is multiplied by the bulk surface area A_m (i.e., 4.0×10^6 m^2/m^3 for iron). Precipitation rates in this study are reported in units of mol/m^3/s ($A_m k_m$).

In addition to the iron oxidations in Equations 2 and 3, there are two other parallel iron reactions involving the reduction of dissolved oxygen and reduction of water:

$$2Fe^0 + 2H_2O + O_2 \text{ (aq)} \Leftrightarrow 2Fe^{+2} + 4OH^- \qquad (5)$$

$$Fe^0 + 2H_2O \Leftrightarrow Fe^{+2} + H_2(aq) + 2OH^- \qquad (6)$$

The rate law (Equation 4) for the dissolution reaction with oxygen (Equation 5) has a relatively large rate constant, 4×10^{-7} mol/m^2/s, which is multiplied by the O_2(aq) activity. It is the only inorganic rate law in the model that has a first-order dependency on the activity of a species (i.e., O_2(aq)). The rate constant for the parallel iron dissolution reaction involving the reduction of water (Equation 6) was derived from a column study (PRC Environmental Management, Inc., 1995) using the granular iron from Peerless Metal Powders, Inc., and Moffett Field groundwater. In this study, a 1.22-m- (4-ft-) long, 10.16-cm- (4-in.-) diameter column was packed to a porosity of 0.38 with a 50:50 mass ratio of sand to iron. The resulting bulk iron surface area was 1.88×10^6 m^2/m^3. For the 5-ml/min feed rate of Moffett Field groundwater (0.888 m/day Darcy flux), rate constants for hydrolysis ranging from 3×10^{-12} to 5×10^{-12} mol/m^2/s best captured the observed chemistry.

Table 5 Mineral Reaction Rates	
Mineral	Log k moles/m³/s
Fe(OH)$_2$(s)	-5.9
Ferrihydrite	-5.9
Siderite	-6.9
Aragonite	-6.1
FeS(am)	-6.9
Brucite	-7.4
Green Rust	-6.9

Rate laws for the seven secondary minerals are based on reversible mineral reaction rates (Table 5) from an earlier study (Mayer 1999) of a reactive iron permeable barrier at the U.S. Coast Guard Support Center near Elizabeth City, NC. Their respective rates were adopted for the calcium, magnesium, and sulfur sinks to the aragonite, brucite, and FeS/green rust minerals used in this model.

Model geometry. The model uses a one-dimensional representation of the gate that includes the up-gradient pea gravel zone (0.6 m (2 ft)) and the reactive iron cell (1.8 m (6 ft)). The down-gradient pea gravel zone was neglected because of contamination from the down-gradient aquifer. The system is discretized into 60 grid cells of uniform size (0.04 m (0.13 ft)).

Flow and transport. Pore velocity in the iron cell was measured by a variety of techniques: water levels (0.46-0.52 m/day (1.5-1.7 ft/day)), tracer tests (0.06-0.18 m/day (0.19-0.59 ft/day)), and down-hole velocity meter (0.34–1.86 m/day (1.12-6.1 ft/day)) The estimated range of likely pore velocities was 0.06–0.6 m/day (0.19-1.97 ft/day), which is equivalent to a Darcy velocity range of 0.04–0.4 m/day (0.13-1.3 ft/day) (based on iron porosity of 0.66). Dispersion and diffusion were assumed to be negligible.

Boundary and initial conditions. The boundary condition and the initial conditions for the model are based on an April 1997 sampling event. The field data are used to create two sets of equilibrated species concentrations. The first set is used for the up-gradient boundary condition and the initial condition for the pea gravel, whereas the second set is used for the initial condition of the iron zone. The significance of equilibrating the two geochemical conditions is based on the assumption that the observed conditions are at quasi-equilibrium. Thus, there was an attempt to prevent unrealistic transient behavior, such as the sudden precipitation or dissolution of minerals due simply to the initial chemical specification.

A geochemically consistent boundary condition was generated using the OS3D reactive transport simulator that reflects the measured background aquifer water chemistry. The following constraints were used:

a. pH fixed at 7.1, CO_2(aq) at 4.0E-4.

b. Total iron, oxygen, and ethene at 1.0E-10 M, reflecting their below-detection concentrations.

c. Total calcium at 3.9E-3 M.

d. Total magnesium at 2.7E-3 M.

e. Total sulfate at 3.5E-3 M.

f. Total nitrate at 3.9E-5 M.

g. Total chloride at 1.1E-3 M.

h. TCE at 9.1E-6 M.

i. *cis*-1,2,-DCE at 2.2E-6 M.

The boundary condition was also the initial condition for the pea gravel zone. The porosity of this zone was 0.33 although no reactive minerals were specified. The boundary condition concentrations for the primary components are summarized in Table 6.

Table 6 Initial and Boundary Conditions		
Species	**Boundary Condition and Pea Gravel Initial Condition (Molality)**	**Initial Condition for Iron Cell (Molality)**
H^+	7.94E-08	3.16E-11
Fe^{+3}	5.93E-20	1.16E-31
Ca^{+2}	3.07E-03	7.50E-05
Mg^{+2}	1.79E-03	7.00E-05
HCO_3^-	2.28E-03	3.55E-11
Cl^-	1.10E-03	1.10E-03
$O_2(aq)$	1.00E-10	2.26E-73
TCE(aq)	9.10E-06	1.00E-10
cis-1,2-DCE(aq)	2.20E-06	4.20E-08
$C_2H_4(aq)$	1.00E-10	7.80E-07
SO_4^{-2}	1.88E-03	9.73E-11
NO_3^-	3.90E-05	3.59E-82

Mineralogically, the reactive cell is initially Fe^0 occupying 34 percent of the volume. A geochemically consistent aqueous initial condition for the reactive cell was calculated by OS3D using the following constraints: pH of 10.5; an arbitrarily small concentration (1.E-10 M) specified for total iron, total sulfate, total nitrate, total carbonate, total oxygen, and TCE; total calcium at 7.5E-5 M; total magnesium at 7.0E-5; total chloride at 1.1E-3 M; ethene at 7.8E-7M; and *cis*-1,2-DCE at 4.2E-8 M. The aqueous initial condition, summarized in Table 6, will essentially be flushed out of the system after 1 pore volume. From a modeling perspective, the initial condition should not result in nonphysical transients that significantly alter immobile phases.

Results

With $O_2(aq)$ nearly absent and chlorinated hydrocarbons at relatively low concentrations in the background aquifer, the reduction of water by iron oxidation is the dominant iron corrosion reaction as well as the principal mechanism for elevating pH and lowering the redox potential in the iron cell at Moffett Field. pH

and redox conditions control the behavior of many of the chemical components in the iron cell; consequently, any attempt to reproduce spatially variable concentrations of chemical components in the iron cell must first consider the interplay between this relatively slow hydrolysis reaction and the rate of transport, which controls the residence time in the iron cell. Based on the laboratory column studies and the field observations, there is a range of possible rates for the hydrolysis reaction (intrinsic rate constant $\leq 5 \times 10^{-12}$ mol/m^2/s) and water flux (0.04–0.40 m/day (0.13-1.3 ft/day)) in the iron cell. In this case, however, there is only one combination that can systematically account for the observed behaviors in the iron cell: a hydrolysis reaction rate constant of 5×10^{-12} mol/m^2/s and a Darcy velocity of 0.04 m/day. A slower hydrolysis reaction rate would require a Darcy velocity below the lowest field estimate, whereas a faster Darcy velocity would require a hydrolysis reaction rate greater than observed in the laboratory.

The subsequent discussion is based on the incorporation of the aforementioned rates into an OS3D simulation of the Moffett Field funnel and gate treatment system for one year of operation, April 1996 to April 1997. One-dimensional modeling results are compared with field observations from 14 monitoring wells in the gate, of which 8 are designed for multilevel sampling. In general, the principal variability of the observed aqueous components is along the longitudinal axis of the gate. In the accompanying figures, the modeling results are compared with the projection of the three-dimensional field data onto this axis.

Chlorinated hydrocarbons. The modeled TCE concentrations reflect the rapid degradation observed in the field (Figure 21), supporting, to some degree, the TCE degradation rate derived in the laboratory. For *cis*-1,2-DCE, the laboratory rate used in the model appears to be high (Figure 21) as the *cis*-1,2-DCE is predicted to be eliminated after 0.1 m in the iron cell compared with 0.5 m observed in the field. Relative to the overall system of chemical components, the chlorinated hydrocarbon chemistry has minimal impact.

pH. The modeled pH tracks the observed rapid increase and plateau in the iron cell very well (Figure 22). The hydrolysis reaction, which acts to elevate pH, is always active throughout the iron cell. Conversely, protons are continually released during the precipitation of secondary minerals, buffering the initial pH increase at the iron cell entrance, and then stabilizing pH at 10.4 for the final 1.5 m (5 ft).

E_H. Modeled concentrations of redox couples were used to calculate E_H under the assumption of global redox equilibrium. All the redox couples are connected through the equilibrium reactions so it is not necessary to identify the dominant redox couple. The calculation is based on half redox reactions:

$$E_H = \frac{2.3RT}{F}\left(pe^0 - \log\frac{[Red]}{[Ox]}\right) \tag{7}$$
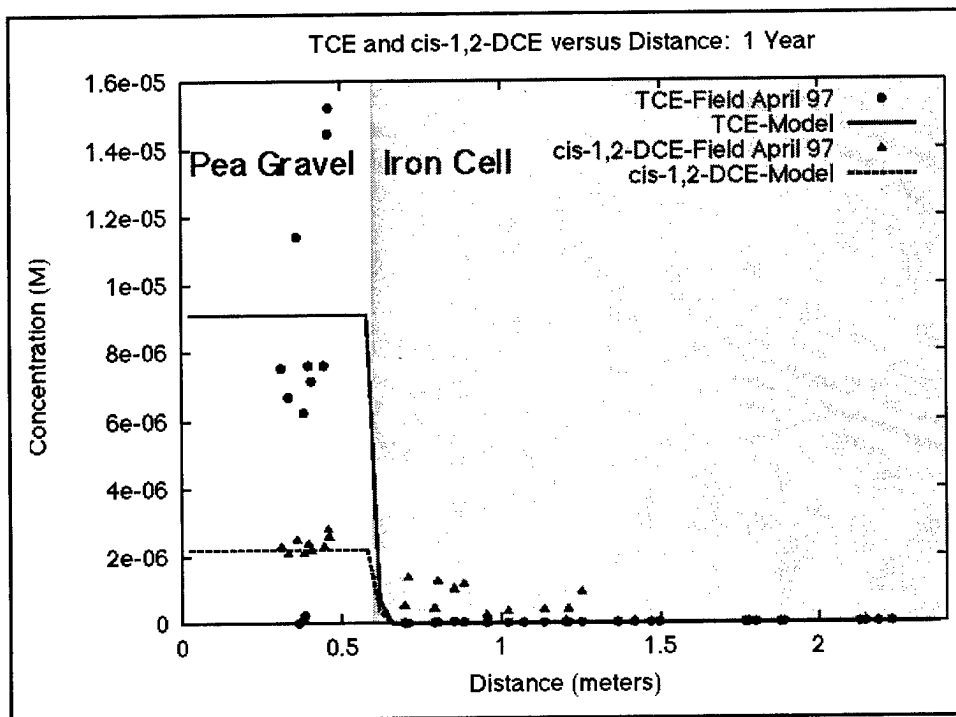
Figure 21. Comparison of model predictions and field observations after 1 year of reactive barrier operation: TCE and *cis*-1,2-DCE

Figure 22. Comparison of model predictions and field observations after 1 year of reactive barrier operation: pH

where

R = universal gas constant

T = temperature, °K

F = Faraday constant, electric charge of 1 mole of electrons, 96,500 coulombs

pe^0 = log (*equilibrium constant*)

$Ox + e^-$ = Red

Ox = oxygen concentration

For 25 °C, 2.3RT/F is 0.059 v.

The model reproduces the trend of positive E_H in the up-gradient aquifer and negative E_H in the iron cell; however, all predictions are more extreme, nearly double the field measurements (Figure 23). The reasons for this lack of agreement cannot be determined with certainty. However, it should be noted that measured species concentrations were available to calculate E_H in the aquifer for two of the redox couples. In this case, E_H for the $O_2(aq)/H_2O$ (720 mV) and $N_2(aq)/NO_3^-$ (690 mV) redox couples compare more favorably with the modeled E_H of 700 mV than the down-hole probe readings of ~300 mV.

Figure 23. Comparison of model predictions and field observations after 1 year of reactive barrier operation: E_H

Alkalinity (as CaCO₃). The modeled alkalinity reproduces the steady decrease from 0.003 M to 0.0002 M observed in the first 0.5 m (1.6 ft) of the iron cell (Figure 24). The decrease in alkalinity in the iron cell is due primarily to the precipitation of carbonate (siderite, aragonite) and hydroxide ($Fe(OH)_2$, ferrihydrite, brucite) minerals. In the model, carbonates are completely depleted from solution in the first 0.24 m (0.79 ft) of the iron cell. The predicted reduction of aqueous inorganic carbonates to methane is a relatively minor process, having little impact on alkalinity. Furthermore, the highest predicted methane concentration can be over an order of magnitude smaller than methane concentrations measured in the reactive cell. The elevated methane concentrations indicate the presence of an uncharacterized carbon source in the field; carbon impurities in the Peerless iron are known to be 3-4 percent (Fort 2000; Phillips et al. 2000).
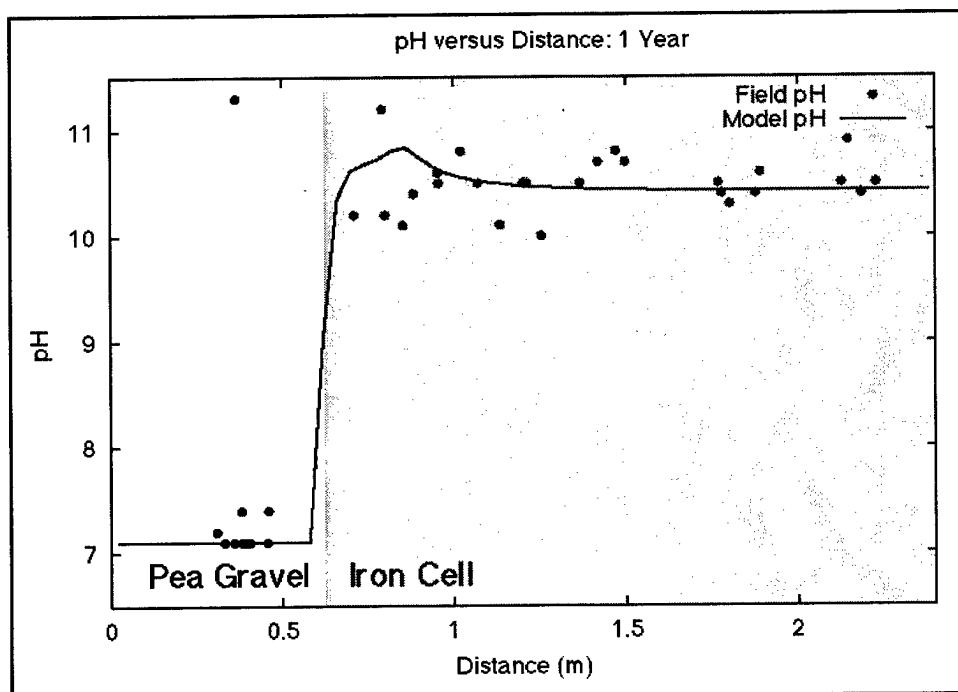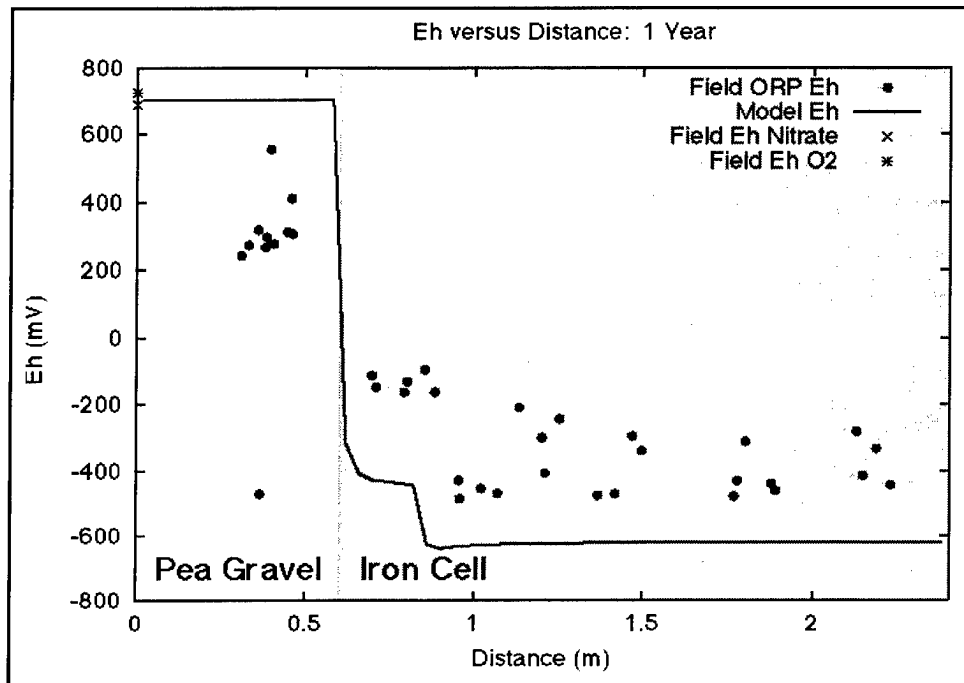

Figure 24. Comparison of model predictions and field observations after 1 year of reactive barrier operation: alkalinity (as CaCO₃)

Dissolved hydrogen. $H_2(aq)$ was not detected ($<4 \times 10^{-5}$ M) in the field despite being a product of the principal iron oxidation reaction that drives this chemical system. In the reactive transport model, $H_2(aq)$ concentrations increase until the dissolved gas pressure exceeds the hydrostatic pressure at middepth in the iron cell, 1.25 bars. At that point, hydrogen gas is assumed to outgas, maintaining a saturated concentration of 1×10^{-3} M.

Major ions. In the reactive transport model, magnesium is removed from solution by the precipitation of brucite. The predicted magnesium concentrations track the field observations very well (Figure 25), matching the decline and subsequent leveling from 2.7×10^{-3} M to less than 1×10^{-4} M over the first 0.3 m (10.98 ft) of the iron cell.

Figure 25. Comparison of model predictions and field observations after 1 year of reactive barrier operation: magnesium

Sulfate appears to have similar behavior with considerably more scatter in the field measurements (Figure 26). Two competing pathways for the removal of sulfate from solution are modeled: precipitation of green rust and reduction of sulfate to sulfide followed by precipitation of FeS(am). While the precipitation of green rust is a likely sulfur sink in the iron cell, the thermodynamics of this reaction limits the amount of sulfur that can be removed from solution. In contrast, the precipitation of FeS(am) is capable of removing essentially all of the aqueous sulfide in the iron cell. Since sulfate concentrations are very low after the first 0.5 m (1.6 ft) of the iron cell and sulfide is always below detection, it appears that aqueous sulfate that could not be precipitated as green rust is rapidly reduced to sulfide and removed from solution during the precipitation of FeS(am). This is precisely how sulfate removal in this system is modeled.

In the iron cell, nitrate transformation is so rapid and complete that nitrate is always below detection. Nitrate in the model is quickly reduced to ammonia via equilibrium homogeneous reactions that match the field observations quite well (Figure 27). $N_2(aq)$ does not appear to be part of the nitrate/ammonia redox chemistry as evidenced by fairly unchanging measurements in the field.

Calcium is also rapidly and nearly completely eliminated from solution in the iron zone. In this case, however, the precipitation thermodynamics of the secondary mineral, aragonite, can account for only half of the calcium (~0.002 M) that needs to be removed from solution. This implies that additional mechanisms for calcium to be removed from solution need to be investigated (e.g., precipitation of other calcium minerals, complexation of calcium on mineral surfaces).
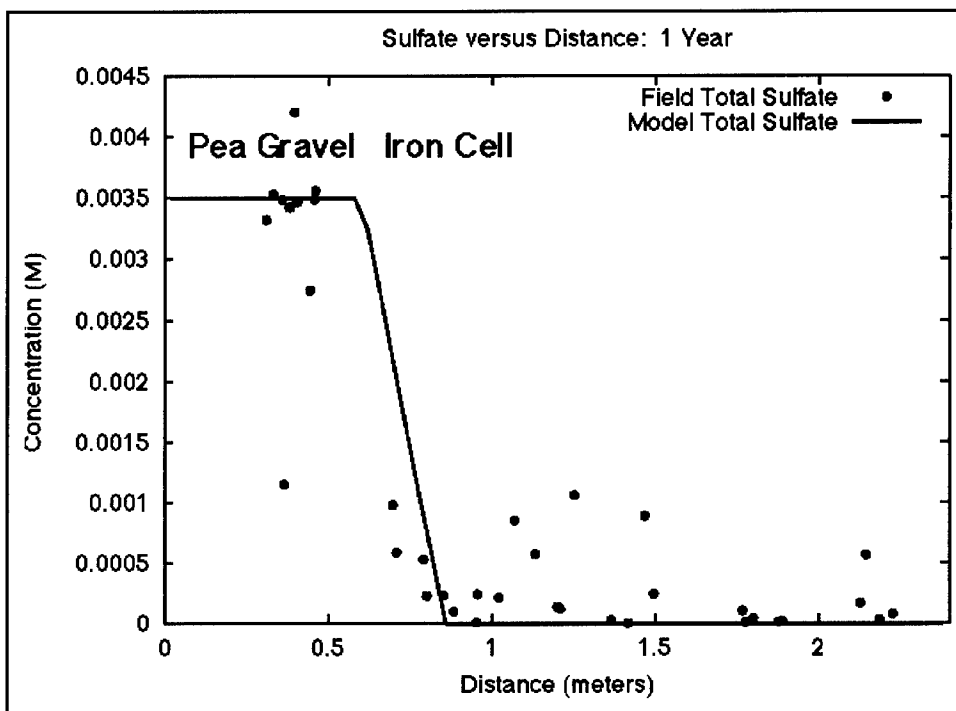
Figure 26. Comparison of model predictions and field observations after 1 year of reactive barrier operation: sulfate

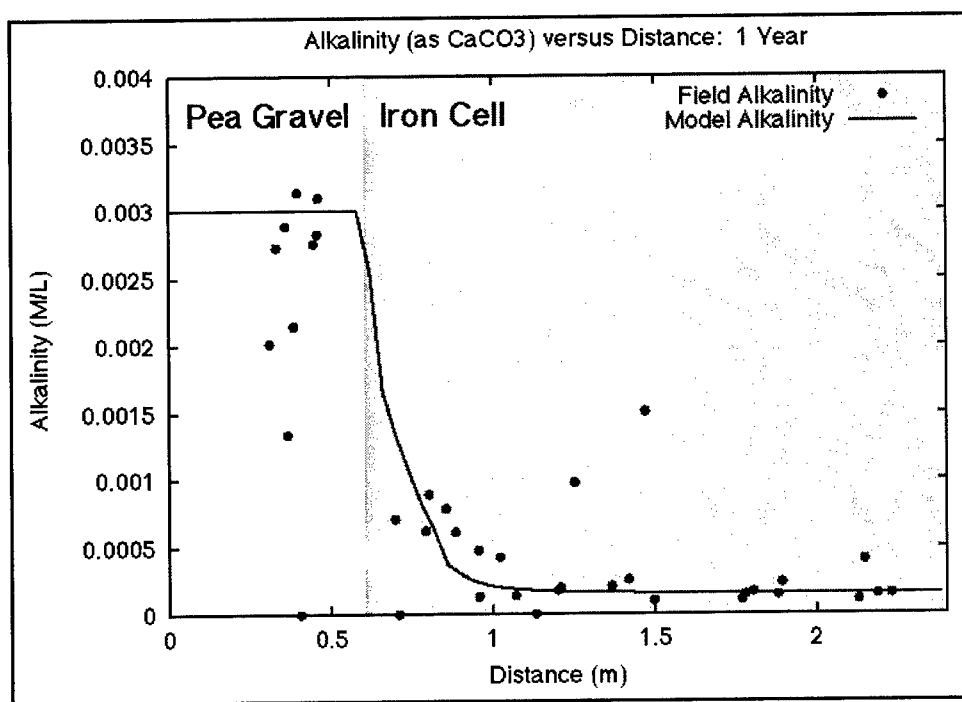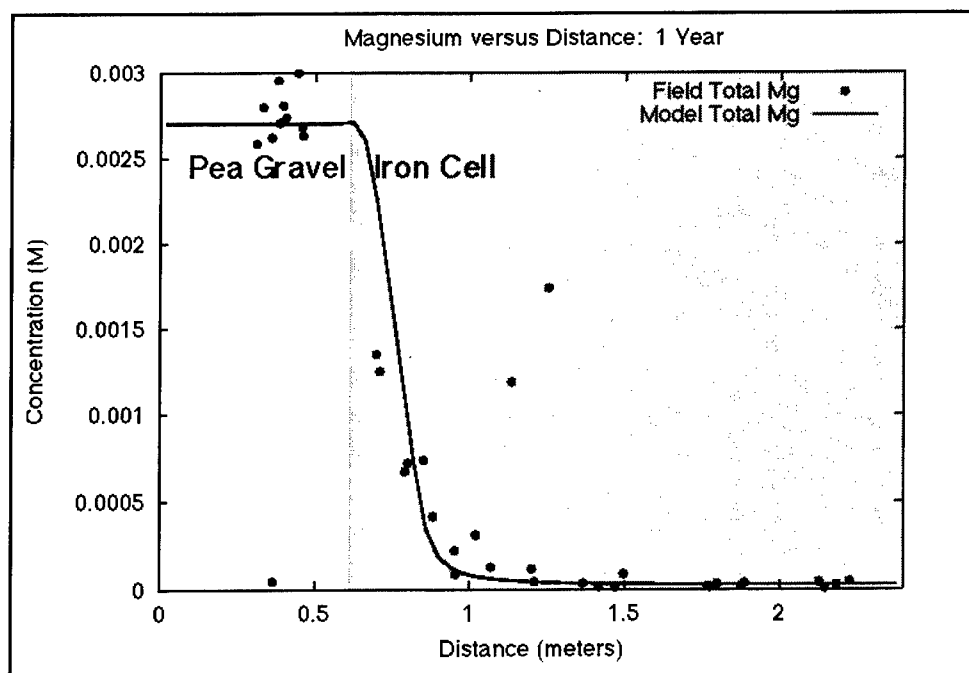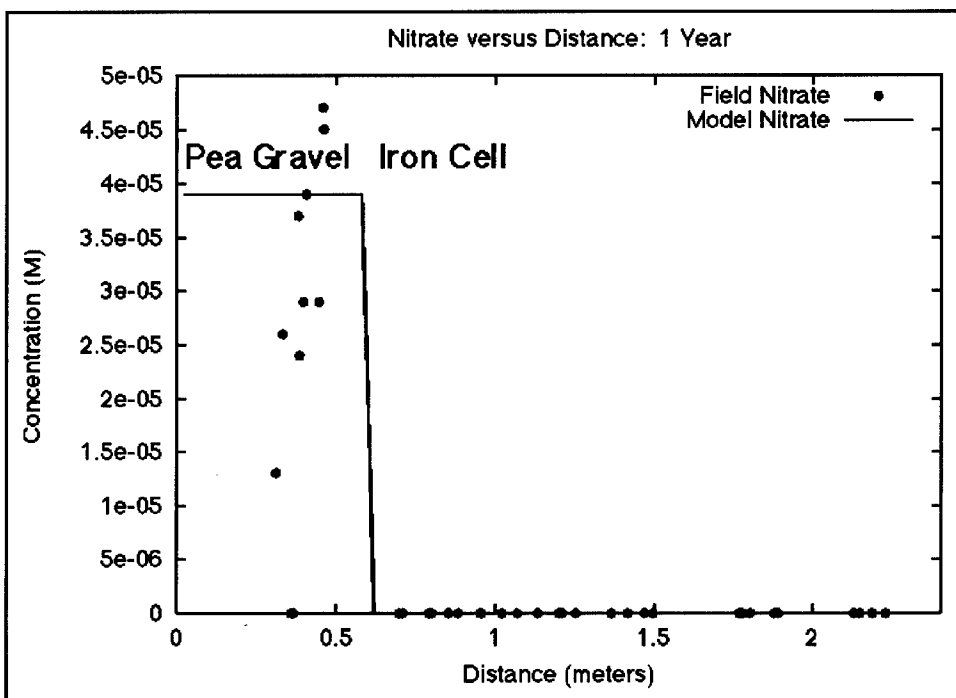
Figure 27. Comparison of model predictions and field observations after 1 year of reactive barrier operation: nitrate

Iron dissolution. The hydrolysis reaction is the dominant iron dissolution mechanism. In the first 0.3 m (0.98 ft) of the reactive cell, the predicted iron mineral volume fraction is reduced by 0.44 percent. Beyond this initial zone, the reduction is predicted to be uniformly 0.38 percent.

Secondary minerals. After 1 year of simulation, the precipitation of secondary minerals is predicted to be highest near the reactive cell entrance where aragonite and siderite dominate the new mineral assemblage (Figure 28). Porosity is reduced at this location from 0.6600 to 0.6344. FeS(am), green rust, brucite, and to a lesser degree, ferrihydrite, are actively precipitating over the initial 0.3 m (0.98 ft) of the iron cell, with moderate accumulations (mineral volume fractions <0.5 percent). After the first 15 cm of iron, the carbonate minerals are essentially absent and $Fe(OH)_2(am)$ comes to dominate the rest of the iron zone with a 1.4 percent mineral volume fraction. The model assumes that $Fe(OH)_2(am)$ is the stable phase.
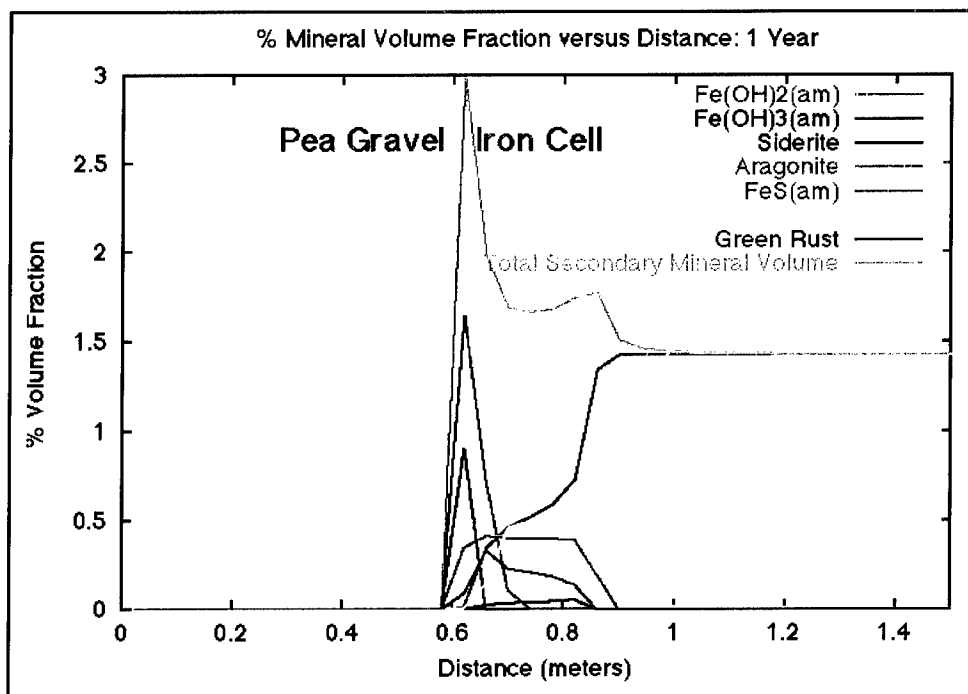
Figure 28. Predicted mineral volume fractions after 1 year of reactive barrier operation

Discussion

Reactive cell performance. The Darcy velocity of 0.04 m/day in conjunction with the hydrolysis rate from the laboratory (5×10^{-12} mol/m^2/s) was clearly consistent with the observed behavior of pH, alkalinity, Mg, SO_4^{2-}, and NO_3^-. However, this should be a concern because the preconstruction Darcy velocity in the

Mineral precipitation in the iron cell could potentially shorten the longevity of the reactive barrier and thus is of concern to the future deployment of similar in situ chemical treatment technologies. In the initial part of the iron zone there is a net reduction in porosity of 0.015-0.03 each year, due principally to the precipitation of aragonite and siderite. If the precipitation is confined only to the entrance of the iron zone, there could be significant reduction in porosity and permeability over many years that would result in the buildup of head on the up-gradient side of the iron barrier. Furthermore, the predicted volume of out-gassed hydrogen is significant, and it is possible that hydrogen gas bubbles are occupying a portion of the void space, resulting in a reduction of permeability. Precipitation of secondary minerals also has the potential to alter the reactivity of the iron cell. Iron surfaces may become less accessible to the aqueous components in the groundwater, and/or the precipitated secondary minerals may provide new sites for sorption and nucleation. The modeling results underscore the need for more detailed studies of the nucleation mechanics of secondary minerals on Fe^0 surfaces.

Ammonia was not part of the sampling program but was included in the modeling because it is a hazardous chemical and part of the nitrate redox couple that was postulated to be active in the iron cell. The modeling shows ammonia to be a thermodynamically favored component that is consistent with the disappearance of nitrate in the iron cell and the lack of significant change to the $N_2(aq)$ concentrations. It should be considered for field sampling analyses at iron barrier sites whenever nitrate is known to be present.

Model assessment. The reactive transport system is the amalgam of several interdependent processes. The ability to mechanistically simulate the multifaceted behavior of this system without significant calibration reflects the quality and consistency of the data, and builds confidence in the conceptualization of the system.

Modeling provided a way to test the understanding of reactive transport at the Moffett Field Site and a way to systematically identify plausible process mechanisms. The flow through the reactive barrier and the selection of chemical components are based on field observations. Once these decisions are made, there are very few "knobs" to tune the model. The stability constants for all the reactions are from well-established databases and are not adjustable. Furthermore, boundary and initial concentrations for the selected species are constrained by total concentrations measured in the field and speciation that satisfy the reaction thermodynamics. In this study, the reaction rates are derived from the literature, not calibrated. The fidelity of the model predictions with field observations is good; and where discrepancies do exist, the mechanistic modeling approach provides insight on what processes need to be examined and how they might be updated.

Using 36 chemical components and 8 minerals to model a system may appear to be too complicated for routine engineering of an in situ reactive barrier; however, the model was built up in a straightforward fashion from the observed behavior in the system. Because of the systematic coupling of transport and reactions for multiple chemical components, simply adjusting precipitation rates to match the disappearance of certain ions will not necessarily be consistent with other measured properties of the reactive cell (e.g., pH, alkalinity). Furthermore,

the reaction rates are operating within the context of flowing groundwater. The character of spatial variations in species concentrations in the reactive cell is the direct result of the interplay between rates of transport and rates of reaction.

Engineered in situ reactive cells are highly amenable to reactive transport modeling. The system being modeled is better controlled and characterized than most environmental situations. In this case, the chemical components and their concentrations entering the reactive cell were comprehensively studied and Fe^0 was initially the only mineral in the cell.

GMS Implementation

In the GMS, the OS3D reactive transport simulator can be used in a stand-alone mode or in conjunction with multidimensional flow fields generated by the MODFLOW groundwater flow simulator. In standalone mode, OS3D can solve batch and reaction path chemistry and reactive transport systems with steady, uniform velocity fields in one, two, and three dimensions. OS3D coupling with the MODFLOW groundwater flow simulation application allows for reactive transport in steady or transient, nonuniform, multidimensional flow fields. This linkage occurs through (a) the transfer of hydrologic problem specification parameters from MODFLOW (e.g., model dimensionality and geometry, time-stepping, spatial distribution of properties) to OS3D using the GMS interface; and (b) the generation of output files (velocities, sources, sinks) by the GMS version of MODFLOW that are read by OS3D.

The GMS interface for OS3D was still under development at the time this report was written, but the plan is to have the GMS interface take the user through the OS3D input data specification, which includes solution options as well as the transport and chemistry. Default values will exist for all solution options. Generally, the principal tasks for the user will be to specify the transport parameters, primary and secondary chemical species, minerals, kinetic rates, and constraints for the geochemical conditions. Transport parameters that can be specified by the user will be spatially variable diffusion coefficients, dispersivities, and the ability to account for tortuosity through formation factors as well as cementation factors. These can be specified using the GMS interface for cell properties. Temperature-dependent diffusion can be specified with an activation energy.

For the chemistry, the user will be presented with a list of primary species to select from. Once the list of primary species is set, the user will then be presented with a list of all possible secondary species to select from. The user has the option to select all the possible secondary species, which can be useful during the pre-liminary screening of species for inclusion in the model. With the primary and secondary species lists, OS3D will automatically define the stoichiometry and stability constants for each reaction (including minerals). The user can then build speciated geochemical conditions (i.e., sets of equilibrated species concentrations) that honor particular constraints for the primary species. For each geochemical condition, the GMS interface will present the user with a choice of one of six possible constraints that are to be used for each of the primary species: fixed total concentration, fixed species concentration, fixed activity, equilibrium with a

selected mineral, equilibrium with a selected gas at a selected partial pressure, and concentration that charge-balances the solution. It is at this point that the user will eliminate species with relatively small concentrations from the final set of modeled species. The GMS interface will allow the user to iteratively build, modify, and speciate a set of chemical components for the modeling study. Once the user is satisfied with the set of chemical components and speciated geochemical conditions, the conditions can then be assigned to specific cell locations as boundary and/or initial conditions.

A restart option can be invoked that will allow a previously run simulation to continue from the last saved time plane when it was originally terminated. The saved restart file can also be used as the initial condition for a new simulation that uses the same problem geometry and chemical components. Results that can be reported include total and individual species concentrations; mineral saturation state, reaction rates, and volume fractions; and aqueous reaction rates. A variety of options for writing results to files are available to the user including time series of selected component concentrations at specific locations and snapshots of the entire spatial domain at a given time. GMS visualization utilities can then be used to examine spatial and temporal distributions of selected parameters.

Recommendations

OS3D is recommended for use on multidimensional advection-diffusion-reaction problems where the numerical stability criteria for the advective transport scheme does not severely limit the time-step size relative to the desired simulation periods. It appears to be an ideal design and performance assessment tool for in situ chemical treatment as well as other subsurface characterization and engineering activities.

The OS3D simulator can be operated by users of varying expertise in reactive transport modeling but does require familiarity with basic concepts of hydrogeology and aqueous chemistry. The user is expected to specify reasonable and appropriate sets of primary and secondary species, minerals, reaction kinetics, and sorption parameters, as well as meaningful geochemical conditions.

The user should understand that while the thermodynamics of most inorganic chemical reactions of interest are well known and exist in the EQ3/EQ6 database, some of these reactions are kinetically controlled with rate laws that are generally developed under specific experimental conditions. To get the most benefit from the OS3D simulation technology, the user should become familiar with the supported rate law forms and be prepared to modify and augment the default database.

The solver technology in OS3D has been shown to be quite robust in solving a variety of nonlinear reaction systems under computationally demanding conditions; however, convergence is not guaranteed. It is recommend that users not adjust the convergence criteria unless they have a full appreciation for the potential consequences these adjustments may have on the accuracy of the simulation.

Because of the large number of chemical components that might be employed, a minimum of 128 MB of memory for general use and 256–512 MB of memory for larger three-dimensional problems are recommended. Large, high-resolution three-dimensional problems should be run using the parallel processing version of OS3D.

6 Conclusions

Four simulators for modeling in situ subsurface remediation were advanced and incorporated into the GMS during this project: MT3DMS/SEAM3D, UTCHEM, NUFT, and OS3D. The latest version of the OS3D code is now being referred to as CRUNCH. These four simulators are a significant advancement in the present status of subsurface modeling for remediation evaluation and design. Each of these four simulators has unique capabilities for simulating innovative in situ treatment technologies. There is some overlap of these models in terms of capabilities, but this is viewed as an advantage.

The MT3DMS code is a multispecies transport code with significant advancements over the previous version, MT3D. MT3DMS is the transport module for SEAM3D and RT3D, both reactive models in the GMS. SEAM3D has many features for simulating intrinsic and engineered bioremediation. The model can handle the full suite of aerobic and anaerobic degradation processes for petroleum and chlorinated hydrocarbons under saturated flow conditions.

The UTCHEM code is probably the most versatile of the simulators as it allows for multiphase, multicomponent flow and transport. The primary emphasis of this model is simulating surfactant and cosolvent flushing of the oil phase. UTCHEM is not well suited for simulating some other multiphase flow problems, such as soil venting and steam injection. However, the model also has modules for simulating bioremediation and geochemical reactions, although features for the latter module have not been interfaced with the GMS. UTCHEM will handle variably saturated flow conditions.

The NUFT code also simulates multiphase, multicomponent flow and transport. NUFT was originally developed for simulating steam injection and soil heating and venting technologies for in situ remediation. Thus, this code is well suited for these types of applications, but it is not well suited for modeling surfactant and cosolvent flushing technologies for oil removal. NUFT also has a bioreactions component, but this feature has not been interfaced with the GMS. NUFT will handle variably saturated flow conditions.

The OS3D code is a versatile geochemical code best suited for in situ chemical treatment technologies, such as permeable treatment walls. This model is intended only for application to groundwater plumes under saturated flow conditions.

At the time of this publication, three of the four featured simulators, plus MT3DMS, have been implemented into the GMS. Work on implementing OS3D was still in progress. Tutorials for all of these simulators either have been or are being developed to aid users in applications. As a result of this project, the GMS now has extensive capabilities for modeling a wide array of subsurface and groundwater flow and reactive transport problems involving a host of cleanup and/or management alternatives.

Some of the advanced features of these simulators will present a challenge for less experienced groundwater modelers. Thus, it is recommended that modelers take the time to become closely acquainted with the model processes being used. Due to the comprehensive features of these four simulators, these models are well suited for detailed design and evaluation of in situ treatment alternatives prior to field-scale implementation. However, with the Map Tool and other site conceptualization/characterization features of the GMS, once a site study has been set up, it is relatively straightforward to apply various GMS models to the site, enabling multiple simulation alternatives to be conducted and evaluated expeditiously, even during the alternatives screening phase of a project. The GMS models will provide an invaluable tool for improving subsurface, in situ remediation selection, design, and operation, thus potentially providing significant reductions in site cleanup costs.

References

Appelo, C. A. J., and Postma, D. (1993). *Geochemistry, groundwater, and pollution.* Balkema, Rotterdam.

Aziz, K., Ramesh, A. B., and Woo, P. T. (1987). "Fourth SPE Comparative Solution Project - A comparison of steam injection simulators," *Journal of Petroleum Technology* 39(12), 1576-1584.

Battelle. (1998). "Performance evaluation of a pilot-scale permeable reactive barrier at Former Naval Air Station Moffett Field, Mountain View, California," Prepared for Naval Facilities Engineering Service Center, Port Hueneme, CA.

Beljin, M. S. (1988). "Testing and validation of models for simulating solute transport in groundwater," GWMI 88-11, International Groundwater Modeling Center, Golden, CO.

Bethke, C. M. (1996). *Geochemical reaction modeling.* Oxford University Press, New York, 397 pp.

Brauner, J. S., and Widdowson, M. A. "Numerical simulation of a natural attenuation experiment with a NAPL source: Contaminant dissolution and reactive transport" (accepted for publication), *Ground Water.*

Brown, C. L. (1993). "Simulation of surfactant enhanced remediation of aquifers contaminated with dense non-aqueous phase liquids," M.S. thesis, University of Texas at Austin.

Brown, C. L., Delshad, M., Dwarakanath, V., McKinney, D. C., and Pope, G. A. (1996). "Design of a field-scale surfactant enhanced remediation of a DNAPL contaminated aquifer." Presented at the *ACS Industrial and Engineering Chem. Div. Special Symposium,* American Chemical Society, Birmingham, AL, Sept. 9-12, 1996. Abstract.

Carrigan, C. R. (1999). "Understanding the fate and transport of multiphase fluid and colloidal contaminants in the vadose zone using an intermediate-scale field experiment," Report No. UCRL-JC-133819, Lawrence Livermore National Laboratory, Livermore, CA.

Carrigan, C. R., and Nitao, J. J. (2000). "Predictive and diagnostic simulation of in situ electrical heating in contaminated, low-permeability soils," *Environmental Science and Technology* 34(22), 4835-4841.

Carrigan, C. R., Heinle, R. A., Hudson, G. B., Nitao, J. J., and Zucca, J. J. (1996). "Trace gas emissions on geological faults as indicators of underground nuclear testing," *Nature* 382, 528-531.

Chien, M. C. H., and Northrup, E. J. (1993). "Vectorization and parallel processing of local grid refinement and adaptive implicit schemes in a general purpose reservoir simulator." 12th SPE Symposium on Reservoir Simulation, New Orleans, LA, U.S.A., February 28-March 3, 1993. Society of Petroleum Engineers, Dallas, TX, Paper No. 25258.

Davis, J. A., and Kent, D. B. (1990). "Surface complexation modeling in aqueous geochemistry." *Mineral-water interface geochemistry*. Reviews in Mineralogy 23, M. F. Hochella and A. F. White, ed., Mineral Society of America, Washington, DC, 177-260.

de Blanc, P. C. (1998). "Development and demonstration of a biodegradation model for non-aqueous phase liquids in groundwater," Ph.D. dissertation, University of Texas at Austin.

Demir, Z., Ferry, L., Green-Horner, L. K., Madrid, V., Maley, M., Mansoor, K., and Haar, S. V. (1999). "Assessment of impact to ground water from vadose zone sources for the site 300 site-wide feasibility study," Report No. UCRL-AR-135312, Lawrence Livermore National Laboratory, Livermore, CA.

Duke Engineering and Services. (1998). "Demonstration of surfactant-enhanced aquifer remediation of chlorinated solvent DNAPL at Operable Unit 2, Hill AFB, Utah," prepared by Duke Engineering and Services for Air Force Center for Environmental Excellence and OO-ALC/EMR, Hill AFB, Ogden, UT.

Fort, J. R. (2000). "Physical performance of granular iron reactive barriers under aerobic and anaerobic conditions," M.S. Thesis, University of Wisconsin, Madison, WI.

Hadala, P. F., Butler, D. K., Cullinane, M. J., Holland, J. P., May, M., and McDaniel, T. (1993). "Army groundwater modeling use and needs workshop," Technical Report IRRP-93-1, U.S. Army Engineer Waterways Experiment Station, Vicksburg, MS.

Hansen, H. C. B., Borggaard, O. K., and Sorensen, J. (1994). "Evaluation of free energy of formation of iron (II), iron (III) -hydroxide-sulfate (green rust) and its reduction of nitrite," *J. Geochim. Cosmochim. Acta* 58(12), 2599-2608.

Jin, M. (1995). "A study of nonaqueous phase liquid characterization and surfactant remediation," Ph.D. diss., The University of Texas at Austin.

Jin, M., Jackson, R. E., Pope, G. A., and Taffinder, S. (1997). "Development of partitioning tracer tests for characterization of nonaqueous-phase liquid-contaminated aquifers," SPE 39293 Proceedings of the SPE 72nd Annual Technical Conference and Exhibition (919-930), San Antonio, TX, 5-8 October 1997.

Johnson, T. L., Scherder, M. M., and Tratnyek, P. G. (1996). "Kinetics of halogenated organic compound degradation by iron metal," *Environ. Sci. Technol.* 30, 2634-2640.

Julian, H. E., Boggs, J. M., Zheng, C., and Feehley, C. E. "Numerical simulation of a natural gradient tracer experiment for the natural attenuation study: Flow and physical transport" submitted to *Ground Water*.

Kueper, B. H. (1989). "The behavior of dense, non-aqueous phase liquid con-taminants in heterogeneous porous media," Ph.D. dissertation, University of Waterloo, Ontario, Canada.

Lasaga, A. C. (1984). "Chemical kinetics of water-rock interactions," *Journal Geophysical Research* 89, 4009-4025.

Lee, K., and Nitao, J. J. (2000). "Geostatistical characterization and numerical modeling of the vadose zone transport of tritium released from an under-ground storage tank," Report No. UCRL-JC-131756, Lawrence Livermore National Laboratory, Livermore, CA.

Lennie, A. R., and Vaughan, D. J. (1996). *Mineral spectroscopy.* Special Publication No. 5, The Geochemical Society, M. D. Dyar, C. McCammon, and M. W. Schaefer, ed., St. Louis, MO.

Lin, H-C. J., Richards, D. R., Yeh, G-T., Cheng, J-R., Cheng, H-P., and Jones, N. L. (1997). "FEMWATER: A three-dimensional finite-element computer model for simulating density dependent flow and transport," Technical Report CHL-97-12, U.S. Army Engineer Waterways Experiment Station, Vicksburg, MS.

Martino, R. "Comparison between field data and UTCHEM simulations for the SEAR demonstration at Hill Air Force Base, Utah" (in preparation), Internal report for SERDP, U.S. Army Engineer Research and Development Center, Vicksburg, MS.

Mayer, K. U. (1999). "A numerical model for multi-component reactive transport in variably saturated porous media," Unpublished Ph.D. diss., University of Waterloo, Waterloo, Canada.

Maxwell, R. M., Tompson, A. F. B., Rambo, J. T., Carle, S. F., and Pawloski, G. A. (2000). "Thermally induced groundwater flow resulting from an underground nuclear test." *Computational methods in water resources*, Proceedings of the XIII International Conference on Computational Methods in Water Resources, Calgary, Canada, June 25-29, 2000. L. R. Bentley, J. F. Sykes, C. A. Brebbia, W. G. Gray, and G. F. Pinder, ed., A. A. Balkema, Rotterdam, the Netherlands.

McDonald, M. G., and Harbaugh, A. W. (1988). "A modular three-dimensional finite-difference ground-water flow model," *Techniques of water-resources investigations* 06-A1, U.S. Geological Survey, Reston, VA.

McGrath, C. J. "Cosolvent enhanced recovery of non-aqueous phase liquids (NAPL) from saturated porous media by ethanol flushing B physical and numerical modeling" (in preparation), Ph.D. diss., University of Virginia, Charlottesville, VA.

Newmark, R., and Aines, R. (1998). "They all like it hot: Faster cleanup of contaminated soil and groundwater," Report No. UCRL-ID-130186, Lawrence Livermore National Laboratory, Livermore, CA.

Newmark, R. L., Aines, R. D., Knauss, K. G., Leif, R. N., Chiarappa, M., Hudson, G. B., Carrigan, C. R., Nitao, J. J., Tompson, A., Richards, J., Eaker, C., Weidner, R., and Sciarotta, T. (1999). "Visalia field tests," Report No. UCRL-JC-136771, Lawrence Livermore National Laboratory, Livermore, CA.

Nitao, J. J. (1998a). "Reference manual for the NUFT flow and transport code, version 2.0," Report UCRL-MA-130651, Lawrence Livermore National Laboratory, Livermore, CA.

_____. (1998b). "User's manual for the USNT module of the NUFT code, version 2.0 (NP-phase, NC-component, thermal)," Report UCRL-MA-130653, Lawrence Livermore National Laboratory, Livermore, CA.

Nitao, J. J., and Buscheck, T. A. (1995). "Discrete-fracture modeling of thermal-hydrological processes at Yucca Mountain and the LLNL G-tunnel field test." *Scientific Basis for Nuclear Waste Management XIX*. W. M. Murphy and E. K. Knecht, ed., Materials Research Society, Boston, MA, 747-754.

Nitao, J. J., Martins, S. A., and Ridley, M. N. (2000). "Field validation of the NUFT code for subsurface remediation by soil vapor extraction," Report No. UCRL-ID-141546, Lawrence Livermore National Laboratory, Livermore, CA.

Parkhurst, D. L. (1995). "User's guide to PHREEQC - a computer program for speciation, reaction-path, advective-transport, and inverse geochemical calculations," Water Research Investigations Report 95-4227, U.S. Geological Survey, Reston, VA.

Phillips, D. H., Gu, B., Watson, D. B., Roh, Y., Liang, L., and Lee, S. Y. (2000). "Performance evaluation of a zero-valent iron reactive barrier: Mineralogical characteristics," *Environ. Sci. Technol.* 34(19), 4169-4176.

Pope, G. A., and Nelson, R. C. (1978). "A chemical flooding compositional simulator," *Soc. Petrol. Engr. Jour.* 18, 339-354.

PRC Environmental Management, Inc. (1995). "Iron Curtain Bench-Scale Study Report, Moffett Federal Airfield, California," Prepared for the Department of the Navy, Contract No. N62474-88-D-5086, Task Order No. 0237, San Bruno, CA.

Reservoir Engineering Research Program. (2000a). "UTCHEM-9.0: A three-dimensional chemical flood simulator; Volume I: User's guide," Reservoir Engineering Research Program (RERP), Center for Petroleum and Geosystems Engineering, The University of Texas at Austin, Austin, TX.

_____. (2000b). "UTCHEM-9.0: A three-dimensional chemical flood simulator; Volume II: Technical documentation," Reservoir Engineering Research Program (RERP), Center for Petroleum and Geosystems Engineering, The University of Texas at Austin, Austin, TX.

Roberts A. L., Totten, L. A., Arnold, W. A., Burris, D. R., and Campbell T. J. (1996). "Reductive elimination of chlorinated ethylenes by zero-valent metals," *Environ. Sci. Technol.* 30(8), 2654-2659.

Rueth, L. S., Ferry, R. A., Green-Horner, L. K., DeLorenzo, T. H. (1998). "Remedial design document for the General Services Area Operable Unit treatment facilities," Lawrence Livermore National Laboratory, Site 300, Report No. UCRL-AR-127465, Lawrence Livermore National Laboratory, Livermore, CA.

Sahni, A., Kumar, M., and Knapp, R. B. (2000). "Electromagnetic heating methods for heavy oil reservoirs," Report No. UCRL-JC-138802, Lawrence Livermore National Laboratory, Livermore, CA.

Semprini, L., and McCarty, P. L. (1991). "Comparison between model simulations and field results for in situ biorestoration of chlorinated aliphatics: Part 1. Biostimulation of methanotrophic bacteria," *Ground Water* 29(3), 365-374.

_____. (1992). "Comparison between model simulations and field results for in situ biorestoration of chlorinated aliphatics: Part 2. Co-metabolic transformations," *Ground Water* 30(1), 37-44.

Starr, R. C., and Cherry, J. A. (1994). "In situ remediation of contaminated groundwater: The funnel and gate system," *Ground Water* 32(3), 465-476.

Steefel, C. I. "CRUNCH, software for multicomponent-multidimensional reactive transport, user manual and programmer's guide" (in preparation), Lawrence Livermore National Laboratory, Livermore, CA.

Steefel, C. I. (2000). "New directions in hydrogeochemical transport modeling: Incorporating multiple kinetic and equilibrium reaction pathways." *Computational methods in water resources,* Proceedings of the XIII International Conference on Computational Methods in Water Resources, Calgary, Canada, June 25-29, 2000. L. R. Bentley, J. F. Sykes, C. A. Brebbia, W. G. Gray, and G. F. Pinder, ed., A. A. Balkema, Rotterdam, the Netherlands, 331-338.

Steefel, C. I., and Yabusaki, S. B. (1996). "OS3D/GIMRT, software for multicomponent-multidimensional reactive transport, user manual and programmer's guide," Technical Report PNL-11166, Pacific Northwest National Laboratory, Richland, WA.

Sun, Y., Demir, Z., Delorenzo, T., and Nitao, J. J. (2000). "Application of the NUFT code for subsurface remediation by bioventing," Report No. UCRL-ID-137967, Lawrence Livermore National Laboratory, Livermore, CA.

Tompson, A. F. B., Bruton, C. J., Pawloski, G. A., Smith, D. K., Bourcier, W. L., Shumaker, D. E., Kersting, A. B., Carle, S. F., and Maxwell, R. M. (2000). "On the evaluation of groundwater contamination from underground nuclear tests," Report UCRL-JC-140435, Lawrence Livermore National Laboratory, Livermore, CA.

U.S. Environmental Protection Agency. (1999). "Field application of in situ remediation technologies: Permeable reactive barriers," EPA 542-R-99-002, U.S. Environmental Protection Agency, Washington, DC.

Waddill, D. W., and Widdowson, M. A. (1998). "Three-dimensional model for subsurface transport and biodegradation," *ASCE J. Environ. Engr.* 124(4), 336-344.

_____. (2000). "SEAM3D: A numerical model for three-dimensional solute transport and sequential electron acceptor-based biodegradation in ground water," Technical Report ERDC/EL TR-00-18, U.S. Army Engineer Research and Development Center, Vicksburg, MS.

Wolery, T. J. (1992). "EQ3/6, a software package for geochemical modeling of aqueous systems, package overview and installation guide, Version 7.0," Technical Report UCRL-MA-110662 Part I, Lawrence Livermore National Laboratory, Livermore, CA.

Wu, W. J., Delshad, M., Oolman, T., and Pope, G. A. (2000). "Remedial options for creosote contaminated sites," *Ground Water Monitoring and Remediation,* Winter, 2000, 78-86.

Yabusaki, S. B., Cantrell, K. J., Sass, B. M., and Steefel, C. I. (2001). "Multi-component reactive transport in an in situ zero-valent iron cell," *Environmental Science and Technology* 35(7), 1493-1503.

Zheng, C. (1990). "MT3D: A modular three-dimensional transport model for simulation of advection, dispersion and chemical reactions of contaminants in groundwater systems," S. S. Papadopulos and Associates, Rockville, MD.

Zheng, C., and Wang, P. P. (1999). "MT3DMS: A modular three-dimensional transport model for simulation of advection, dispersion, and chemical reactions of contaminants in ground water systems," Contract Report SERDP-99-1, U.S. Army Engineer Research and Development Center, Vicksburg, MS.

Zheng, C., Wang, P. P., and Dortch, M. S. "A general third-order TVD scheme for modeling advection-dominated solute transport in porous media," submitted to *Ground Water*.

Appendix A
Publications

This appendix lists all previous publications partially or fully resulting from the SERDP CU-1062 project. This list includes peer-reviewed papers that are either still in press or in review and are expected to be accepted for publication. The section at the end of this appendix lists those remaining publications for this work unit that were still in preparation at the time that this report was prepared. These papers/reports are expected to be published or submitted for publication during 2001.

Abstracts of Presentations

Brown, C. L., Delshad, M., McKinney, D. C., Pope, G. A., and Wade, W. H. (1997). "Demonstration of surfactant flooding of an alluvial aquifer contaminated with DNAPL," presented at the 5th Chemical Congress, November 11-15, 1997, Cancun, Mexico.

de Blanc, P. C., Brown, C. L., McKinney, D. C., Speitel, G. E., and Pope, G. A. (1997). "Design of a bioremediation system to remove residual surfactant and chlorinated solvents from an aquifer following surfactant flushing," presented at the National Ground Water Association National Convention and Exposition, September 3-6, 1997, Las Vegas, Nevada.

McGrath, C. J., Dortch, M. S., and Ruiz, C. E. (1997). "Development of simulators for in-situ remediation evaluation, design, and operation," poster presentation for 3rd Annual SERDP Symposium, December 3-5, 1997, Washington, DC.

McGrath, C. J., and Zakikhani, M. (1998). "Numerical modeling of the natural attenuation of explosives," presented at the 3rd Tri-Service Environmental Technology Workshop, 18-20 August, San Diego, CA.

Pope, G. A., McKinney, D. C., Delshad, M., and Brown, C. L. (1997). "A successful example of predictive modeling of a surfactant remediation field test," presented at the 4th SIAM Conference on Mathematical and Computational Issues in the Geosciences, June 16-19, 1997, Albuquerque, New Mexico.

Pope, G. A., Delshad, M., Wang, C., and Wade, W. (1997). "Characterization and surfactant remediation of multicomponent NAPLs," invited presentation, Amer. Geophysical Union (AGU), Fall Meeting, *EOS*, Transactions of AGU, 78(46, suppl.), p. F261.

Yabusaki, S. B. (1997). "Implementing reactive transport algorithms on multi-processor computers," presented at a Workshop on Subsurface Reactive Transport Modeling, October 29-November 1, 1997, Richland, WA.

_____. (1998). "Reactive transport in a funnel and gate treatment system," presented at the AGU Spring Meeting, May 26-29, 1998, Boston, MA.

_____. (1998). "Modeling transport reactions in nonuniform flows," presented at the Gordon Research Conference on Modeling of Flow in Permeable Media, August 2-7, 1998, Proctor, NH.

_____. (1998). "In situ chemical treatment in a funnel and gate treatment system," presented at the 2nd Annual Department of Defense Environmental Security Modeling and Simulation Conference, May 4-6, 1998, Alexandria, VA.

Zakikhani, M., McGrath, C. J., and Pennington, J. C. (1997). "Study of natural attenuation of selected explosive chemicals at a DoD site," presented at the International Conference on Advances in Groundwater Hydrology, A Decade of Progress, Am. Inst. of Hydrology, November 16-20, 1997, Tampa, FL.

Zheng, C., Wang, P. P., and Dortch, M. S. (1997). "Three-dimensional modeling of multicomponent transport in heterogeneous aquifer: The ULTIMATE conservative difference scheme," presented at Amer. Geophysical Union (AGU), Spring Meeting, *EOS,* Transactions of AGU, 78(7).

Internal Reports

Martino, R. (1999). "Comparison between field data and UTCHEM simulations for the SEAR demonstration at Hill Air Force Base, Utah," Internal report for SERDP, May 1999, U.S. Army Engineer Research and Development Center, Vicksburg, MS.

McGrath, C. J. (1997). "The use of isotopic data in modeling the natural attenuation of explosives, within the general NAX simulator," Internal report for SERDP, April, 1997, U.S. Army Engineer Waterways Experiment Station, Vicksburg, MS.

_____. (2001 in review). "Cosolvent enhanced recovery of non-aqueous phase liquids (NAPL) from saturated porous media by ethanol flushing – Physical and numerical modeling," Ph.D. dissertation, University of Virginia, Charlottesville, VA.

Technical Reports

Reservoir Engineering Research Program. (2000a). "UTCHEM-9.0: A three-dimensional chemical flood simulator; Volume I: User's guide," Reservoir Engineering Research Program (RERP), Center for Petroleum and Geosystems Engineering, University of Texas at Austin, 153 pp (See http://www.pe.utexas.edu/CPGE/UTCHEM/)

_____. (2000b). "UTCHEM-9.0: A three-dimensional chemical flood simulator, Volume II: Technical documentation," Reservoir Engineering Research Program (RERP), Center for Petroleum and Geosystems Engineering, University of Texas at Austin; 256 pp (See http://www.pe.utexas.edu/CPGE/UTCHEM/)

Nitao, J. J. (1998). "Reference manual for the NUFT flow and transport code, version 2.0," Report UCRL-MA-130651, Lawrence Livermore National Laboratory, Livermore, CA.

_____. (1998). "User's manual for the USNT module of the NUFT code, version 2.0 (NP-phase, NC-component, thermal)," Report UCRL-MA-130653, Lawrence Livermore National Laboratory, Livermore, CA.

Nitao, J., Martins, S., and Ridley, M. (2000). "Field validation of the NUFT code for subsurface remediation by soil vapor extraction," Report UCRL-ID-141546, Lawrence Livermore National Laboratory, Livermore, CA.

Sun, Y., Demir, Z., Delorenzo, T., and Nitao, J. J. (2000). "Application of the NUFT code for subsurface remediation by bioventing," Report No. UCRL-ID-137967, Lawrence Livermore National Laboratory, Livermore, CA.

Waddill, D., and Widdowson, M. (2000). "SEAM3D: A numerical model for three-dimensional solute transport and sequential electron acceptor-based bioremediation in groundwater," ERDC/EL TR-00-18, U.S. Army Engineer Research and Development Center, Vicksburg, MS.

Zheng, C. P., and Wang, P. P. (1999). "MT3DMS: A modular three-dimensional multi-species transport model for simulation of advection, dispersion, and chemical reactions of contaminants in groundwater systems; Documentation and user's guide," Contract Report SERDP-99-1, U.S. Army Engineer Research and Development Center, Vicksburg, MS.

Journal Papers

Brauner, J. S., and Widdowson, M. A. (2001, in press). "Numerical simulation of a natural attenuation experiment with a NAPL source: Contaminant dissolution and reactive transport," *Ground Water*.

Julian, H. E., Bogg, J. M., Zheng, C., and Feehley, C. E. (2001, in press). "Numerical simulation of a natural gradient tracer experiment for the natural attenuation study: Flow and physical transport," *Ground Water*.

Waddill, D. W., and Widdowson, M. A. (1998). "Three-dimensional model for subsurface transport and biodegradation," *J. of Environmental Engineering*, ASCE, 124(4), 336-344.

Yabusaki, S. B., Steefel, C. I., and Wood, B. D. (1998). "Multidimensional, multispecies reactive transport in nonuniform velocity fields: Code verification using an advective reactive streamtube approach," *Journal of Contaminant Hydrology* 28(2), 299-331.

Yabusaki, S. B., Cantrell, K. J., Sass, B. M., and Steefel, C. I. (2001). "Multicomponent reactive transport in an in situ zero-valent iron cell," *Environ. Sci. & Technol.* 35(7), 1493-1503.

Zheng, C., Wang, P. P., and Dortch, M. S. (2001). "A general third-order TVD scheme for modeling advection-dominated solute transport in porous media," submitted to *Ground Water*.

Conference Papers

deBlanc, P. C., McKinney, D. C., and Speitel, G. E., Jr. (1999). "UTCHEM: A multiphase flow and biodegradation model." SPE/EPA Exploration and Production Environmental Conference, Austin, TX, 28 February-3 March 1999, Society of Petroleum Engineers, paper number SPE 52734, 1-8.

Zheng, C., Feehley, C. E., Wang, P. P., and Dortch, M. S. (1998). "The ULTIMATE scheme for modeling three-dimensional multicomponent transport in heterogeneous aquifers," *Proceedings of MODFLOW'98 Conference*, E. Poeter, C. Zheng, and M. Hill, ed., Colorado School of Mines, Golden, CO.

Zheng, C., Wang, P. P., and Dortch, M. S. (2000). "Subsurface contaminant transport modeling: Challenges and resolutions," *Proceedings* of 16th IMACS World Congress, August 21-25, 2000, Lausanne, Switzerland.

Remaining Publications in Preparation

Addendum report for the SEAM3D documentation and user's manual to include the chlorinated solvents package for reductive dehalogenation and cometabolism

Peer-reviewed journal paper documenting the validation application of the SEAM3D chlorinated solvents package at Pensacola Naval Air Station

Paper documenting the validation application of UTCHEM for cosolvent flushing
at the Dover AFB test site

REPORT DOCUMENTATION PAGE

Public reporting burden for this collection of information is estimated to average 1 hour per response, including the time for reviewing instructions, searching existing data sources, gathering and maintaining the data needed, and completing and reviewing this collection of information. Send comments regarding this burden estimate or any other aspect of this collection of information, including suggestions for reducing this burden to Department of Defense, Washington Headquarters Services, Directorate for Information Operations and Reports (0704-0188), 1215 Jefferson Davis Highway, Suite 1204, Arlington, VA 22202-4302. Respondents should be aware that notwithstanding any other provision of law, no person shall be subject to any penalty for failing to comply with a collection of information if it does not display a currently valid OMB control number. **PLEASE DO NOT RETURN YOUR FORM TO THE ABOVE ADDRESS.**

1. REPORT DATE (DD-MM-YYYY) September 2001	2. REPORT TYPE Final report	3. DATES COVERED (From - To)

4. TITLE AND SUBTITLE	5a. CONTRACT NUMBER
Development of Simulators for In Situ Remediation Evaluation, Design, and Operation: Final Report	5b. GRANT NUMBER
	5c. PROGRAM ELEMENT NUMBER
6. AUTHOR(S)	5d. PROJECT NUMBER
Mark S. Dortch, Christian J. McGrath, John J. Nitao, Mark A. Widdowson, Steve Yabusaki	5e. TASK NUMBER
	5f. WORK UNIT NUMBER WU CU-1062

7. PERFORMING ORGANIZATION NAME(S) AND ADDRESS(ES) See reverse.	8. PERFORMING ORGANIZATION REPORT NUMBER ERDC/EL TR-01-33

9. SPONSORING / MONITORING AGENCY NAME(S) AND ADDRESS(ES) U.S. Army Corps of Engineers, Washington, DC 20314-1000; Strategic Environmental Research and Development Program ATTN: SERDP, 901 North Stuart Street, Suite 303 Arlington, VA 22203	10. SPONSOR/MONITOR'S ACRONYM(S)
	11. SPONSOR/MONITOR'S REPORT NUMBER(S)

12. DISTRIBUTION / AVAILABILITY STATEMENT

Approved for public release; distribution is unlimited

13. SUPPLEMENTARY NOTES

14. ABSTRACT

Four simulators for modeling in situ, subsurface remediation were advanced and incorporated into the Groundwater Modeling System (GMS) during SERDP Project CU-1062. The four simulators are MT3DMS/SEAM3D, UTCHEM, NUFT, and OS3D. The addition of these four simulators to the GMS provides a significant advancement in the present status of subsurface modeling for remediation alternatives evaluation and design. Each of these four simulators has unique capabilities for simulating innovative in situ treatment technologies, including intrinsic and engineered bioremediation, surfactant and cosolvent flushing to remove oil phase contaminants, venting technologies (e.g., soil vapor extraction, air sparging, and bioventing), and in situ chemical treatment (e.g., Fe^0 permeable treatment walls). Each of the simulators was modified/improved, documented, validated against field-scale studies, and incorporated into the GMS. The GMS models will provide an invaluable tool for improving subsurface, in situ remediation selection, design, and operation, thus potentially providing significant reductions in site cleanup costs. This report provides an overview of results of the CU-1062 project and recommendations for future enhancements to the simulators.

15. SUBJECT TERMS

Groundwater modeling	In situ remediation	Subsurface simulators

16. SECURITY CLASSIFICATION OF:			17. LIMITATION OF ABSTRACT	18. NUMBER OF PAGES	19a. NAME OF RESPONSIBLE PERSON
a. REPORT UNCLASSIFIED	b. ABSTRACT UNCLASSIFIED	c. THIS PAGE UNCLASSIFIED		89	19b. TELEPHONE NUMBER (include area code)

7. (Concluded)

U.S. Army Engineer Research and Development Center
Environmental Laboratory
3909 Halls Ferry Road, Vicksburg, MS 39180-6199

U.S. Department of Energy
Lawrence Livermore National Laboratory
7000 East Avenue, Livermore, CA 94550-9234

The Charles E. Via, Jr., Department of Civil and Environmental Engineering
Virginia Polytechnic Institute and State University
Blacksburg, VA 24061-0105

U.S. Department of Energy
Pacific Northwest National Laboratory
P.O. Box 999
Richland, WA 99352